7-12-2014

# UNM Shock Tube Modernization

Clinton Lee Corbin

Clinton Lee Corbin

*Candidate*

Mechanical Engineering

*Department*

This thesis is approved, and it is acceptable in quality and form for publication:

*Approved by the Thesis Committee:*

Dr. Peter Vorobieff, Chairperson

Dr. Randall Truman

Dr. Juan Heinrich

# UNM Shock Tube Modernization

by

**Clinton Lee Corbin**

B.S., Mechanical Engineering, University of New Mexico, 2012

THESIS

Submitted in Partial Fulfillment of the
Requirements for the Degree of

Master of Science
Mechanical Engineering

The University of New Mexico

Albuquerque, New Mexico

May, 2014

# Dedication

*To my family. My mom for believing in me and pushing me to be my best. And to my sister Rena Marr. Without her support, this never would have happened.*

# Acknowledgments

I would like to thank my adviser, Professor Peter Vorobieff, for pushing me to pursue a Masters degree in the first place. Without his ongoing support and encouragement, the end of this particular road might not be in sight.

I also have to thank all the other students helping out in the shock tube lab, either as graduate students or undergraduate students. We argued. We disagreed. And we got a lot of good word done! Thanks for the guidance and the help. And the arguments.

In addition, I must thank my sister, Rena Marr for proof reading the draft of my thesis and marking up nearly every page with red ink! This thesis is better for her assistance. And any remaining errors are of my own devising! As this is an acknowledgment, I must also acknowledge that without her willingness to keep a roof over my head while I went back to school, it would not have been possible for me to have pursued this deegree in the first place. Thanks Sis!

# UNM Shock Tube Modernization

by

**Clinton Lee Corbin**

B.S., Mechanical Engineering, University of New Mexico, 2012

M.S., Mechanical Engineering, University of New Mexico, 2014

## Abstract

The UNM shock tube in the Mechanical Engineering department has been in continuous operation since its creation in 2007. During this time, significant discoveries in the field of Richtmyer-Meshkov instabilities has been made with this shock tube. While conducting these experiments, limitations on the operational aspects and data quality aspects of this research tool have been found. To further advance the state of the art, it was necessary to address these limitations to allow the research to continue to push boundaries and discover new science.

# Contents

# List of Figures

# List of Tables

# Glossary

| | |
|---|---|
| $CCD$ | Charge-Coupled Device - A light sensitive integrated circuit used as the imaging element in many cameras. |
| $DMM$ | Digital Multimeter - A piece of electronic test equipment that measure voltage and current among other features. |
| $IC$ | Initial Condition - Usually a column of $SF_6$ with a tracer gas added |
| $M\ or\ Mach$ | Mach number - Ratio of speed to local speed of sound. |
| $PIV$ | Particle Image Velocimetry - A method where the velocity of a flow field is measured with the use of small tracer particles |
| $RMI$ | Richtmyer-Meshkov instabilities. |
| $SF_6$ | Sulfur Hexafluoride - A very dense, odorless, tasteless gas. |

# Chapter 1

# Introduction

## 1.1 Overview

Science is data driven. The limitations on science are also often limitations on the quality and quantity of data that can be economically collected in the time frame allocated. The shock tube at Mechanical Engineering at the University of New Mexico (UNM) has been in continuous operation since 2007. During this time, a significant amount of high quality data has been collected at this facility.

Shock tubes are used around the world to collect data on interesting (and usually very fast moving) behaviors with gasses and particles. The shock tubes can range in size from just 1m long with a bore of only 5mm, to over 250m long with a bore of 2m. The UNM shock tube is on the lower end of this size scale with a bore of 76.2mm. These devices are used to collect data on everything from micro explosions at the small end to coal dust mine explosions at the large end.

At UNM, our shock tube is generally used to collect data on three different types of of experiments:

- RMI
- Multiphase RMI
- Particle sweep-up

RMI experiments are experiments where there is only one phase of material (generally a gas) in the "Initial Conditions" IC column and the shock-induced accelerations within the IC cause initial instabilities to develop into turbulence. A classic example of this is when sulfur hexafluoride ($SF_6$) is saturated with acetone vapor (which is used as the tracer gas) and is then illuminated with the 266nm laser to cause the tracer to fluoresce, creating the image. There are many different ways of conducting this experiment by varying the timings, the laser position (upper, center, lower, boundary layers, etc.) or orientation of the laser sheet (horizontal to capture the x-z cross-section or vertical to capture the x-y plane of the entire IC column).

A very beautiful example of this was recently captured. In Figure 1.1 we see a very clear RMI image that is also developing secondary instabilities. It has been false colored by intensity.

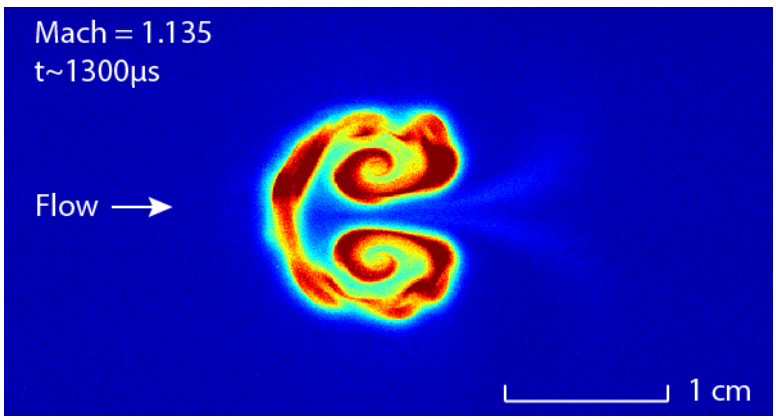


Figure 1.1: RMI image showing development of secondary instabilities

Figure 1.2 is a false color example of the vertical plane of an inclined shock experiment.

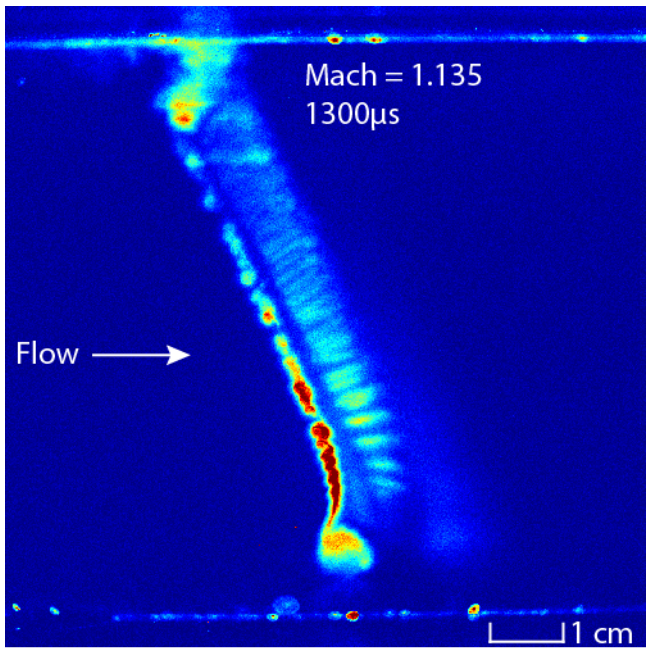


Figure 1.2: RMI with 30° incline and vertical laser plane

This shock tube has also been used to conduct multiphase RMI, where multiple phases of material are in the IC column. In our case, we have conducted experiments with $SF_6$ and glycerin droplets produced from a commercial fog machine that produces droplets of glycerin in the 0.5 micron to 5 micron size range. These droplets remain in suspension with $SF_6$ and form the IC column. A visible laser light sheet of 532nm is used to directly illuminate the droplets in the IC to capture the image. Figure 1.3 below is a classic example of multiphase RMI.

While not directly a focus of this thesis, it must be noted that the RMI and multiphased RMI research at UNM has led to the discovery of a new type of instability in multiphase flows that has been labeled "particle lag instability".

The final type of experiments conducted with the UNM shock tube are particle

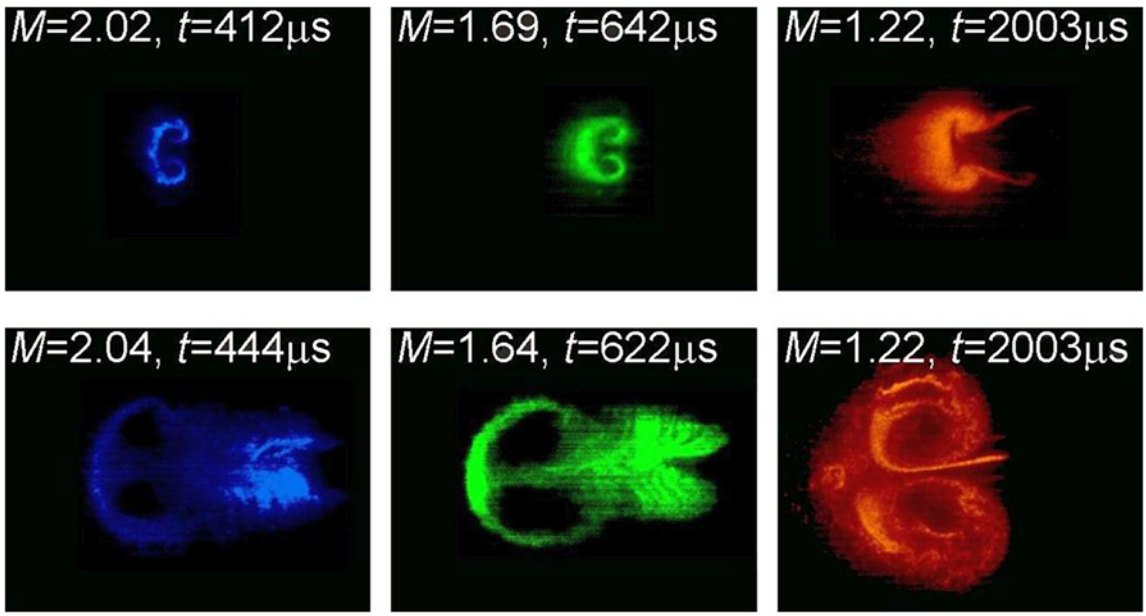


Figure 1.3: Multiphase RMI development [1]

sweep-up experiments. In these experiments, instead of an IC column, particles are carefully "attached" to a test surface that is then installed in the bottom of the test section so that the surface is flush with the inside bottom surface of the test section. As the shock wave passes over the surface, the particles are swept up into the air stream behind the shock wave. This type of experiment has many applications in understanding how dust is lifted by an explosion or the redistribution of biological and radiological materials due to other explosions after the particles originally settled. Figure 1.4 shows particles being swept up behind a Mach 1.7 shock wave after it passed over the particles on the surface.

In all of these experiments, the timing of the lasers is adjusted shot to shot to capture the development at different times to better understand the evolution of the phenomena of interest.

Figure 1.5 is a montage of 32 images taken with the same setup and Mach number (within the limitations of the shock tube at that time) with the time after shock

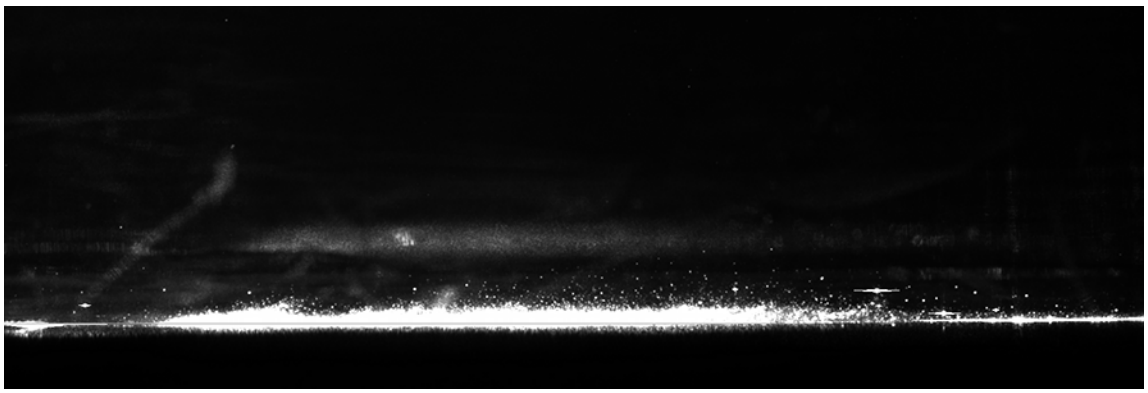

Figure 1.4: Particles swept up after passage of shock wave

varying from approximately $50\mu s$ for image 1 to $1060\mu s$ for image 32. The time span is only $1ms$ for the whole montage, yet you can see the extremely rapid development of the RMI feature as it goes from initial perturbation to well-mixed turbulence.

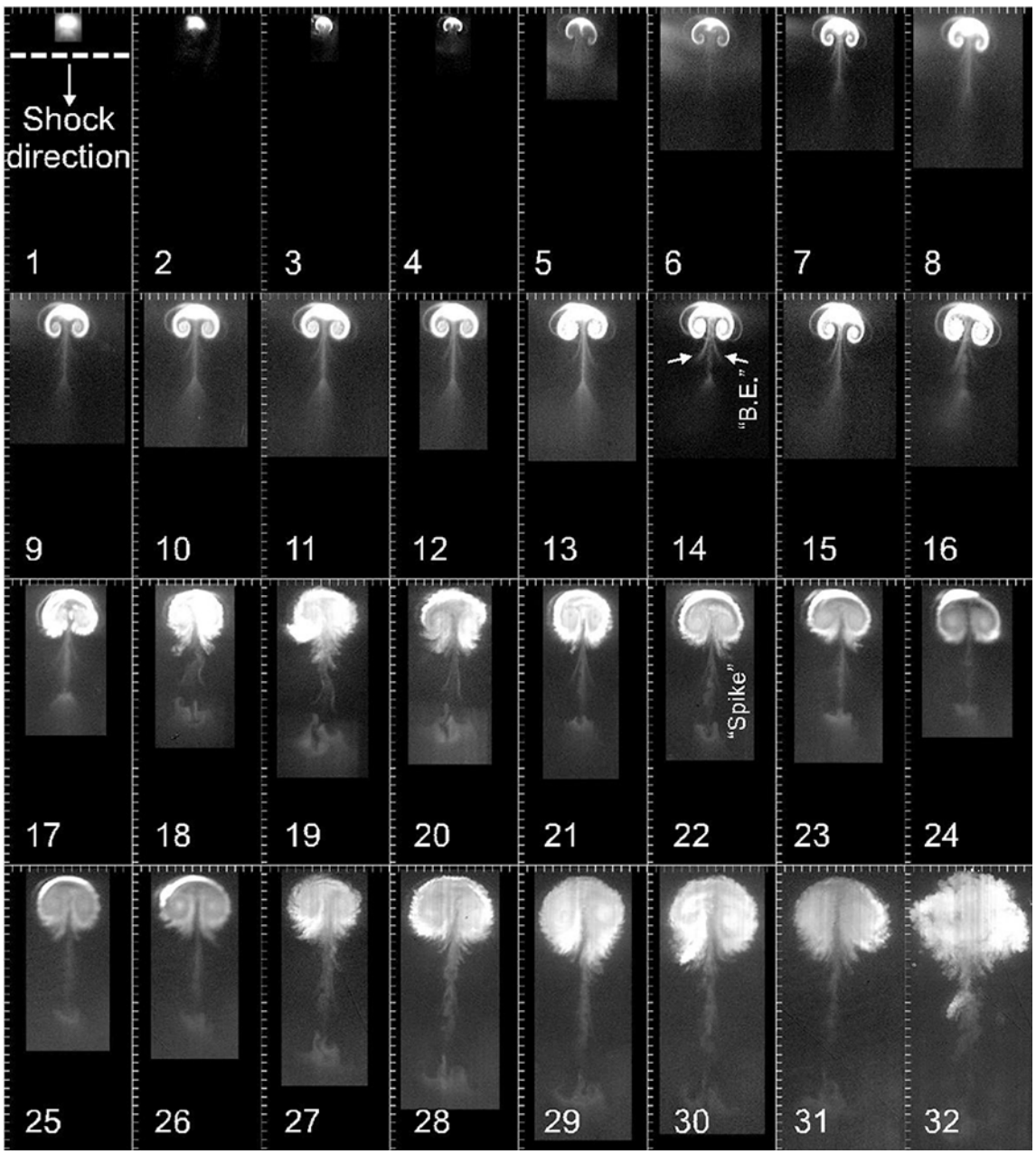


Figure 1.5: Montage showing development of RMI over 1ms [2]

## 1.2 Original Shock Tube Configuration

This shock tube is fairly conventional in its overall configuration with one distinct feature: it can be tilted from 0° (horizontal) to 45°, allowing for data to be collected on normal and tilted initial conditions, when the angle between the shock and, for example, the axis of the gravity-driven heavy gas cylinder is oblique.

Figure 1.6 below is a diagram of the system.

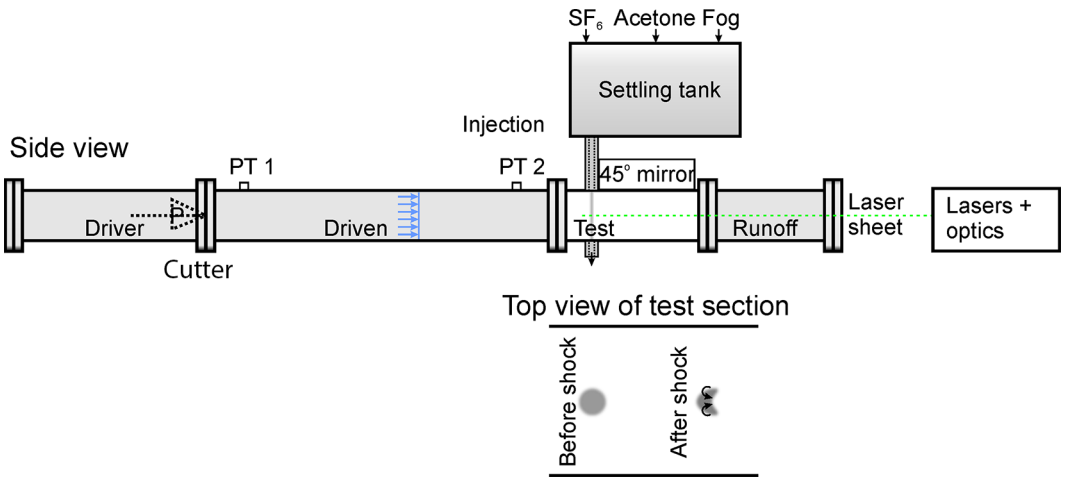


Figure 1.6: Diagram of the UNM shock tube [3]

The shock tube is composed of several basic components. The driver section shown on the far left side is where the pressurized gas is held. The cutter inside the driver section is used to rupture the diaphragm that initially separates the driver section from the driven section. The driven section allows for the normal shock wave to form from the expansion waves. It guides the shock wave to the test section and contains two high speed pressure transducers that are used to time the shock wave and trigger the lasers.

After leaving the driven section, the shock wave enters the test section which is constructed of clear polycarbonate to allow for the experiment to be imaged. The

ICs are flowing through the IC injector system into the test section when the shock wave impacts and passes through the ICs. The transfer of momentum and vorticity to the ICs leads to the rapid development of Richtmyer-Meshkov instabilities (RMI) in the ICs.

After passing through the test section, the shock wave enters the run off section before leaving the end of the shock tube. The runoff section gives the shock wave more distance to travel before it exists the shock tube and a reflected shock wave is then sent back up the run-off section towards the experiment in the test section. The longer the run-off section, the more time for the experiment before the reflected shock wave arrives back at the rapidly moving gas column and further disturbs it.

The final components of the shock tube are the laser assembly (or assemblies) and their associated optics system to produce the proper laser sheet and position it in the correct location in the test section. The laser is triggered from a precision delay generator that is started when the shock wave passed the downstream pressure transducer, PT 2. Finally, a high sensitivity camera is used to capture the light produced by the laser pulse and produce the output image.

To image the gas column, a nominally 200 mJ per pulse laser from New Wave Research, the Gemini PIV, is triggered at the correct moment by the delay generator to illuminate a slice of the gas column with either a 266nm or 532nm pulse to provide illumination of the ICs at that instant in time. The orientation (horizontal or vertical) and position (top, bottom, center, etc.) of the beam sheet can be adjusted using the optics held in the laser path. An Apogee U42 camera with a cooled CCD image sensor is then used to capture either the reflected light (532nm) or the laser induced florescence of the acetone tracer gas in the ICs caused by the 266nm laser pulse. Due to the extremely fast nature of a shock wave and the subsequent rapid development of the features in the gas column, the triggering of the lasers must be very precise and repeatable.

The accuracy of the triggering is achieved by using the pressure pulse of the shock wave as it passes under the downstream pressure transducer, PT 2, to trigger a precision delay generator that then counts down the correct delays before triggering from one to four lasers, each with their own programmed delay. As each laser is triggered, it emits a 4ns long pulse that illuminates the flow features brightly enough for the camera to capture the image in that instant. Following a small delay (dependent upon the exact experiment being performed) which allows the flow volume of interest to move further down the test section and the RMI features to further develop, the next laser is triggered to capture an additional image of the same volume.

The camera shutter is held open during the firing of the shock tube as the iris is orders of magnitude too slow to open after the shock wave forms. To prevent overexposure of the image and to maximize the signal to noise ratio, the lab is blacked out during firing.

To fire the shock tube, the cutter head, which is inside the driver section, is pushed forward where the blades of the cutter head come in contact with the burst diaphragm which then ruptures. Mach waves begin rapidly propagating down the driven section due to the rapidly expanding helium. These Mach waves very quickly coalesce into a planar shock wave traveling at the desired Mach number down the driven section. The shock wave forms before the first pressure transducer, PT 1.

The pressure transducers PT 1 and PT 2 are both high speed Omega piezoelectric transducers that perform two important functions in the system:

- Indirectly measure the velocity of the shock wave
- Trigger the delay generator to fire the lasers

The first task is performed by accurately measuring the time it takes for the shock wave to travel between the upstream pressure transducer PT 1 and the downstream pressure transducer PT 2. The distance between the two pressure transducers is

known and fixed at 2.60 meters. With this and the timing data, the velocity can be calculated as

$$Velocity\ V_a = \frac{2.60\ m \cdot 10^3 \frac{ms}{s}}{\Delta t\ ms} \tag{1.1}$$

To calculate the Mach number, the local speed of sound is needed. The Mach number is a function of the gas properties and the local temperature

$$V_s = \sqrt{\gamma RT} \tag{1.2}$$

where

$\gamma$ = Ratio of specific heats
$R$ = Gas constant
$T$ = Absolute temperature

The temperature in the shock tube lab remains at a fairly constant 20C° year round (one advantage of working in the dungeon!) with any variance in the $\pm 0.5C°$ range. If we assume that the temperature is 20C°, and that $\gamma$ for air is 1.401 at 20C° and $R = 286.9\ J/kg\ K$, we find that the local speed of sound is

$$V_s = \sqrt{1.401 \cdot 286.9\ J/kg\ K \cdot (20 + 274.15)K} \tag{1.3}$$

$$V_s = \sqrt{118,232.7\ m^2/s^2} = 343.8\ m/s \tag{1.4}$$

With the known shock wave travel time and the calculated local speed of sound, the Mach number can be calculated as

$$M = V_a/V_s \tag{1.5}$$

To get the shock timing data, we must interrogate the "pressure trace", which is just a recording of the pressure transducer data captured by the oscilloscope for that "shot". Figure 1.7 is a pressure trace of a shot taken on June 6, 2012. This was before the isolation of the pressure sensors discussed in a later section.

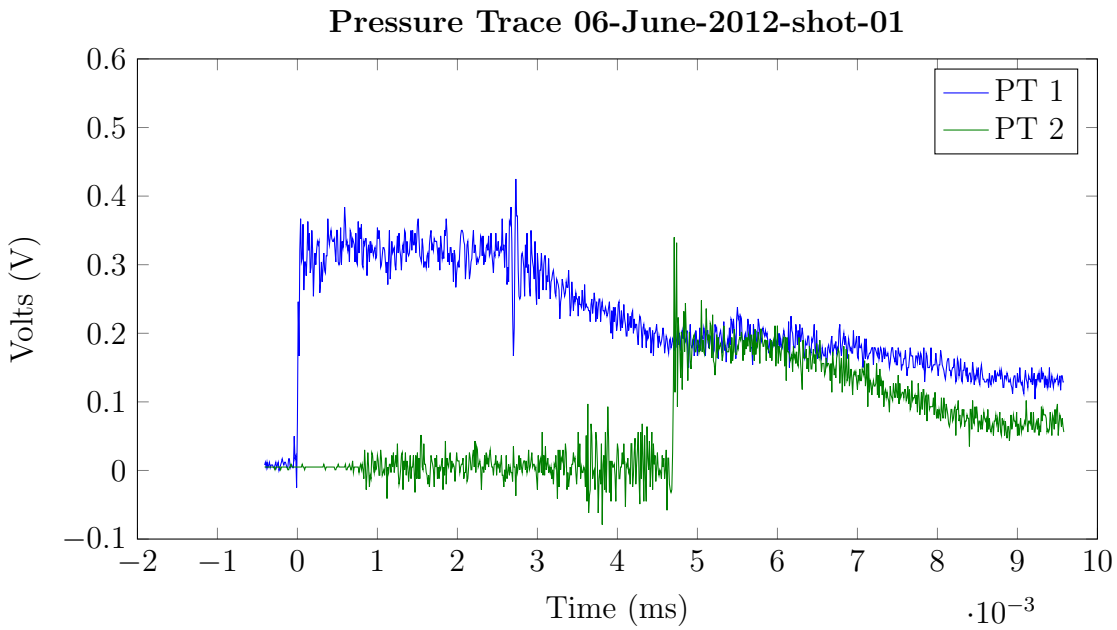


Figure 1.7: Pressure Trace, 2012-06-01-shot-01, pre isolation

The blue line is the signal from the upstream pressure trace (from PT 1) while the green line is the signal from the downstream pressure trace (from PT 2). You can see the very sharp rise in pressure in the blue trace at t=0 as PT 1 triggers the oscilloscope in single shot mode. This very sharp rise is also indicative of a shock wave, as opposed to subsonic (and gradual)pressure increase due to the expanding helium. The timing for the shock wave is measured from the initial sharp rise at PT 1 to the initial sharp rise at PT 2, which is when the shock wave arrives at that sensor. You can also clearly see the conducted noise in the signal at PT 2 before the shock wave arrives. In this image, the specific timing of the pressure rises are not clearly readable, but reviewing the data shows the pressure spiked at $4.71ms$ from

trigger. The pressure spike on PT 1 occurred effectively at $t = 0ms$. This gives a travel time of $4.71ms$ for this specific shock wave.

Using equation 1.1 and equation 1.5 above, we can calculate the Mach number for this shot to be

$$V_{shot} = \frac{2.60\ m \cdot 10^3 \frac{ms}{s}}{\Delta t\ ms} = \frac{2.60\ m \cdot 10^3 \frac{ms}{s}}{4.71\ ms} = 552.02 m/s \tag{1.6}$$

$$M = \frac{V_{shot}}{V_s} = \frac{552.02 \frac{m}{s}}{343.8 \frac{m}{s}} = 1.606 \tag{1.7}$$

Given that we have not recently targeted $M = 1.6$, it is safe to say this was a slow shot that day. There are many reasons for a slow (or fast!) shot that will be discussed in other chapters.

## 1.3 The Issues

While this shock tube has been a significant success for UNM, several limitations have been identified which have impacted the ability of this system to collect data. These issues fall into two distinct groups:

- Qualitative
- Quantitative

The issues that are categorized as "Qualitative" are issues that directly impact the QUALITY of the data collected. This could be due to incorrect disturbance growth due to timing or Mach number issues, or problems with the image clarity.

The issues that are categorized as "Quantitative" are issues that directly impact the QUANTITY of data collected. Generally, these are issues that lead to failures in the shock tube firing, cameras triggering, or lasers triggering at the correct time.

Some issues will have an impact on both categories and will generally be placed in the Qualitative category.

### 1.3.1 Qualitative Issues

From a pure science point of view, the qualitative issues are the largest issues as they directly impact the quality of the collected data. Some of the qualitative issues we have encountered are:

- Mach number variation
- Focal plane variation
- Laser trigger timing variation
- Initial Conditions (IC) poorly formed
- Laser plane alignment
- Noisy images

The Mach number variations are generally caused by a single issue: controlling the pressure in the driver section at the moment the diaphragm is ruptured. Several changes have been made both to the design of the shock tube and firing procedure to address this issue.

The focal plane variation had several root causes and required several different changes to fully address. Even at this time, making sure that the camera focal plane and the laser sheet plane are aligned properly is still time consuming, but the process is much more repeatable due to improved equipment and procedures.

The laser triggering is actually a two step process. First, the flash lamp is fired to begin the laser cascade, then $180\mu s$ later, the internal timer activates the Q-switch, allowing the beam to exit the resonating cavity. For most experiments, this internal timer is sufficiently accurate. However, for some types of experiments such as

particle velocimetry, the variation of the internal timer is too great. This is especially true when multiple lasers are used in the same experiment. When four lasers are used simultaneously, the limitations of the internal timer become all too apparent. Thankfully, we were able to resolve this issue as well.

Perhaps more than any other aspect of running the shock tube, the ICs were either "on" or "off". Usually with nothing in between. The objective in forming the IC gas column is to have a very uniform and perfectly round column of heavy gas (with or without particles or tracer gasses) falling very steadily through the test section with no variations or disruptions. When it was "on", you couldn't even tell the column was moving or see any variation from top to bottom inside the test section. When it was "off", it seemed that nothing you did could make it better. Several changes were made to the IC injector system that mostly addressed this. But I am sad to say it STILL has an "off" day from time to time... But we are working on it!

To capture a clear, bright image, we must first make sure that the camera is precisely focused at the required location, then we have to create a laser sheet that passes exactly through the middle of this focal plane. In addition, because we are focusing the beam, then spreading it into a sheet and then directing it into the test section, fine adjustments of the assorted lenses are required. The original system was not capable of the precise and independent adjustments required to get a high quality laser sheet to its proper location. Significant changes were made to the mounting of the optics to address this limitation. In addition, the alignment methods were refined (and documented) to allow anyone with a bit (or maybe a lot) of patience to properly align the laser.

As was mentioned, this system is triggered with the camera shutter open during the whole shot. It is opened just before the diaphragm is punctured and normally stays open for 2 full seconds. The Apogee U42 has a very high quantum efficiency of

over 98% which means any stray light in the lab is translated to noise in the image. Background subtraction has been used in the past to subtract out some of the noise, but you can't help but subtract out real information as well. Eliminating most of the noise in the first place is a much better solution.

All of these issues were addressed and they will be discussed in the Qualitative Issues chapter of this thesis.

### 1.3.2 Quantitative Issues

The quantitative issues, while they do not impact the quality of the data recorded, greatly impacted the rate that data can be collect and therefore the speed of completing the science as well as the cost of that research in terms of salaries and supplies used. Some of the quantitative issues encountered are:

- Failure to fire when triggered
- Lasers not triggered correctly
- Camera iris not open

There were two different failure to fire: the first one is when the fire button is pressed (hopefully at the correct time), but all you hear is silence because the cutter didn't so much as move. The occasional failure would not be too bad, but when it starts to happen every third or even every other shot, it becomes a great hindrance to getting the job done. Not to mention, it tends to cause steam to come out of the ears of certain research techs... The shock tube improvement question that led to this thesis all started with my desire to address this particular failure. And I am very glad to say that address it we did!

One of the more irritating aspects of operating the shock tube was when a perfect shot is set up, the ICs looked perfect prior to shooting, the camera shutter was opened

at the correct time, the cutter fired just like it should. Even the pressure trace showed you had a perfect Mach number, but you captured no image because the lasers were either triggered too early or too late!

There are two basic causes of this failure. The batteries in the pressure transducer power supplies were too low (I think we have bought enough 9V batteries to keep the Energizer Bunny running for the rest of my life!), or worse yet, not turned on at all. Or there was a noise spike in the pressure trace that caused the delay generator to trigger too early.

We were not able to do anything about the batteries as the manufacturer swears any AC power supply will introduce too much noise into the transducer, but we were able to deal with most of the false triggers due to noise. Other causes of false (or failed) triggers are also discussed.

To understand the problem with the camera iris not being open, you first have to understand the standard operating procedure of firing the shock tube. And, you have to understand this is all being done in a nearly completely blacked out lab.

First, one research assistant has to get the ICs flowing and verify that they are flowing smoothly and with no aberrations. Once the ICs are verified, the research assistant who is firing the shock tube takes over and begins charging the driver section with helium. A toggle switch is thrown which operates a solenoid that opens to allow helium into the driver section. The pressure at the helium regulator is adjusted so it takes around 3 to 4 seconds to fill the driver to the correct pressure.

It becomes a bit more interesting when you realize that the RA is determining the pressure by watching the readout on a Fluke 87 DMM connected to the Omron pressure transducer. While the pressure transducer has an update rate of 1000Hz, the Fluke 87 however only updates at 4Hz... In the original system, the shock tube was fired dynamically as the cutter would not be able to puncture the diaphragm

if the driver was brought up to pressure slowly and allowed to sit. The diaphragm would bow out into the driven section and the cutter couldn't reach it.

So the tube was fired as the pressure was rising... This leads to a bit of "Kentucky Windage" as they had to fire the tube at the correct time so that when the system responded and did cut the diaphragm, it was at the correct pressure. Several of the RAs became quite adept and could generate fairly consistent Mach numbers with dynamic firing. Others fought with it to the bitter end.

The reason the camera iris is an issue with this procedure is that the iris was only open for 2 seconds (to keep image noise down) and it took around 3 to 4 seconds to charge the driver section for a shot, so the camera could NOT be opened before filling the test section. In fact, it was triggered (with one hand on the computer mouse...) approximately 1/2 second before the firing button was pressed.

Usually.

More than one shot was missed because the operator opened the camera iris AFTER everything of interest had already occurred. Or, they opened it so soon that it closed before the shock wave arrived. I personally have managed to capture the iris opening on four separate occasions. Two were back to back!

In Figure 1.8, you can also see the "triplets" used for particle velocimetry where we are working to determine the velocity and boundary layer profile of particles seeded in the stream. The spacing between the "triplets" is used to calculate the velocity of that particle at that location. The timing for these pulses is very critical and led to the discovery of another issue that we had to address. This specific issue is discussed in more detail in a later chapter.

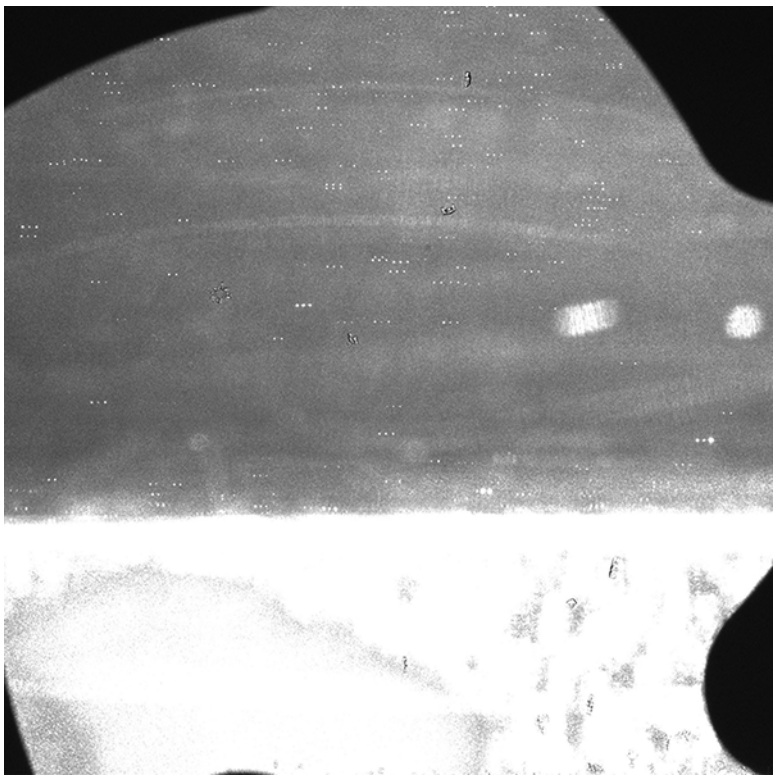

Figure 1.8: Particle Image Velocimetry with the iris just opening and three laser pulses

## 1.4 Summary

Addressing each of these issues has not only increased the quality of the data collected significantly, but has also increased the quantity of data that can be collected in any given lab session. The increased reliability of the shock tube has also led to a less stressful working environment for the research assistants conducting the research. Thankfully, they still have each other to maintain the "proper" level of stress for the working environment!

The rest of this thesis will go into the specific details of each of the improvements to document not only what was done, but why.

# Chapter 2

# Earlier RMI Results

## 2.1 Pre Upgrade RMI Results

While the theme of this thesis is discussing the improvements that have been made to the UNM shock tube over the last few years, that does not imply that the original configuration was sub-par. It is far from it in fact. It DID have limitations, but many of those limitations were not known until advances were made. For example, something as simple as purchasing a new lens with a much sharper focal plane brought forward the issues with the then current methods for aligning the camera and laser sheet. Ignorance apparently IS bliss!

With that said, there were areas that needed to be addressed, such as the Mach number variation between shots. Thankfully, the efforts made to improve the reliability of the shock tube also ended up leading us down a path to address these issues as well.

### 2.1.1 Mach Number Variation Visualization

The images used to make the montage of Figure 1.5 are a great example of Mach number variation. If you compare sequence 3 and sequence 4, even though the first image was taken $65ms$ after the shock while the second image was taken $100ms$ after the shock, just by looking at them you would never know that the second image had 50% more time to develop. Sequences 11 and 12 are also very similar where sequences 22 and 23 actually look out of order.

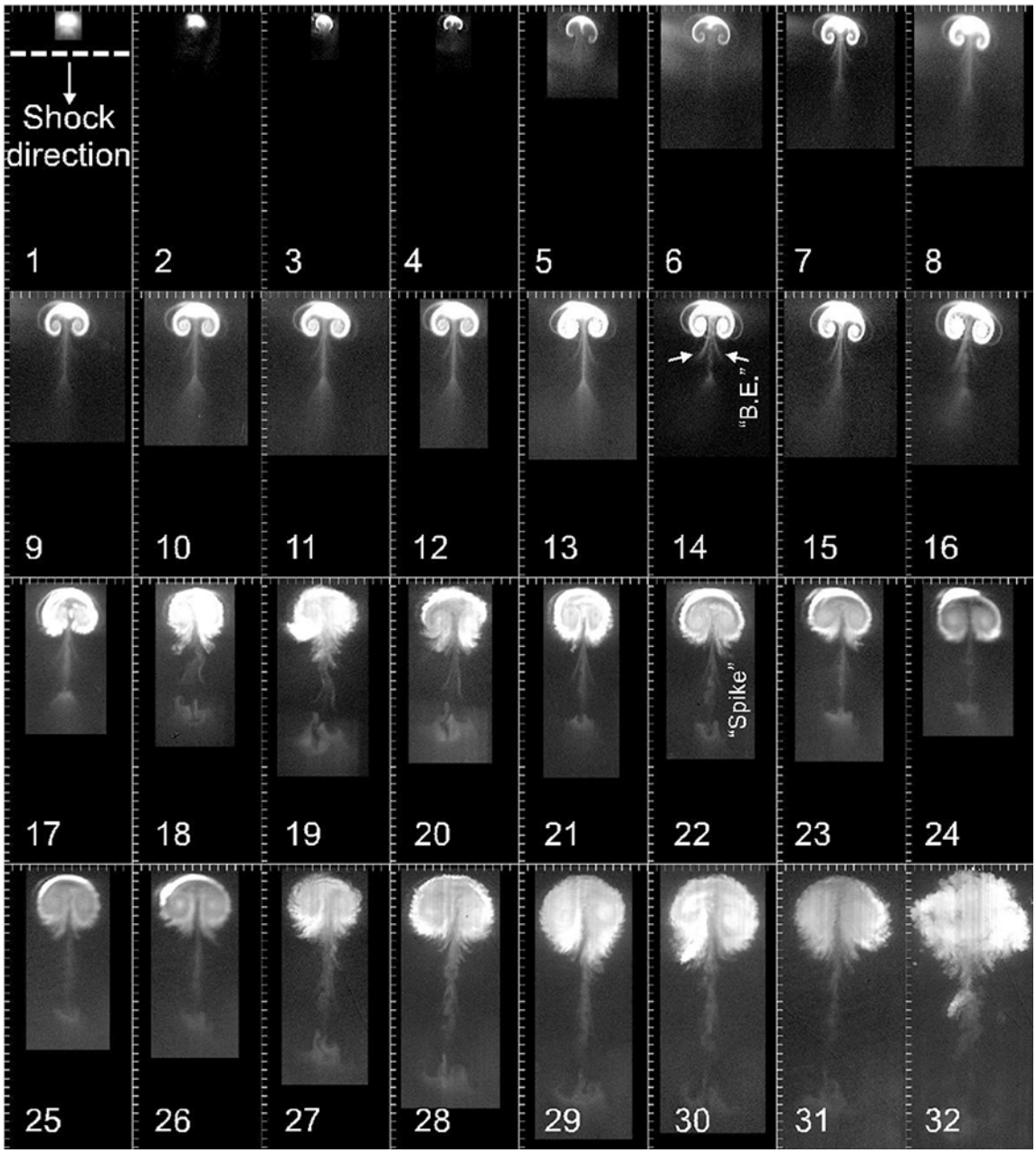


Figure 2.1: Montage showing development of RMI over 1ms [2]

If we look at the early linear model for the development of the instability growth as originally proposed by R. D. Richtmyer we can shed some light on these images. Richtmyer started with the equation originally proposed by Taylor [4] as a linear solu-

tion for the growth of amplitude $\eta$ of small single mode perturbations on an interface between two incompressible fluids that are acted on by gravitational acceleration $g$

$$\frac{d^2\eta(t)}{dt^2} = kgA\eta(t) \tag{2.1}$$

where

- $k = 2\pi/\eta$ the wave number of the perturbation
- $A = \frac{(\rho_2-\rho_1)}{(\rho_1+\rho_2)}$ the Atwood number

Richtmyer replaced the constant acceleration of gravity with impulsive acceleration and the velocity delta $[u]$ the change in interface velocity induced by the shock wave. He then integrated this equation once to generate an in impulsive growth rate equation

$$\dot{\eta}_{imp} = k[u]A\eta_0 \tag{2.2}$$

where $\dot{\eta}_{imp}$ is the growth rate of the instability of the interface long after the shock, but while the perturbation amplitude is still small enough to be in the linear region.

Reviewing this equation can shed a lot of light on the initial behavior of the Richtmyer-Meshkov instability. First, we see that $\dot{\eta}_{imp}$ is a constant, which implies that the growth rate will be constant and based on the other initial parameters of the equation. Looking at the parameters we see

- k: the wave number of the initial perturbation forces us to maintain a constant IC shot to shot.
- [u]: The velocity change is a function of Mach number, so our Mach number must also be constant shot to shot.
- A: The Atwood number must also remain constant and once again forces us to produce repeatable ICs.

- $\eta_0$: The initial perturbations must be as constant as possible, once again making us look to constant IC conditions shot to shot.

The wave number k, the Atwood number A and initial perturbations in the interface $\eta_0$ all point to the fact that our initial conditions must be as consistent as possible shot to shot. The one parameter we directly measure, the Mach number, directly impacts the velocity change $[u]$.

The ICs have been a problem in the past. If you are using glycerin fog for the experiment, you at least have a visible IC that can be viewed with the naked eye to help and detect disturbances in the IC. When no fog was used, the IC column was invisible and it was "assumed" the ICs were good. Abnormal distortions in the actual image were the only indicator that the ICs were not good for that shot.

Even worse, control of the Atwood number was simply non-existent. No attempt was made to measure or control it other than flowing the ICs into the settling tank long enough and fast enough to mostly ensure the residual air had been displaced by the ICs. Not good.

### 2.1.2 Mach Number Variation Data Analysis

The Mach number was not being controlled as accurately as it should be due to the dynamic firing system used. Table 2.1 shows the average and standard deviation for a group of shots taken at Mach = 1.2, Mach = 1.7 and Mach = 2.0. This is not a statistically random sample by any means, but the data was taken as a generally representative sample of the quality of data generated.

For this sample, the % error in the average velocity ranged from 1.96% to 4.48%. When you take into account the dynamic method firing being used, this is actually a pretty good error. Looking at the standard deviation, we have a range from 0.028

Table 2.1: Pre-upgrade Mach Number Analysis

| **Target Mach Number** | **# Samples** | **Standard Deviation** | **Average** | **% Error** |
|---|---|---|---|---|
| M = 1.20 | 12 | 0.027723 | 1.223516 | 4.476 |
| M = 1.70 | 9 | 0.036513 | 1.623906 | 1.960 |
| M = 2.00 | 13 | 0.075581 | 1.960902 | 1.955 |

up to 0.076.

Thankfully, the upgrades made to modernize the UNM shock tube were effective as will be demonstrated in the post upgrade results section later in this thesis.

# Chapter 3

# Addressing the Qualitative Issues

## 3.1 Introduction

The data collected by the shock tube is of two types:

- Oscilloscope recording of the pressure data from both pressure transducers
- An image of the developing "feature" at a specified time

As was discussed in section 1.2, the pressure trace from the oscilloscope is used mainly as a diagnostic tool to allow the exact shock wave Mach number to be calculated from the time taken by the shock wave to travel between the upstream and downstream pressure transducers mounted on the shock tube. Equations 1.1 and 1.2 demonstrate how this information is used specifically. Needless to say, before an image can be of any real use, we must know the Mach number for that specific shot.

The image of the developing "feature" is the bread and butter of the shock tube. Without high quality visual data, it would not be possible to produce high quality papers and presentations that expanded the understanding of the phenomenon being

researched.

## 3.2 Mach Number Variation

### 3.2.1 Fluke DMM

The pressure in the driver section is measured by an Omega PX303 sensor. This sensor has a rise time of $1ms$ and is very responsive to small changes in the pressure. The output from this transducer is a voltage proportional to the pressure. It was read by the simple expedient of connecting a Fluke 87 hand held DMM to it's output. The meter was "attached" to a shelf behind the shock tube using duct tape.

Because the transducer is outputting a voltage instead of a pressure, the voltage level for a corresponding target pressure (which was determined by the target Mach number) was looked up and used as the target voltage for that shot. When that pressure was displayed on the meter, the firing button was pressed and the helium fill solenoid was turned off.

The Fluke is a great meter. But it only refreshes the display 4 times per second. It is really hard to target a moving pressure to any accuracy with a 1/4 second delay between updates. Combine that with the reflex rate of the average human which is also in the $250ms$ range, and you have a situation ripe for over or undershooting the target pressure with dynamic shots.

Digital control theory shows that the performance of a control system is impacted by the sampling rate and response rate of the system. The transducer is already performing orders of magnitude better than the operator. It is also many times faster than the DMM. In our situation, we have a 1/4 second delay between updates on the meter, then another 1/4 second delay for the operator to react and press the

firing button.

While we can't do much on the reflex rate of the human operator (yet...), we could do something about the Fluke.

So, we switched it out for a bench meter that updated at 10 or 25 times per second. Much better! Plus, the display on that meter never turned off in the middle of a shot like the battery powered Fluke did! That little change actually had a larger impact on the irritation level in the lab than you would expect.

With a 25Hz refresh rate and a bright, vacuum fluorescent display that is easy to see in the dark, this meter change improved the Mach wave variation. We do not have a definitive answer to "how much did it improve it" as several changes were made in short order. And the next change REALLY had an impact.

### 3.2.2 Dynamic shots

Shooting while the pressure is rising is VERY hard to do accurately. We actually can't do it. As it will be discussed in more detail in later chapters, the reason we shot dynamically was that we had to. The original cutter assembly just couldn't rupture the films if the pressure was allowed to sit at the target pressure before firing. While addressing the misfire issues (addressed in the qualitative section 4.1), it had a very positive side effect: We no longer had to fire the shock tube dynamically.

Static firing is really very simple. The first step is to pressurize the driver section to the correct pressure. The final target pressure is approached gradually so we can hit it to within 0.1 psi. The pressure is then allowed to sit and stabilize for a few seconds and if it drops (due to diaphragm stretching), quick bursts of helium bring it back up to the target zone. Once the pressure is stabilized, the ICs begin flowing and are checked for stability. When everything is correct, all lights are turned off

and the monitors are covered to plunge the lab into near total darkness.

Then and only then is the camera triggered followed very rapidly by triggering the cutter. The operator actually has the chance to catch his or her breath and make sure all is well BEFORE the system is fired. That is a huge change from manic race that is dynamic firing. With dynamic firing, once you start filling the driver section, you are committed to either a very quick shot, or a very quick failure.

Static firing by itself addresses much of the precision of shooting. We can now repeatably fire at our target pressure. Figure 3.1 shows six shots taken back to back. The delay timing was fixed at 570$\mu s$ and the firing pressure was varied from 91.5 *psi* down to 88.0 *psi* microseconds.

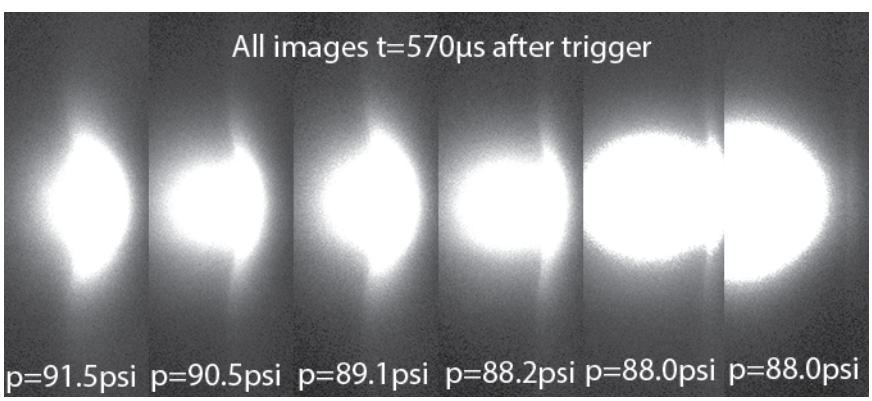


Figure 3.1: Montage of shock captured in the IC six shots in a row.

The first shot has the shock at the front of the IC and the last shot has the shock just almost touching the IC. The middle four have the shock almost in the middle of the IC column. Consider that the shock wave was traveling at Mach 1.7 and it originated 3 meters upstream, capturing the shock wave in almost the exact same position six times in a row is a confirmation of significant improvement. Making this even more impressive, the target pressure was gradually changed shot to shot from 91.5 *psi* down to 88.0 *psi* through this sequence to intentionally move the shock wave to just in front of the IC.

The right most two images were both taken with the same delay and the same target pressure of 88.0 *psi*. With those images, you can see that the shock wave moved approximately 1 *mm* from one shot to the next.

This repeatability has actually had a carry over effect. Originally, we needed to capture at least 7 good shots at a given timing before we could go on so that we knew we had a representative sample at that timing. With this much improved performance, we only need three shots at each sample and for exploratory work, one. This greatly reduces the number of experiments that must be conducted for any given project and greatly speeds up the data collection portion of that experiment.

### 3.2.3 Burst Diaphragm Quality

An additional factor in the Mach number variation was the diaphragm (or film) quality. The original cutter system was very sensitive to the type of film used. In fact, we were only able to identify two different films that would reliably work, the 3M CG5000 and CG6000 InkJet and LaserJet transparency films. They had the property that they were strong enough to support the pressures being applied to them, but were weak enough that they would tear open once the cutter initiated the rupture. There was a very fine line between too weak and too strong and the shock tube was sensitive to that variation.

When a specific film for a shot proved to be weak, it had no impact on the data quality as the shock tube would fire prematurely and there would be no data collected. The worse case scenario was when the film was a bit TOO strong.

For a normal shock wave to form quickly, the diaphragm needs to rupture in an almost brittle fashion once the cutter head has introduced an initial puncture. The forces acting at the stress concentration formed at this puncture should lead to the diaphragm to split into multiple petals that then fold flat against the driven section

and allow the helium to expand unimpeded into the driven section to quickly form a normal shock wave before it reaches the upstream pressure transducer PT 1.

When the film is too strong, it does not split cleanly and quickly. Instead, the plastic material stretches before it tears, stretches a bit more, tears a bit more, etc. This process leads to a very slow rupture of the diaphragm and prevents the driver gas from quickly and cleanly entering the driven section. The result of this is a shock wave that is still in the process of forming when it passes the upstream pressure transducer. Because it is not yet formed, there is no way to accurately time the velocity of this shock wave. Figure 3.2 is a good example of this.

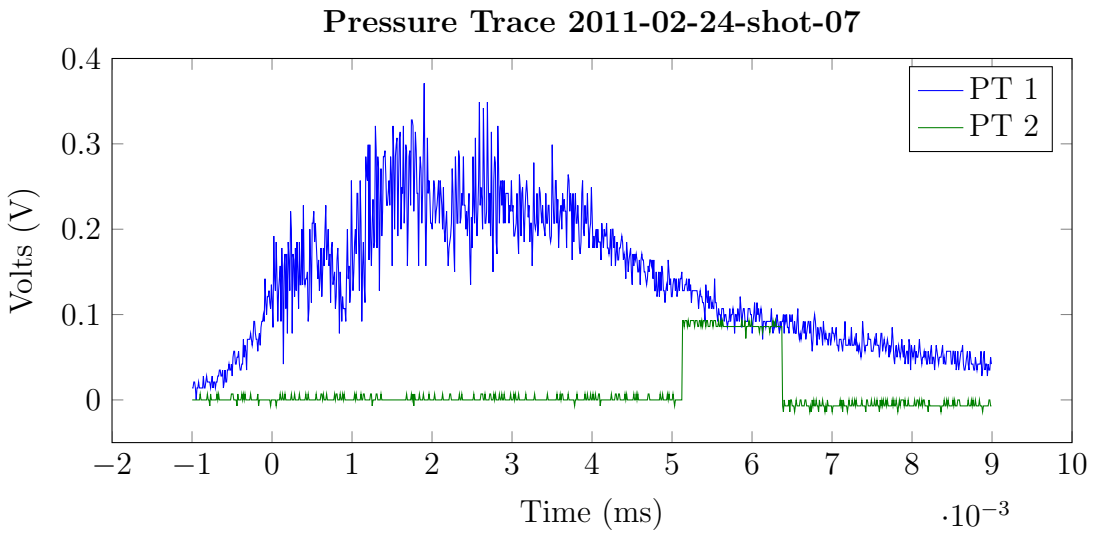


Figure 3.2: Pressure trace, 2011-02-24-shot-07 with poor shock wave at PT 1

Notice how we do not have a true vertical "spike" in the blue trace at what is marked as time $t = 0$. Instead, there is a slow rise (with a great deal of noise) in pressure before it starts to fall off due to the gas expansion. But there is no good evidence that a shock wave was actually formed until you look at the downstream pressure trace where we do have the sharp pressure spike we expect. Using such a pressure trace to calculate Mach number is not much better than a wild guess.

The improvements to the cutter assembly covered in the quantitative section also removed the sensitivity to the films. The switch to static firing also allowed for an improvement in the films as well. We found that films that were too weak to withstand the full pressure of a shot when brought up to pressure in a single charge, could withstand the pressure if they were brought up to pressure in stages.

With these "weak" films in place, the pressure was first brought up to 50% of the target pressure and then held for 10 seconds or so. This hold time allows the film to stretch, which causes the polymer chains to straighten. These straightened chains are better able to resist the pressure being applied. The pressure is then brought up another 10% and allowed to sit for a few seconds. This process is repeated until the pressure has reached the target firing pressure.

At this point, the polymers in the film have strained as much as they can. The chains are stretched out very straight and the diaphragm is now actually very brittle due to the strain hardening that has taken place. This gives us a diaphragm with nearly perfect characteristics: it is strong enough to support the pressure (just) and it is relatively brittle. When the initial puncture is formed by the cutter, the diaphragm ruptures almost instantly leading to a very clean normal shock wave formation and a very good pressure trace as shown in Figure 3.3

Unlike the previous pressure trace, this one has a nearly vertical rise in pressure at the upstream pressure transducer. There is no doubt that the shock wave was fully formed and it is very easy to identify the time when this shock wave passed the pressure transducer. Clean, vertical spikes in the pressure trace eliminate any uncertainty of when the shock wave arrived at each of the pressure transducers, therefore it also eliminated the uncertainty of the velocity of that shock wave as well.

Taken together, the changes that have been made have significantly reduced the

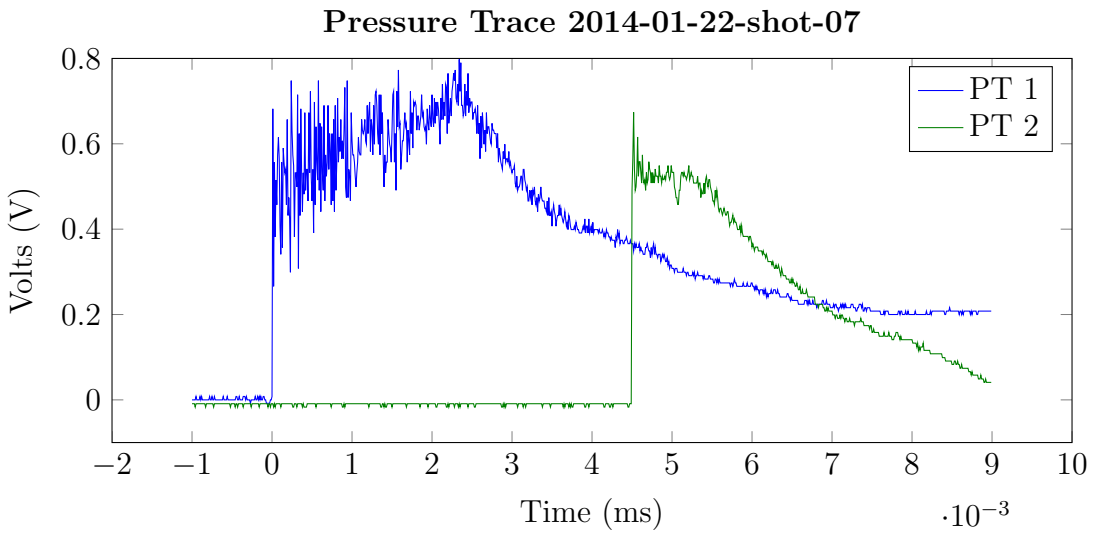


Figure 3.3: Excellent pressure trace, 2014-01-22-shot-07

variation in the actual Mach number as well as the uncertainty in the measurement of this value. This has allowed us to decrease the number of shots taken at a specific Mach number and delay timing.

## 3.3 Focal Plane Variation

### 3.3.1 Laser Plane Alignment

To obtain a high quality image several factors must be satisfied:

- Camera focused at the correct location
- Laser sheet properly formed, focused and aligned to the same plane
- A high quality lens with low f-stop is used
- Low background noise is in the image

The criticality of each of these items was brought to our attention when a new Nikkor 1.2 f-stop lens was purchased for the lab. The previous lens had significantly higher f-stop, and it was focused on a target that was made of an aluminum block with a piece of engineering paper (for the grid) taped to the top face. This target was positioned in the test section under the camera center by sliding it down the driven section while attached to a tape measure. Target images were captured using ambient light and the camera position and focus was adjusted to optimize the image. The laser was then focused and adjusted to shoot the laser sheet right over this same target.

This method had several shortcomings:

- The target did not always sit exactly where it was needed (especially for vertical shots)
- The paper did not sit perfectly flat on the surface of the target
- The texture of the paper provided a 3D surface, so focusing on a plane was difficult
- Adjusting the laser plane was very difficult and time consuming

The target used was a fairly short aluminum block. It was approximately 3.0" x 2.75" x 1.5". With the tape measure attached to the back of it, the tape would often pull the leading edge of the block up slightly, throwing off the plane of the target. The paper on the target did not sit perfectly flat no matter how much care was taken with applying the paper, so we never had a true 2D plane to focuse on. In addition, because the texture of the paper was as thick as the laser sheet we were producing, it was very difficult to know were the exact focal point was when aligning the laser.

We had been able to successfully work with this target for quite some time. When the new lens was brought in, it had a much narrower focal plane, and consequently, needed to be focused more precisely. The solution to this problem was to build an

improved target. The first improved target was machined out of aluminum like the first target, but it had a 1cm x 1cm grid engraved in the surface of the target, so no paper was required for this target. The engraved lines were then blacked out with paint to maximize the contrast of the markings.

This target was very useful, but it was decided that additional improvements could be made. The Rev 3 target differed from the Rev 2 target in that it was nearly 7" long. This additional length was added to prevent the target from tilting up under the weight of the taper measure. In addition, testing had shown that a grid of identical 1cm x 1cm boxes makes it very hard to locate the physical center of the image relative to the target. To resolve this issue, labels were engraved into each block face. This allows instant identification of which block a person is looking at in the image. Figure 3.4 shows the Rev 3 target.

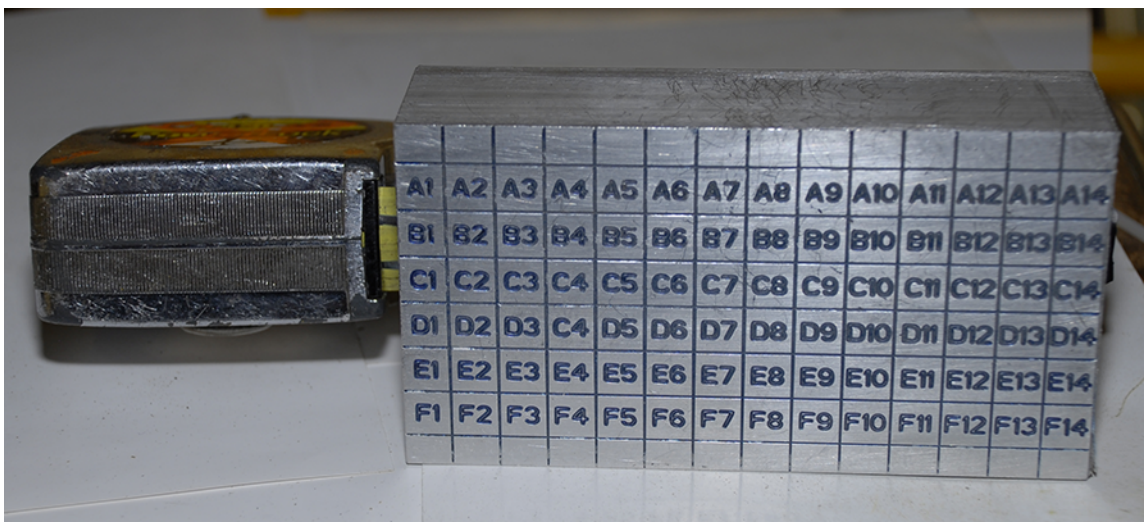


Figure 3.4: Focal target and tape measure

To improve the positioning issues, it was decided that strong rare earth magnets could be used to hold the target in position. The whole of the shock tube is non magnetic aluminum and polycarbonate, so rare earth magnets were embedded in the back of the new target as shown in Figure 3.5.

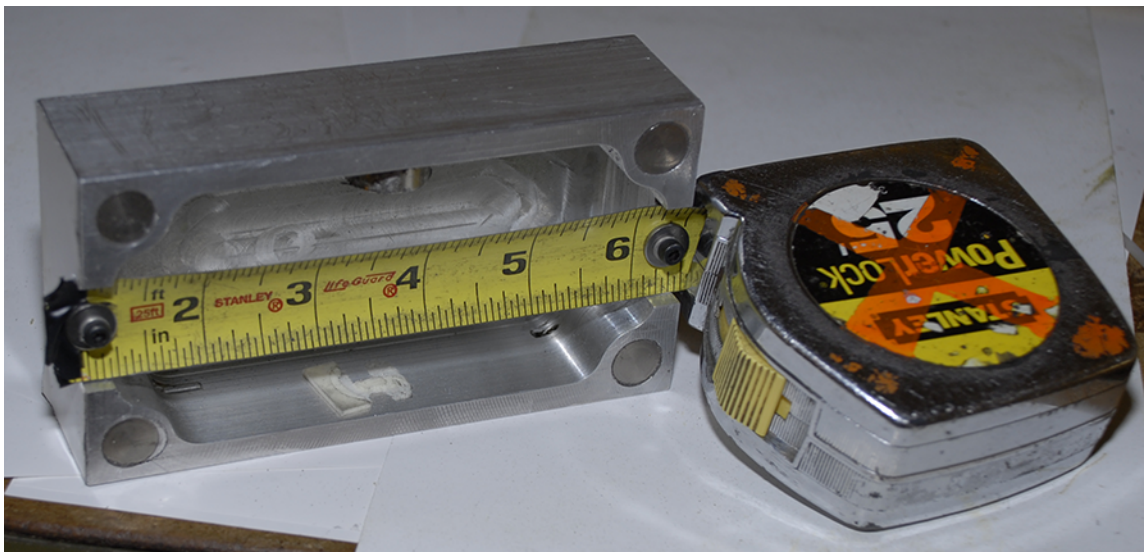


Figure 3.5: Focal target and tape measure, back view

In Figure 3.5, you can clearly see the four rare earth magnets that are embedded in the target. Once the target is moved to the correct position, large rare earth magnets are put in position on the outside of the test section which attracts the rare earth magnets in the target and pulls the target firmly up against the test section and prevents it from moving while the alignment is completed.

In Figure 3.5 you can also clearly see the recess milled out of the block to lighten it. The new target is nearly 2 1/2 times longer than the original, but it has almost the same weight due to this recess.

Finally, the figure also clearly shows how the tape measure was attached to the target. Previously, the tape measure was actually attached to the target with double sided foam tape. Needless to say, this wasn't optimal as it had to be reattached from time to time and it was a messy job removing all the residue of the old foam tape. The screws that attached the tape to the current target do not have to be replace as it does not come off. When the tape measure needs to be removed, it only takes seconds to remove the screws and remove the tape measure.

### 3.3.2 Laser Plane Alignment

With this new target, we now had a planar target of sufficient quality that we could accurately focus the camera. It also provided a great reference surface to focus and adjust the laser sheet as well. Unfortunately, the method used to make those adjustments presented problems as well.

Originally the laser was mounted on a tripod. The optics for that laser were mounted on a 3/8" diameter steel rod that projected from the bottom of the laser housing and pointed in the same direction as the laser beam. The lenses were mounted to the rod with mounts that used thumb screws to clamp the mounts in place.

Unfortunately, it was almost impossible to adjust a lens without tweaking the alignment of the laser as all the lenses were mounted to the laser. In addition, small, careful adjustments were usually needed, and it was impossible to make a small adjustment with the loosen-move-tighten method required by this mounting system. Aligning the laser often became a back and forth battle between focusing and shaping the beam and positioning the beam on the target.

Because of the difficulty, laser alignment was only done when absolutely necessary and it usually took half a day to perform to everyone's satisfaction. Even then, while the alignment might have been satisfactory, it was almost never truly excellent. And the loss of time performing this alignment was significant. With the narrower focal plane of the new lens, alignment became more critical and alignments were performed more and more often with the loss of time growing with each alignment.

Eventually, this came to a head. One of the RAs had previously taken a laser class and had used proper optical mounts in the class. While organizing the shock tube lab, we found a small selection of optical mounts and optical rails. This kicked

off a cleaning/digging session that uncovered many more mounts and rails. Most of them were incorporated in old pieces of equipment that had not been used in decades. These provided the raw material for the improved optical system for the acceptable price of free.

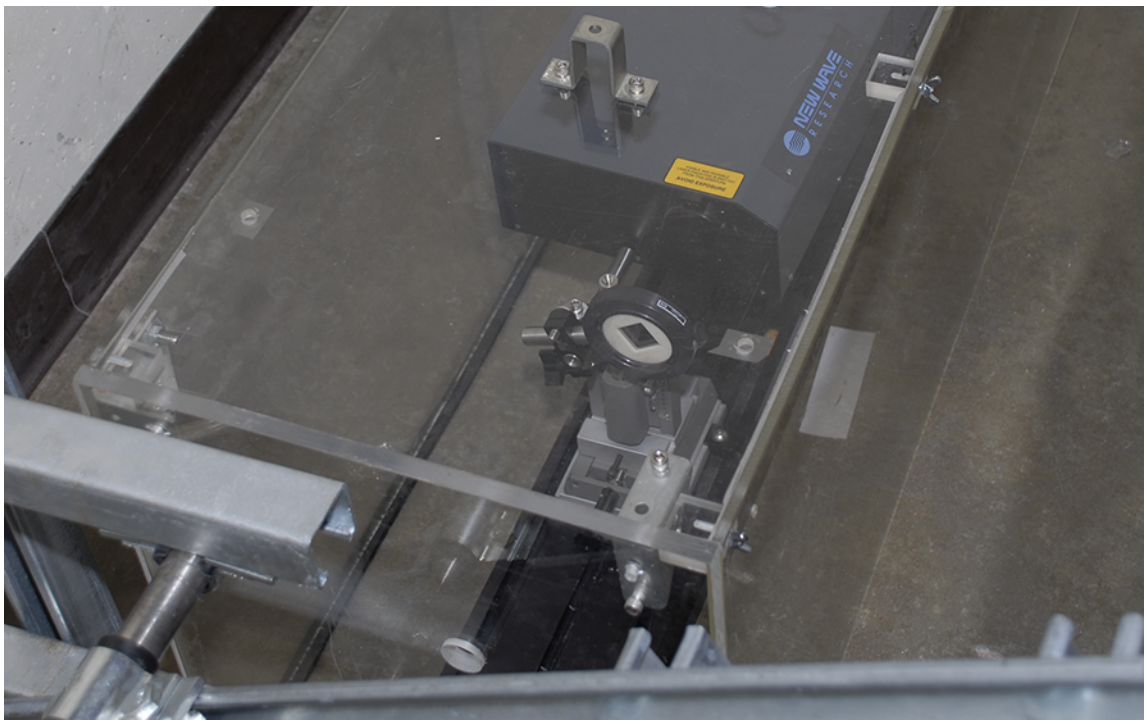


Figure 3.6: Optics on rail

Figure 3.6 shows one lens on its adjustable mount, attached to the black rail sitting in front of the output of the laser. This mount allows the lens to be adjusted in all three axes with micrometer adjusters. You no longer have to loosen the mount and then try to hold the lens in the correct position while you carefully tighten down the mount. The isolation of the each axis was especially welcome to this new system.

Like before, several lens can be mounted on the rail and independently adjusted in each axis as well. Due to strength and mass of the rail, neither the other optical components nor the rail's alignment to the laser are disturbed while making an

adjustment to a lens. For the inclined shots being conducted when this image was taken, the optics rail was set directly on the ground while the laser was attached to the rail with a scissor jack that allowed the height of the laser to be precisely adjusted as required and it prevents it from moving due to being jostled by shock waves or RAs.

The greatly increased precision of the optical system not only sped up the alignment procedure, but allowed a new, improved alignment system to be implemented as well. Originally, just getting the laser sheet formed, focused, and positioned at one edge of the target was extremely difficult. The optical rail and mounts reduced that from a half day chore, to a 15 to 30 minute procedure that could be quickly performed any time there was a question on the alignment. In addition, the greatly increased support of the optical system also meant the alignment stayed true much longer.

With this ease of alignment came the ability to fine-tune the alignment procedure by going to a two point alignment. Where before, the alignment consisted of just getting the laser plane aligned on the leading edge of the target at its current position and was difficult and involved, the two point procedure involved moving the target to the far front and rear of the test section for alignment. Because we are now aligning at both locations, this forces us to get the laser sheet in the exact center of the test section. As you move the camera downstream to capture later time images, the laser plane is not shifting relative to the image plane of the camera so the images captured remain sharply in focus.

One other item is clearly visible in Figure 3.6 that should also be discussed. The shock exits the shock tube just to the left of and below the image of Figure 3.6. This shock wave then bounces off the concrete wall just visible in the figure and then reflects back. This reflected shock wave has significant energy and impacts both the optical components and the laser itself. To help prevent the alignment from shifting

and to protect the sensitive internals components of the laser, a clear polycarbonate housing was placed over the laser assembly. A small hole just visible in the bottom center of the image allows the laser sheet to to exit the housing with no impedance. This housing also has the added benefit of keeping dust and debris off the laser system and protects it from assorted impacts from falling tools or other items.

### 3.3.3 Camera Mirror Mount

For the horizontal slice images, the laser sheet is horizontal in the tunnel and "cuts" an initially circular slice of the IC column. To image this, the camera must be looking straight down the test section. A mirror is used to reflect the image produced from the vertical direction to the horizontal direction so the camera can sit off to the side of the test section and capture the image. Figure 3.7 is a picture of the original mirror mount system.

To use this mount, the two upper rear flange bolts at both ends of the test section are removed and a threaded rod is run the length of the test section and goes through the holes in the mirror mount. When the nuts are tightened on the rod, the tension in the rod pulls the mirror mount down and secures it in position.

While this system worked fairly well, it was not possible to fine-tune the angle of the mirror to accurately position the image on the camera. Instead, the camera often would need to be moved to position the image. This was not optimal. In addition, as the shot delay is increased, the camera (and mirror) had to be moved downstream to keep the IC in the frame during the shot. This led to changes in the relative zoom factor and angle for nearly every other timing set due to inaccuracies in realigning the mirror when it was moved.

To address this issue, a new mounting system was designed that included a rail running behind the test section that allowed a mount to slide along it to reposition

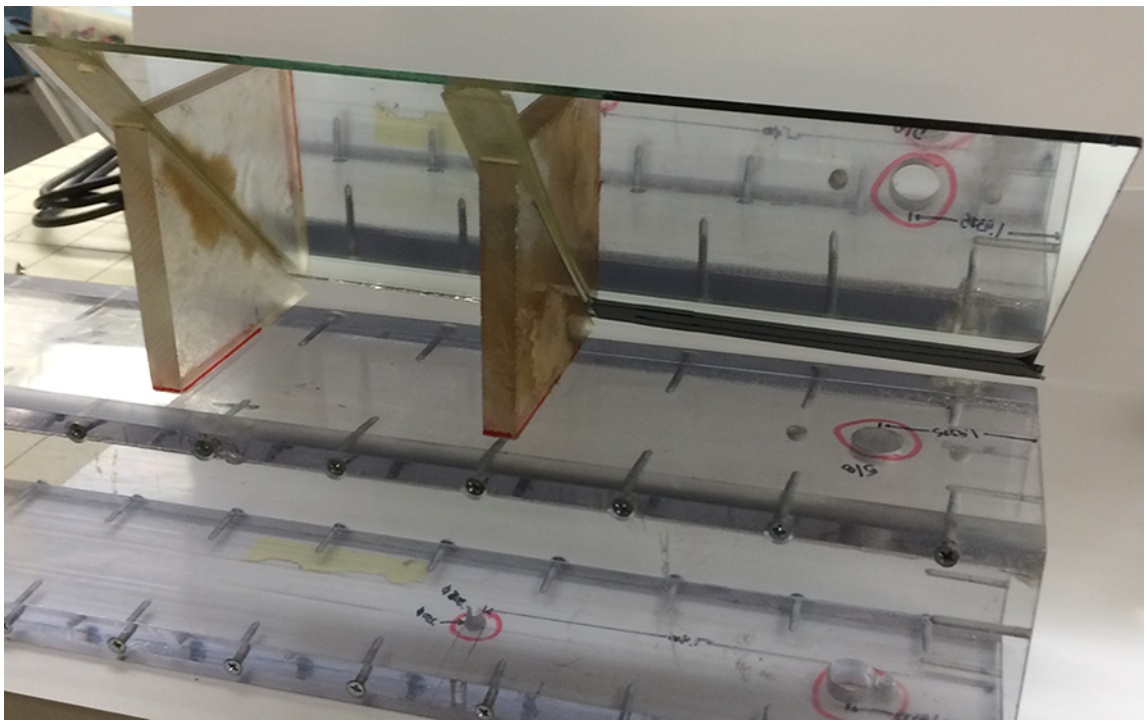

Figure 3.7: Original camera mirror mount

the mirror. The mount incorporated a 2-axis micro adjustable optical mount that the mirror attached to as shown in Figure 3.8

In this image, the camera is on the far right side with only the lens visible and is mounted below the mirror as it is set to capture a vertical plane image through the side of the test section. The mirror mount and mirror is seen in the upper center of the figure, right above the target in the test section. The aluminum rail is seen going off to the bottom left of the figure. Figure 3.9 is a close up of the mount itself.

You can clearly see the adjuster knob that adjusts the mirror in the x-axis. There is another knob behind the mirror that allows the same adjustment to the y-axis. Behind the black adjuster mount, you can also see the nut on the stud. This stud is a T-bolt that runs in the channel on the rail. To reposition the mirror mount, this nut is loosened and the entire mount is slid down the rail to it's new position. The

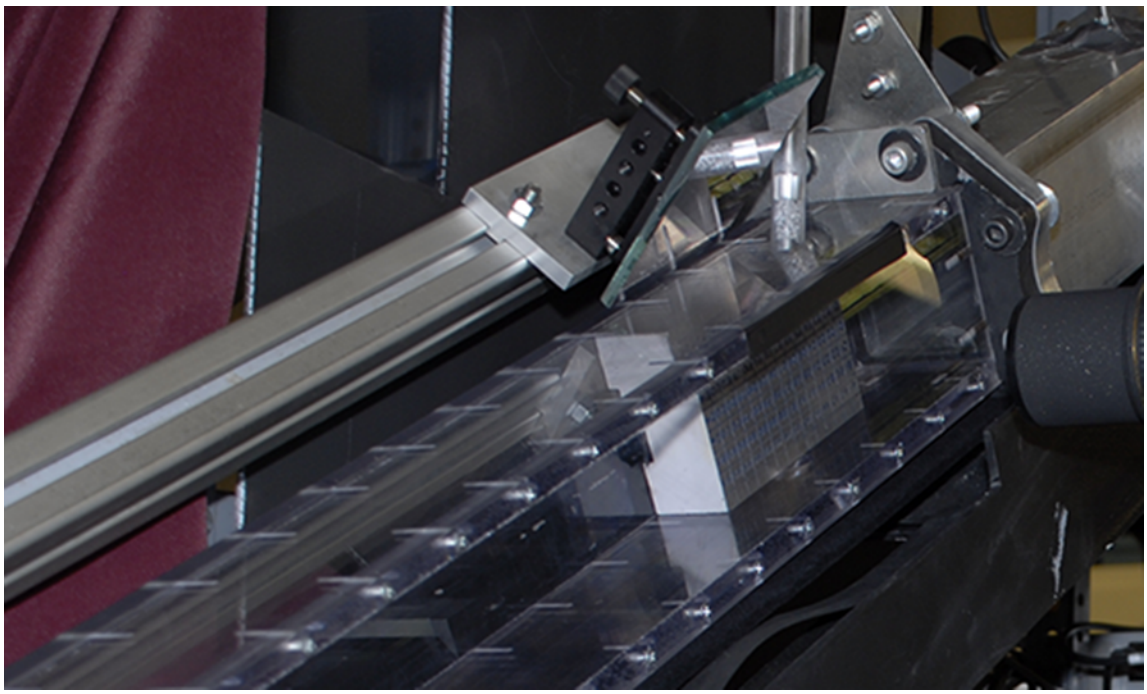

Figure 3.8: New camera mirror mount and rail

mirror mount has a machined key (visible below the nut) that rides in the channel opening and keys mount to the rail so it cannot rotate when it is moved.

Operational experience has shown that the mirror can be repositioned anywhere down the rail and it will generally require no changes to its alignment. The time required to reposition the mirror has gone from several minutes to only a few seconds. And the alignment remains almost perfect after repositioning.

### 3.3.4 Camera Mounting Rail

The camera was originally mounted on a heavy tripod that was set next to the shock tube in the correct position. This mounting system allowed for a great deal of flexibility in positioning the camera, but it also added a great deal of difficulties in positioning it as well. Specifically, to maintain the same scaling of images for each

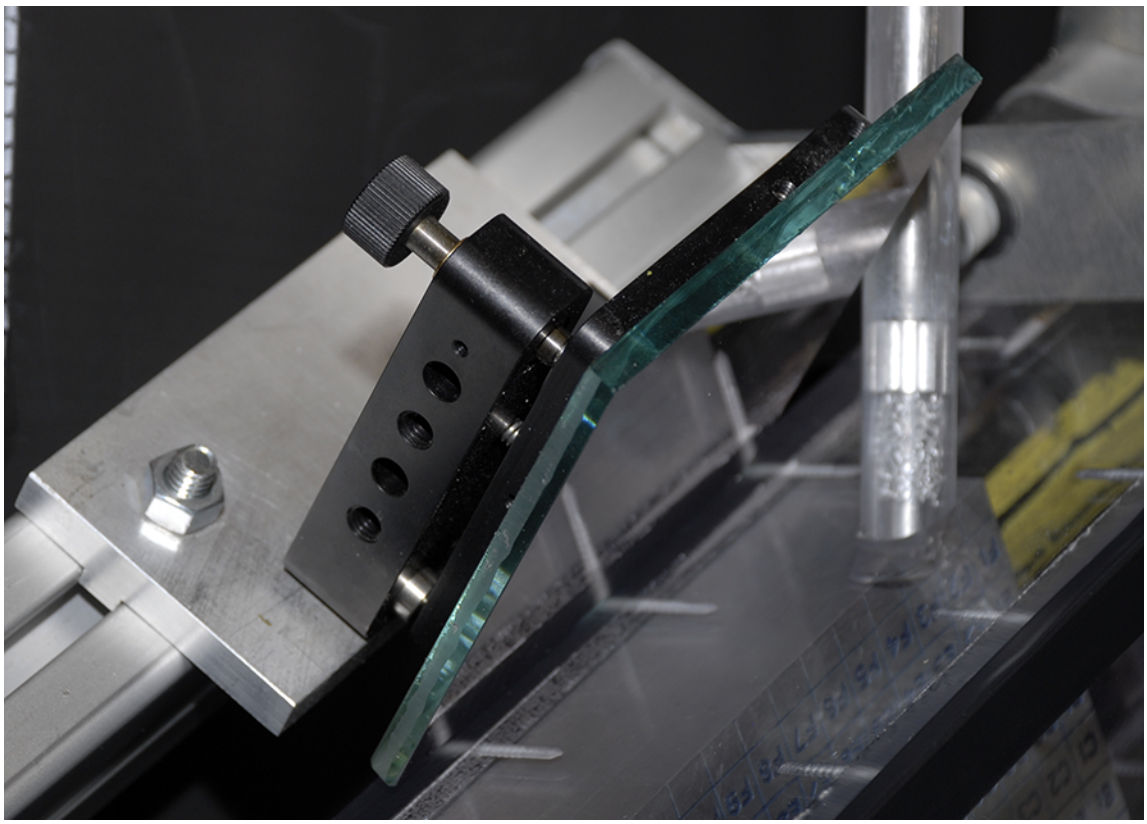

Figure 3.9: Close up of adjustable mirror mount

timing set of a given experiment, it is necessary to keep the lens a fixed distance from the shock tube. The orientation of the camera must also be maintained parallel to the shock tube. Needless to say, getting the distance and orientation set to less than 1mm after moving the whole tripod could be time consuming and generally not as accurate as we would prefer.

In addition to the general alignment issues, the tripod itself was a problem. Much of the work is done right around the camera during a shot and most of that work is done with the lab blacked out except for a few hand held LED lights. Needless to say, more than once a stream of curse words were released by an RA who had accidentally kicked one of the legs of the tripod while trying to get the ICs straightened out... A better system was needed. This came to a head after the current short tripod

basically wore out due to the beating it was taking from the repeated reflected shock waves.

With the current tripod no longer able to accurately and repeatedly hold the camera in the correct position, a new camera mount was designed that basically used the tripod head of one of our very heavy duty tripods (that was too tall to be used for inclined shots) along with a custom base mount and a heavy duty optical rail to attach the camera. Figure 3.10 shows the final result.

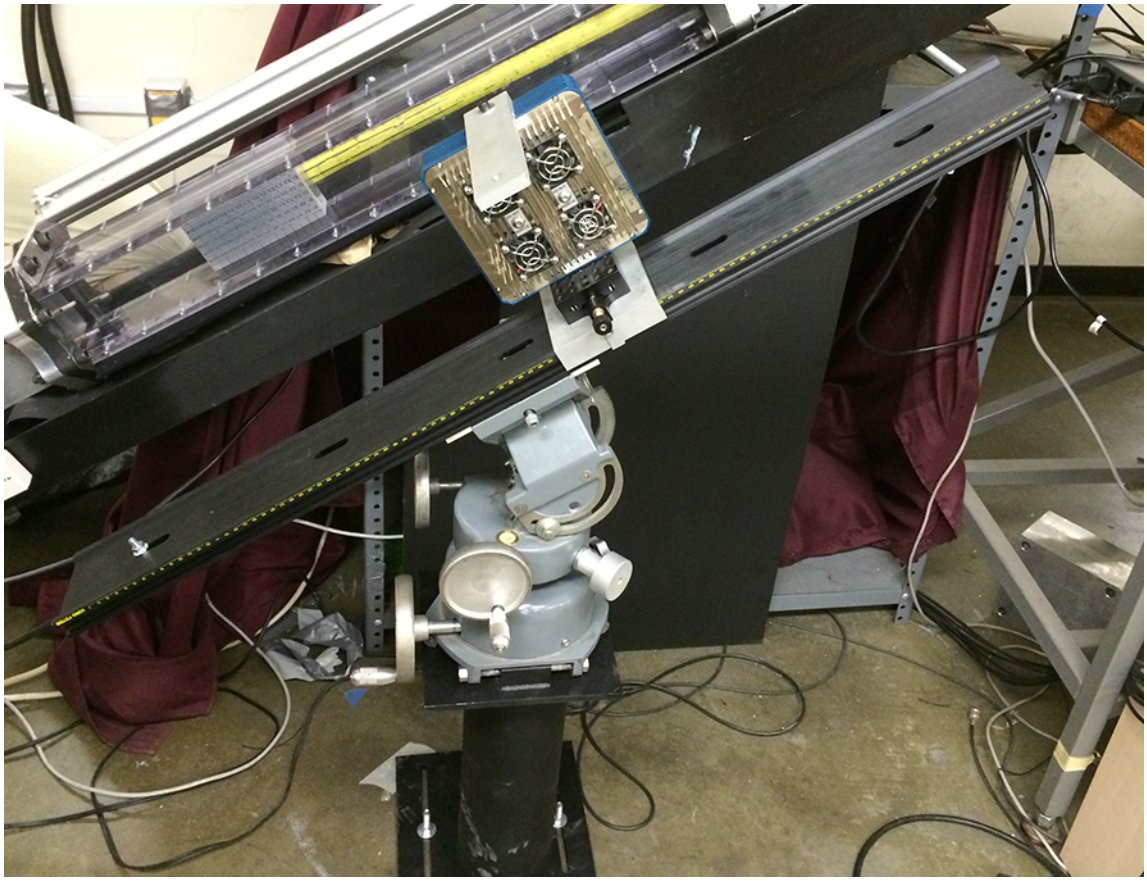

Figure 3.10: New camera mounting system

A new steel mounting stand was built that holds the tripod head and its elevation adjustment system. This base is bolted to the concrete floor to prevent it from moving

with the occasional kick. While the stream of curse words might still be released, at least it won't be from the camera being moved!

On top of the tripod, a heavy optical mount was attached. The camera is mounted on a 2-axis mounting block that allows the camera to slide along the rail but it does not allow the camera to rotate. It has a micrometer adjustment to fine tune the distance the camera is from the shock tube. This rail also has a built in cm scale that allows for precise adjustment of the camera in the shock tubes x-axis.

To use this new mount, the angle of the rail is adjusted using the tripod head until it exactly matches the angle of the shock tube. The base is then shifted in or out to position the distance between the lens and the shocktube to the desired location for the experiment being undertaken. The rail is then squared up to the shock tube so the camera will not change distance as it is moved up stream and downstream along the x-axis. All the bolts are then tightened and the alignment is verified.

The camera is then slid to its initial starting position and the 1-axis mount is then locked down. The distance the camera is from the shock tube is then fine tuned with the micrometer adjuster on the camera mount. Figure 3.11 better illustrates the relationship between the camera mount and the rail.

This new camera mount, in conjunction with the new mirror mount, allows for new shot timings to be taken with only a very minimal delay between shots as the mirror and camera are repositioned. In addition, the scale, angle and focus of the repositioned shots nearly perfectly matches the previous position with almost no work by the RAs. Previously, this could be hit or miss and always took a significant amount of time to realign everything after moving the camera and mirror. The precision of the current system enables better focal plane adjustments and taken together, allows us to resolve finer details in the images.

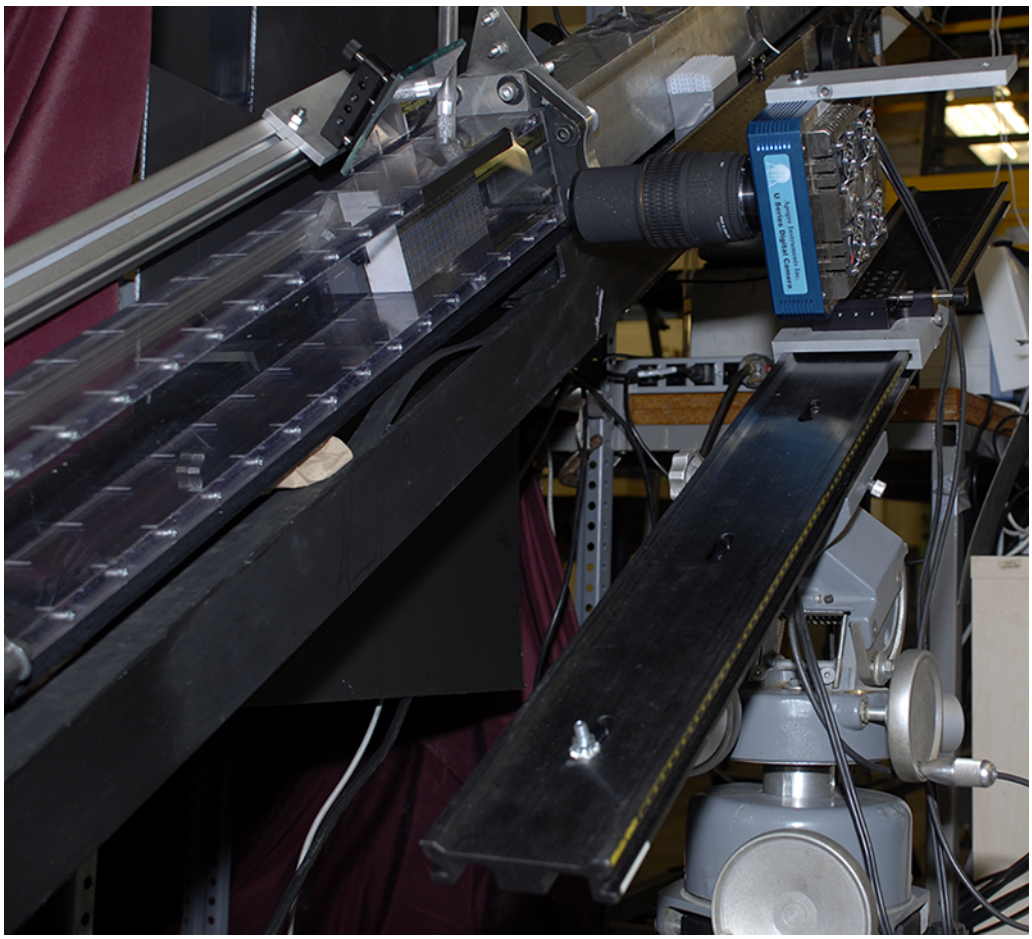

Figure 3.11: New camera mounting system from front

### 3.3.5 First Surface Mirror

One upgrade that had a dual effect on both the qualitative and quantitative improvements was upgrading from standard, "off the shelf" rear surface mirrors to using more expensive, but still reasonable "low cost" first surface mirrors.

The standard mirror we had been using was what was known as a rear surface mirror. This is the same type of mirror you see every morning when you are brushing your teeth. It gets its name from the fact that the silver reflective surface is actually

applied to the back of the mirror. The light then has to pass through the glass on the front before being reflected back out through the glass once more before it continues on its way. The reason this is the default mirror configuration one sees in day to day life is that glass provides excellent scratch protection to the incredibly thin silver coating on the back.

For our use, this actually had two negatives associated with it. First, the light reflects off the glass multiple times while passing through it, reducing the optical clarity of our image. Figure 3.12 shows how light will reflect off the glass multiple times while passing through it.

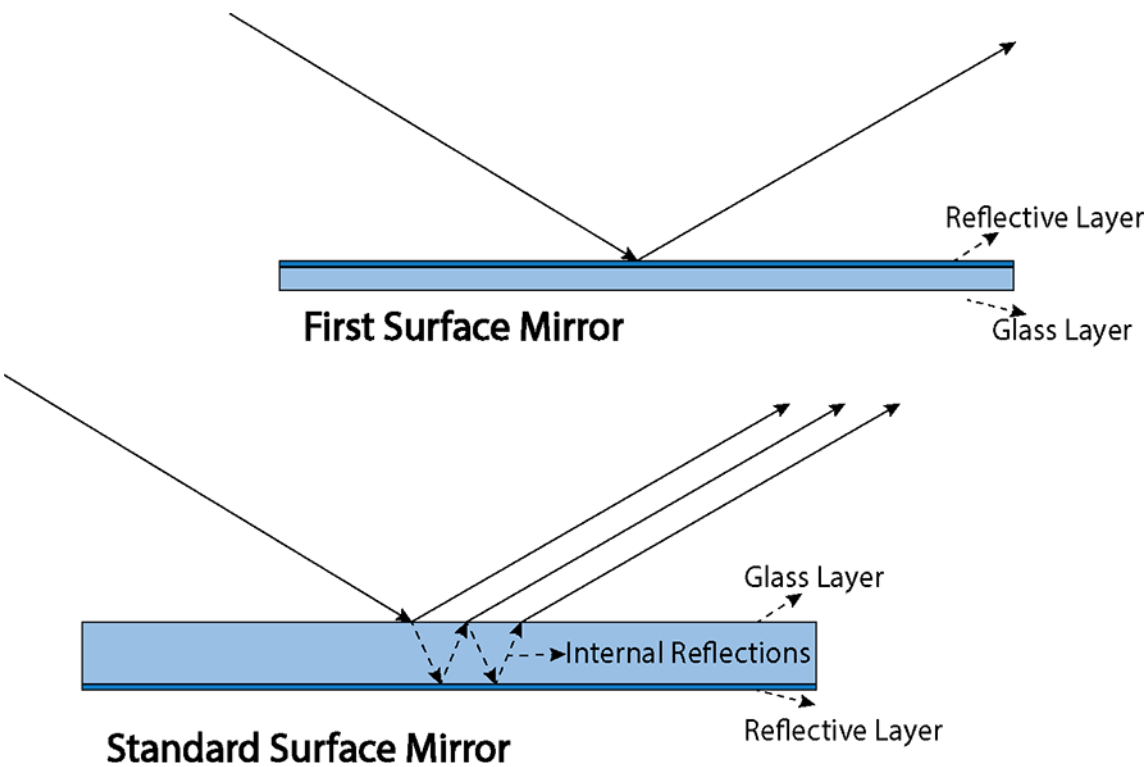


Figure 3.12: Light reflecting off first and rear surface mirrors

Needless to say, these multiple reflections reduce the image quality captured at the camera. As we are attempting to image smaller and smaller and dimmer and

dimmer features, these reflections impact our ability to move forward in the science.

The second issue was actually the trigger to investigate low cost first surface mirrors: The glass at the surface of the mirror was being heated by the laser pulse. This was causing the silver to be vaporized from the mirror. On one experiment that required high power in a narrow beam, the mirror was only good for a few shots before it had to be relocated because there was no longer any reflective material left in that spot and we could no longer capture any data with it.

The first surface mirrors addressed both of these issues. As can be seen in Figure 3.12, with the reflective coating on the top of the mirror, the laser beam can reflect off the mirror with minimal additional reflections. This increases the sharpness of the image when the mirror is used to turn the light to the camera as well as when the mirror is used to turn the laser sheet due to a sharper focal plane of the laser sheet.

When used to turn a high power laser sheet, the first surface mirror also proved to be much better than the rear surface mirror. With the reflective surface on the outside face of the mirror, the energy of the laser beam is more efficiently reflected and dissipated into the air, reducing the energy absorbed by the mirror and subsequent damage to it. In addition, with the mirror mounting system described above, small side to side adjustments could be easily made to move the mirror to provide a "fresh surface" when the laser did burn through the mirror.

## 3.4 Laser Trigger Accuracy

### 3.4.1 Precise Laser Gate Pulse

An additional limitation in our original setup was found while conducting particle image velocimetry (PIV) experiments. For this experiment, extremely sparse glycerin droplets were placed in the shock tube. When the shock tube was fired, the shock wave accelerated the droplets to an unknown velocity. Multiple laser pulses (up to four) were then used to illuminate the particles in a single image, as shown in Figure 3.13 below.

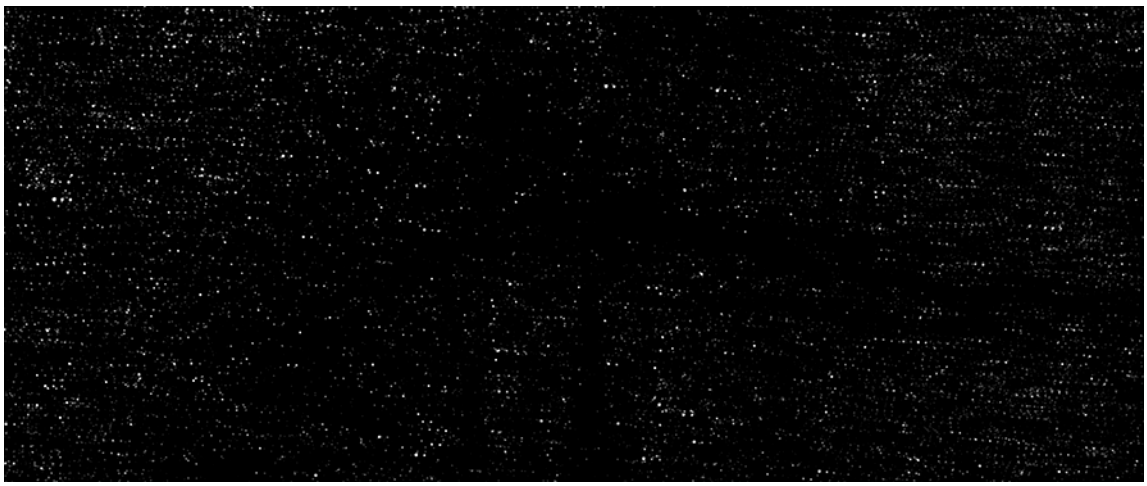

Figure 3.13: PIV triplets, 4-Sept-2013-shot30-subtracted

With this image, only three laser pulses are used and they are spaced $100\mu s$ apart. You can clearly see the distance each particle moved between pulses.

The problem came when we tried to interrogate these images. The velocity varied way too much between pulses and the data could not be trusted. After considering the issue, we decided to investigate how accurate the internal timer was on the laser. Normally, the laser is fired with a single trigger pulse that activates the flash lamp.

The internal timer then waits $180\mu s$ before it triggers the gate which allows the pulse to leave the laser head. It also has an output for both the lamp and gate pulses, so it is possible to measure the time delay directly.

When we connected an oscilloscope to these outputs on each of the lasers, what we found was not encouraging. While each laser appeared to be fairly stable in its timing, the variation laser to laser was over $7\mu s$. We needed to bring the timing uncertainty down to no more than $500ns$ to achieve the level of accuracy we required for PIV.

With the delay generators we had, we could not achieve the necessary delays and accuracy on all eight channels simultaneously. With the aging of the delay generators and their inability it accurately work with the current experiment, we received permission (and funds) to purchase a new, eight channel delay generator, a BNC Model 575. This model allowed us to control the on time and off time of each channel independently with a precision of $250ps$ on both the delay and duration of each pulse.


Figure 3.14: BNC 575 delay generator

Figure 3.14 shows the new delay generator in action, using four of its eight out-

put channels for this experiment. Also in this image, you can see the black heavy paper light shield for the face of this piece of equipment that is used for image noise reduction discussed in later sections.

## 3.5 Initial Conditions Issues

### 3.5.1 Flow Rate Consistency

Producing the IC gas column has often proven difficult. Originally, the gas ($SF_6$ and air, $SF_6$ and glycerin droplets, $SF_6$ and acetone vapor, etc) was injected into a 20 gallon glass aquarium where it was allowed to cool. When the tank was sufficiently full, a valve in the IC system was opened and the gas was allowed to flow out the bottom of the tank via a bulkhead fitting ($SF_6$ is nearly 5 times denser than air) via gravity where it flowed through a 1/4" OD plastic tube, through the ball value and into the injector. The injector was a 1/4" diameter steel tube held inside a plastic outer tube. Coflow air was allowed to flow down between the plastic outer tube and the steel inner tube to stabilize and support the IC column as it entered the test section and then fell smoothly through it and out a small hole in the bottom of the test section.

When things worked as planned, the column would fall perfectly smooth with only a very gradual increase in diameter at the bottom due to diffusion. It would maintain its circular cross section for the whole duration of its time in the test section. This slow, laminar flow would prevent additional fluctuations from being introduced in the ICs before the shock wave arrived.

Unfortunately, things did not always go according to plan. Occasionally, a "tail" would develop in the ICs that left a feature that looked like a flag coming off the

column that got worse and worse as it traveled down in the test section. When this happened, usually, a good cleaning of entire injection system would get things back to normal. But not always. Also, the glycerin tended to condense on the inside of the cool metal tubing. Eventually, it could build up a large enough bubble of glycerin that it would entirely block the flow of the ICs. Cleaning was also the prescribed cure for this issue.

Occasionally, the ICs would "misbehave" and no amount of work would seem to correct the problem. Sometimes, the only solution was to go to lunch and hope things were back to normal when you came back! And occasionally, calling it a day was the only solution. While it may not have solved the root cause of the IC problem, it did usually help prevent RAs from throwing objects at each other!

When you started to get distorted images, you could occasionally get distorted images such as Figure 3.15 below! While this image has little scientific value, it DID provide a bit of much needed levity at just the right time.

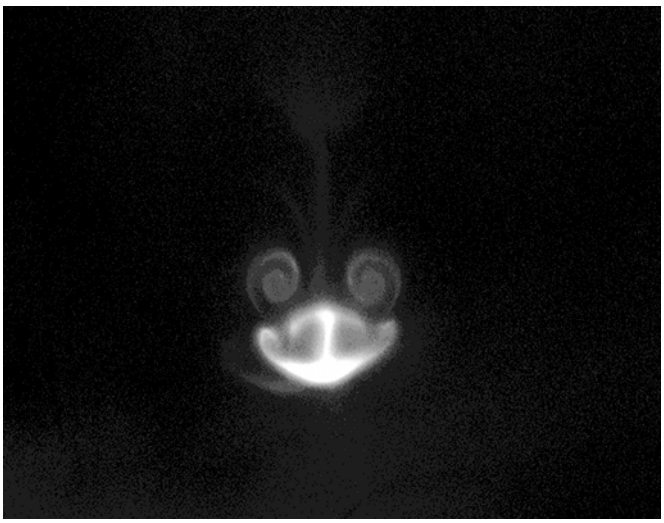

Figure 3.15: Our lab mascot: the gecko. This flow pattern likely developed from irregular initial conditions.

Needless to say, this was not a satisfactory method for solving a research problem.

While we did not know the true root cause of the strange ICs, we did know that it was causing additional rotation and other velocities inside the IC column other than the pure -y laminar velocity we needed.

The initial plan was to enlarge the upstream hose size that connected the tank to the IC injector. We knew that the larger 3/8" ID hose would reduce the incidents of plugging due to glycerin droplet build-ups and we felt the reduced flow rate in this section of the injector system would give the unwanted velocities more time to settle out due to friction.

This was a very simple change and it did improve the IC performance some, it still did not address the occasional hard to correct IC distortion we had been seeing. The next step was to straighten the flow out.

### 3.5.2 Noncircular ICs

After adding the larger inlet tube and seeing its results, we designed a flow straightener that was placed right above the injection tube. The flow straightener was a simple apparatus that first expanded the flow from 1/4" out to 1.25" using a short divergent-convergent nozzle. Right after the expansion, which greatly slowed the gas, a short piece of aluminum foam was placed. This foam broke up all the larger scale motions into much smaller scale motions that then dissipated due to friction as the gas slowly dropped down the flow straightener due to gravity.

At the bottom of the flow straightener, the flow was smoothly accelerated and brought back to a 1/4" diameter to enter the steel tube via a convergent-divergent nozzle. A great deal of effort went into making sure the transition from the flow straightener to the injector tube was as smooth as possible to prevent any new eddies from forming in the IC column.

This flow straightener proved very successful in reducing the occurrence of and the severity of IC disruptions. There are still occasional issues that are usually resolved with a good cleaning. We have not had any occasions where we were not able to resolve any IC issues and continue on with the day's work.

### 3.5.3 IC Injector Alignment

With all the work to improve the IC injection system, the old method of using the aquarium to hold the IC system in alignment with the shock tube was no longer feasible. Nor was it ever perfect. With this method, the alignment was literally controlled by shifting the aquarium on the stand until the flexible tubing between the tank and the IC valve would hold the IC injector in the correct alignment to the shock tube. A careless bump of the stand the tank was on would require a bit of time to realign things.

The flow straightener made that system impractical at best, impossible at worse. Basically, it just added too much height to the injector assembly. In addition, the old method would never very be good at precise alignments and the stand was quite wobbly at time. Figure 3.16 is the solution we developed to resolve this issue.

A bracket was fabricated that mounted a 2-axis optical mount (these have proven very multipurpose!) in the horizontal position next to the IC injector. Another simple bracket was fabricated that was attached to the 2-axis mount and then to the top of the flow straightener.

Looking closely, one can see the duct tape and wire currently used to keep the two sections of the flow straightener together. When time allows and the need pushes for it, a better, more professional closure system will be made for the flow straightener.

In this image, you can also see the IC control valve at the top of the flow straight-

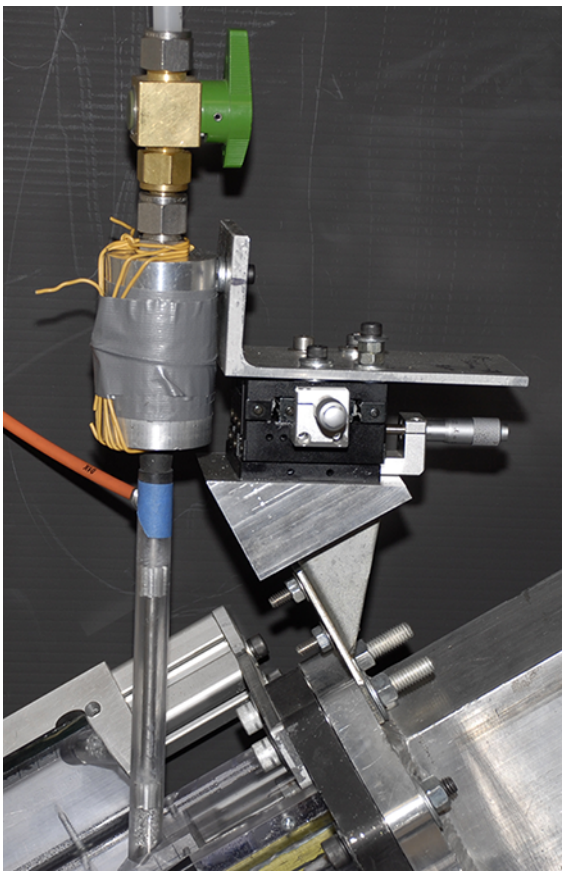

Figure 3.16: New IC Injector system

ener with its 3/8" tube coming in. The bottom of the flow straightener is attached to the IC injector itself. The orange hose going off to the left of the image is where the coflow air is injected. At the very bottom of the image, you can just see where the IC injector is plugged into the opening on the top of the test section.

Using this system is almost trivial. Once the IC injector is assembled and the ICs are flowing, preferably with glycerin fog so it is visible in standard light, the position of the top of the flow straightener is adjusted in the x-z plane using the two micrometer adjustments until the gas column exits the bottom of the test section in the center of the exit hole.

Once adjusted, the rigid adjustment system keeps the IC injector in the proper alignment even when getting nudged about by RAs opening and closing the IC valve. It is also able to withstand the slightly less gentle nudges from the reflected shock wave which can get fairly substantial at Mach 2.0 and higher.

## 3.6 Noise in the Images

To capture any detail in the very fast moving IC column when it gets illuminated by a $4ns$ long laser pulse, the camera system must meet a few criteria:

- Sufficient resolution
- Sufficient light gathering power
- Quality optical components

The camera we currently use meets the first two criteria. It was shown in Figure 3.11 mounted on the camera rail system. The camera is an Apogee U42 2048x2048 high performance cooled CCD camera. its peak quantum efficiency is greater than 90%. The 4 megapixel CCD sensor is more than enough for our current work, and its greater than 90% quantum efficiency means nearly every single photon is captured. The final piece of the puzzle was added when the 1.2 f-stop Nikkor lens was acquired in 2012. This lens had the light gathering power we needed along with an excellent and narrow focal plane.

But, like most things, these high performing optical systems do have their disadvantages. Namely, they capture a significant amount of optical noise as well as the desired image. We took a couple of different approaches to decrease this image noise.

### 3.6.1 Laser Reflection Reduction

When the laser is fired, the pulse is very high power and very short duration ($4ns$). This pulse is spread out into a sheet that is effectively triangular in shape, with it expanding out continuously from the cylindrical lens in the light path. When the sheet hits the side of the aluminum expansion section, the laser is refracted in many different directions and causes additional random light to hit the camera, creating additional noise in the image.

Most of this issue was indirectly resolved with the changes to the laser optical mounting system described earlier. The final resolution came from making simple changes to how we shaped the sheet. Originally, controlling the sheet with accuracy was made very difficult by the course adjustments we had for the optical system. With the micrometer controls we now had, it was very simple to accurately control not only the shape and location of the laser sheet, but the size as well.

The effect of this was that we could keep the laser sheet narrowed down so that it could not expand out to the walls of the shock tube until it was well past the test section. Any reflections produced reflected up the driven section to the driver section where they were attenuated before they could make their way back to the camera system. This resulted in less laser light creating optical noise in the image, both the back ground image and the shot image.

### 3.6.2 Maximizing the Camera Efficiency

From the beginning, the work in the shock tube lab has been conducted in the dark with the lights off. When you first turn off all the lights, it appears pitch black and you literally couldn't see your hand in front of your face. However, as your eyes adjusted, in a few minutes, you would be able to conduct much of your work without

the use of any lighting devices.

The light in the lab was coming from many sources:

- From the small windows in the main door
- Computer monitors
- Illuminated interlock control
- Delay generator display
- Router LEDs
- Power supplies displays
- Assorted LED indicators on various equipment

While each light was not very bright (with the exception of the computer monitors) this extra light is very visible in our images and does mask finer details in the image.

Historically, a background was taken before each image and was subtracted from the dynamic shot to reduce the effects of this noise. This background shot was a simple shot taken once everything was set up for the actual shot. The lights were out, the camera was opened and the lasers were fired. All of this noise was captured in the background.

The problem with this is that while background subtraction can (and does) clean up the image overall by reducing the repeatable light pollution, it also removes image data that occurs in the same location as the light pollution but was of less magnitude than the pollution. And there was no way to reduce the background light without also removing image data.

Once we realized that much of the image detail we wanted to see were occurring in the same intensity zone as the light pollution, we also realized that we had one tool at our disposal to correct this: reduce the background light pollution as much as possible. The beauty of this approach was that we could easily do this with materials

on hand (and free is ALWAYS the preferred cost!) and it didn't make any changes to the operation of the shock tube. Well, almost.

The various LED indicator lights were a fairly simple task to deal with: a small pieces of aluminum foil tape (the LEDs would bleed through even several layers of black electrical tape) were cut and placed over every single LED indicator in the lab. The power supplies and delay generators had black paper shields made that were taped to the top of the instrument and were simply dropped down over the face of the instrument after any adjustments were made. The interlock controls were addressed similarly, but the light block was taped over it permanently as we all knew which button enabled the interlock and which one disabled it without any need to look at it.

The computer monitors posed a slightly more complex problem. All of the image diagnostics as well as camera controls and pressure traces were displayed on the computer monitors. In addition, the camera was still being manually triggered by clicking a button in Maxim DL (the camera control software) during each shot, so they could not be simply turned off. Figure 3.17 shows the solution we came up with.

Heavy black paper was cut and folded to form a simple shield for each monitor. This shield was taped to the top edge of the monitor so it could be easily folded back to use the computer and then flipped forward during each shot to block all the light from the monitor. The monitor on the right displays Maxim DL, so we would need access to it during the shot. To allow this access while still blocking as much light as possible, a small slot was cut out of the shield directly over the software button we needed to click on.

Once the shot was ready, the mouse cursor was positioned over the button and all the shields were dropped in place. The camera was triggered and either the lasers

Figure 3.17: Covers for computer monitors

were triggered (for a background shot) or the shock tube was fired.

The windows in the main doors to the lab still needed to be addressed. This was done by simply cutting heavy pieces of paper to size and then taping them in the windows. This quick and easy method reduced the light coming in from the main doors by 99% or more.

Finally, a curtain system was devised that allowed us to wrap the test section and camera system in a heavy, dark maroon cloth to help absorb even more stray light. This cloth was actually part of one of the table cloths from the wedding dinner for one of our RAs... Never let it be said that we don't push our lab dollars to the limit!

With all these light pollution sources addressed, the amount of light pollution in our background images AND our shot images was dramatically reduced as shown in Figure 3.18.

This figure stands on its own. You can clearly see details inside the test section in the before image due to all the extra light that shouldn't be there. In the after image,

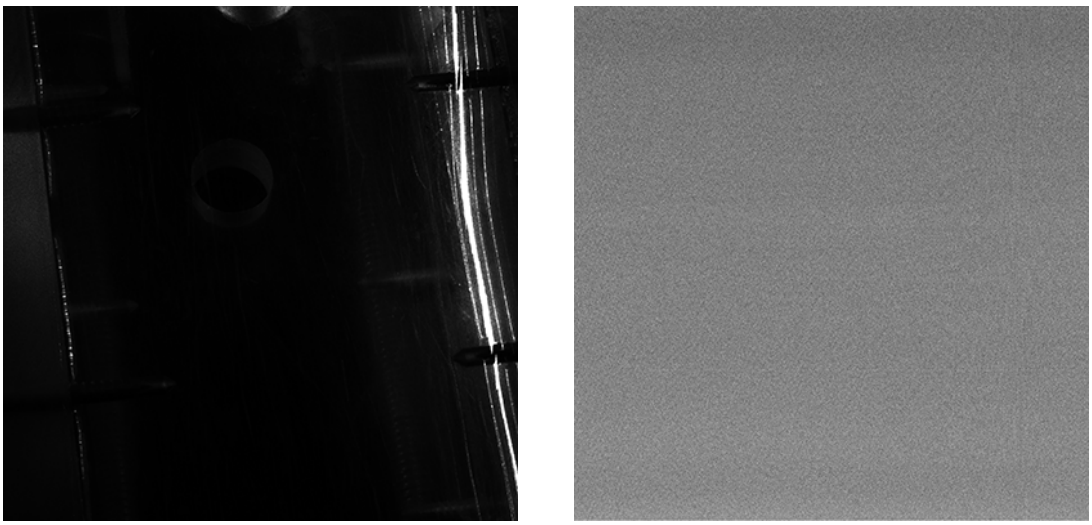

(a) Before: 2011-08-18-19-bg (b) After: 2014-02-24-shot-11-bg

Figure 3.18: Background images before and after upgrades

everything is just a gray blur as there is not enough light even for our camera system to pick up any real details. In fact, the noise appears almost Gaussian, showing that we are getting the light pollution down so low that the limitation of the noise floor of the CCD sensor itself is becoming the limiting factor.

Figure 3.19 is also very interesting.

If you look at the data displayed on each histogram, you will see that the mean for the after image is only $\frac{1}{4}$ the mean of the before image. Perhaps more important, an inspection of the maximum values for each histogram shows that the before image had at least one pixel that was fully saturated with a count of 65535 (16 bit images), even in the background image! In comparison, the max for the after image is only 2048, which is less than 50% higher than the minimum for the before image.

At this point, we feel that we have reduced the light pollution to a level that it is no longer a real concern in our images. The need to subtract backgrounds from the shot image is greatly reduced, though we are still collecting background images

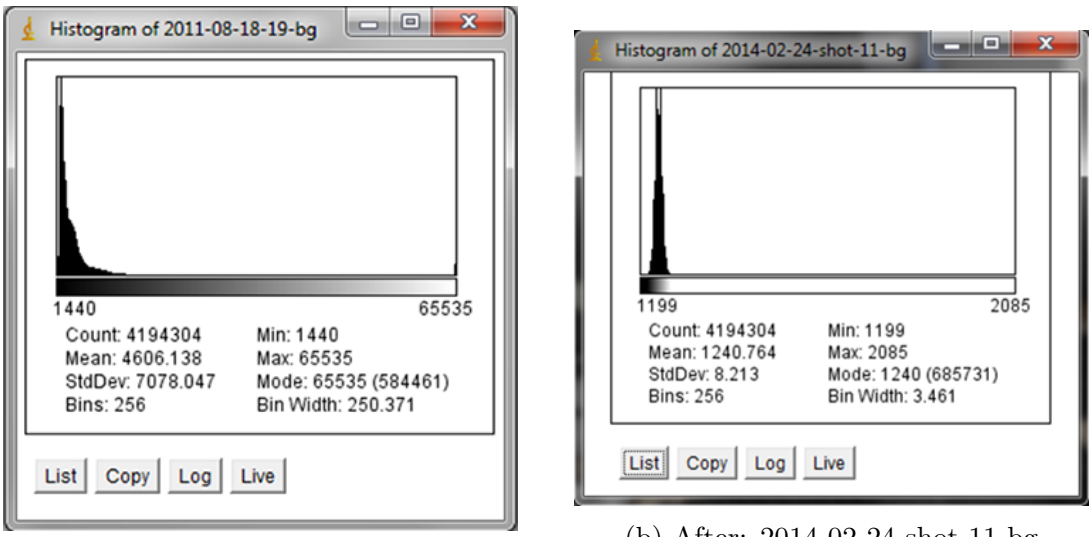


(a) Before: 2011-08-18-19-bg

(b) After: 2014-02-24-shot-11-bg

Figure 3.19: Image histograms before and after upgrades

to support any image processing needed in the future.

Like everything else we have done with this shock tube, there is one down side to these improvements: you can no longer work in the dark! It is simply too dark and even moving from place to place without a light is not really possible.

We resolved this slight hiccup by purchasing three low cost LED rechargeable flash lights. The operators each keep one with them and when we are not shooting, they are turned on and shined towards the ceiling to provide enough illumination for everyone to do there jobs. And they can be used for spot illumination if you really need to brighten things up to address a specific issue, or find a lost tool.

## 3.7 Burst Diaphragm Quality

The diaphragms originally used in the shock tube for most of the shots were 3M CG5000 transparency films. These were simply a type 1 polyester film that had

the right thickness so that a single sheet would hold up to the pressures of a Mach 1.7 shot while two sheets would support a Mach 2.0 shot. The diaphragm supply was expanded in 2010 by adding the CG6000 film, also from 3M, that was found to support Mach 2.0 shots with a single sheet due to their extra thickness versus the CG5000 films.

Both of these films were found by trial and error. Other films simply wouldn't work as they either couldn't support the pressure or they couldn't be fired by the original cutter system. There are three issues with the use of these films:

- They are expensive. Each shot cost $1 for diaphragms.
- The coatings on the films could contaminate the image
- They are in 8 1/2" x 11" sheets which does not fit the shock tube well

While these films were not perfect, the continued use of these films became a huge issue when we noticed it was getting harder and harder to find supplies in stock at the usual suppliers. A phone call to 3M confirmed our worst fears: They had discontinued these films.

The initial concerns about finding a replacement were tempered by the knowledge that significant improvements had been made to the cutter system and it should be much less picky about the films it fires. This also allowed us to investigate industrial sources of rolled film instead of sheets as well.

We already knew the type of film used in the CG5000 and CG6000 films, thanks to the help given to us by the 3M Corporation. Searches turned up a couple of sources of this type 1 polyester film. We had measured the thickness of the original films, 4.5 mil and 7.5 mil, so samples of these films were ordered in various thicknesses ranging from 3 mil to 10 mil for testing.

To make a long story shorter, the 5 mil film was found to be perfect for Mach

1.7 shots and two layers of this film were perfect for Mach 2 shots. In addition to the cutter improvements that allowed the system to have the throw to reach bowed films, it also had the force to puncture stiffer films.

Interestingly, the initial testing showed this particular film to be a failure. It couldn't hold the pressure of a Mach 1.7 shot with a single film reliably. Every other shot or so it would burst prematurely. Testing showed an interesting behavior though. If the pressure was brought up in the driver section in stages and allowed to sit at each of these lower pressures for four to five seconds before raising it to the next pressure step, the films WOULD hold every single time.

The root cause of this strange behavior was strain hardening of the film, as discussed previously.

This strain hardening also had another beneficial side effect. The strain hardened dome was also significantly less elastic than undeformed film. When the cutter was activated and it initially punctured the dome, instead of acting like a tough, elastic material, the dome would "unzip" rapidly with an almost brittle failure mode. This rapid failure of the diaphragm increased the speed in which the shock wave could form from the initial Mach waves and produced a much better formed shock wave passing the upstream pressure transducer PT 1.

With these prestrained diaphragms, the pressure rise as the shock wave passes the upstream pressure transducer is basically perfect. There is no doubt that a fully formed normal shock wave passed this transducer before any Mach waves passed it. The gas in the driven section was stationary and at ambient pressure, then the shock passed and the pressure spiked up through the discontinuity of the shock wave, so the pressure rise is basically vertical on the pressure trace. Needless to say, it is absolutely trivial to trigger the oscilloscope and to calculate shock wave velocities with such a well formed pressure trace.

Shot after shot has been taken with the new system with this type of pressure trace. Even the shots that are now considered "ok" have better upstream pressure results than previous "exceptional" pressure traces from the past. A new level of quality and consistency has been established for this shock tube.

One additional benefit of these new films is packaging. The original films were ordered as letter sized transparency and were not available in any other format. It was possible, with care, to get two shots per sheet. The new films could be ordered in 48" wide by 100 ft long rolls. And this roll could be cut into eight 6" wide rolls for a nominal fee. With care, only 4" of the strip is used for each shot which means we can get up to 2400 films from a single $250 roll. This dropped our film cost from $1 per shot to 10 cents per shot!

With the films in 6" wide rolls, it was also trivial to attach a hanger to the shock tube to hold two rolls of films right in front of the driver/driven section flange. After a shot, the driver is pulled back, the film is pulled up and the ruptured section is carefully cut off and discarded. The clean film is then slid back down between the two flanges and the toggle clamps operated to securely clamp the driver section to the driven section. All in 20 seconds or less. It was no longer necessary to have a person dedicated to changing the diaphragms (and preparing the next diaphragms for the next shot) as it could be done so quickly. This directly increased the amount of time the shock tube is spending collecting data as now two people can effectively operate this shock tube with no impact to effectiveness versus having three people.

# Chapter 4

# Addressing the Quantitative Issues

## 4.1 Shock Tube Misfires

There is nothing worse when you have expensive $SF_6$ flowing in the test section and you press the fire button and nothing happens! You wasted the $SF_6$, the helium AND the diaphragm. Not to mention 5 to 10 minutes of everyone's time.

So we tried to fix that...

As it was mentioned in the introduction section, misfires were the issue that first got me into thinking about upgrades for the shock tube. Initially, it was just to fix the things that were driving people (myself included!) up the wall. A single misfire isn't that bad. On "good" days when they only occurred every eight to ten shots, they could be lived with. But on the days where you were fighting other issues, such as bad ICs or delay generator not being triggered by the pressure sensors, then it was a huge issue as you go from one failure to another to another. More than one long day of shooting was called off at lunch because everyone was just so sick of the failures.

Prior to coming back to school to finish my undergraduate degree, I spent over a decade working at Intel at Fab 11. Most of this time was spent as a process engineer, and equipment engineer, or both. The entire philosophy at Intel is centered around a perfect process with zero defects on any wafer. Continuous improvement is not just a good idea there, but it is the law. You will improve your area of the process, or they will find someone that will! It must be working because usually once or twice a year, a wafer would come out that had zero detectable defects! Knowing that the target was achievable always made the battle to achieve it that much easier.

Switching to an academic setting was definitely a change! The resources were greatly reduced as was the necessity to make those improvements. The general attitude was that if a shot fails, we can always "rinse and repeat." This led to fairly significant resistance to making improvements initially. No one wanted to take the time out from shooting to make improvements that would decrease the chance of misfires.

That all changed one particularly bad summer day when it seemed like two out of every three shots failed because the cutter head refused to move when the firing button was pressed. Out of sheer frustration, I was given the go ahead to implement the first of what would eventually be many improvements.

### 4.1.1 Guide Rails

To understand the original failure to fire issues, once has to understand how the system was originally fired. Many shock tubes are fired by the use of burst diaphragms. A metal diaphragm is used to separate the driver section from the driven section. The driver section was then slowly charged with the driving gas until the diaphragm burst under the applied pressure. With properly made (and expensive!) metal burst diaphragms, the burst pressure is fairly consistent. The biggest limitation (besides

cost) with this system is that you do not know exactly WHEN the diaphragm will burst. Camera shutters are simply too slow to open at the bursting of the diaphragm, so the shutter must be held open for a very long time once the pressure has exceeded some critical value. Any stray photons will lead to noise in the image.

Our shock tube uses a type 1 polyester film as a diaphragm. They start life as commercially available 3M CG5000 and CG6000 transparency films. This film separates the driver section from the driven section to allow the helium to pressurize the driver section just like the burst diaphragm does. But these are not precision manufactured films and do not have specific pressure that they will burst at. Instead, inside the driver section, there is a cutter assembly. Figure 4.1 shows most of what is inside the driver.

Figure 4.1: Solenoid, coupler, rod and support bearing

The solenoid itself is attached to the flange at the back of the driver section by a pair of metal stand-offs. The output from the solenoid was connected to a 0.25" diameter steel rod via a metal coupler. The rod was supported by two linear bearings that are positioned in the center of the driver section by a pair of metal legs as shown in Figure 4.2.

The cutter head is at the far end of the driver section, right up against the diaphragm. It is attached to the rod with a set screw. This cutter head, shown in

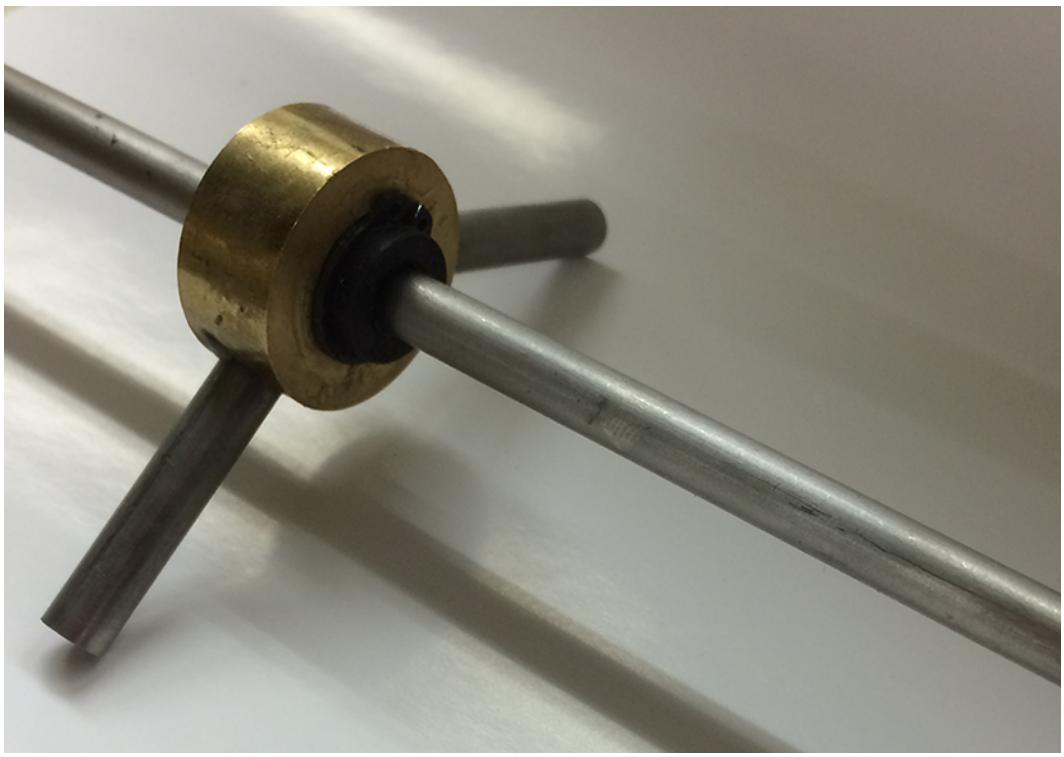

Figure 4.2: Linear bearing on cutter head firing rod

Figure 4.3, is a simple aluminum block with a mounting hole for the shaft and the retaining set screw and two orthogonal slots that have modified utility knife blades mounted in place with JB-Weld epoxy.

The linear bearings were not attached to the driver section, but instead floated inside. The cutter head firing rod that passed through each of the bearings prevented them from falling over. The legs on the bearing assembly held the rod up. Unfortunately, linear bearings do not handle misalignment well. Depending on the exact position of the bearing on the shaft, the would either operate smoothly, or they would bind up.

When the cutter head is retracted before a new diaphragm is installed, the bearings are pushed back slightly. But more importantly, they were also tilted backwards.

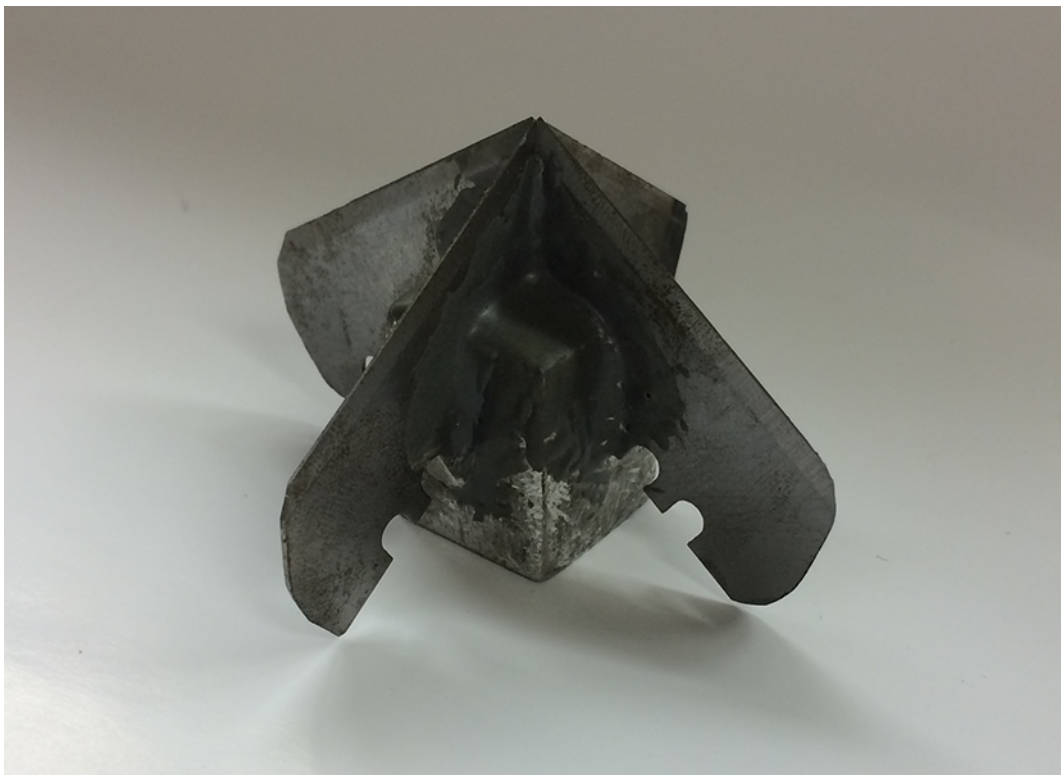

Figure 4.3: Closeup of the original cutter head.

The initial movement of the rod would not be a sliding motion through the bearing, but instead would be a tilting motion as the bearing rotated slightly on it's two legs towards the diaphragm. In some areas of the rod, when the bearings approach vertical, the rod starts to slide through the bearing as designed. In other areas, however, the rod never starts to slide through the bearing and, instead, the bearing is accelerated by the rod towards the diaphragm. This acceleration reduces the velocity of the cutter head and increases the chance that it will not have sufficient energy to puncture the diaphragm.

In addition, because the linear bearings were not mounted to the driver section, they also moved with every single shot. Because firing the tube generates more acceleration on the cutter rod than retracting the cutter head by hand does, the

bearings would inevitably move towards the diaphragm a small amount with every shot. Eventually, they would get far enough forward that they would end up right behind the cutter head itself. As the cutter head has very sharp blades on it and the RA is working in tight confines and poor lighting conditions, the cutter head is pushed backwards fairly gently. When the head hits the bearing, the RA could mistake this for the solenoid being fully retracted. This mistake is found out the next shot when the shock tube fires on it's own at around 90% of the target pressure due to a tiny prick at the center of the diaphragm from the cutter head being slightly too far forward.

These issues led to the very first modification for the shock tube: a set of guide rails shown in Figure 4.4 to hold the linear bearings vertical and maintain the proper spacing between the bearings.

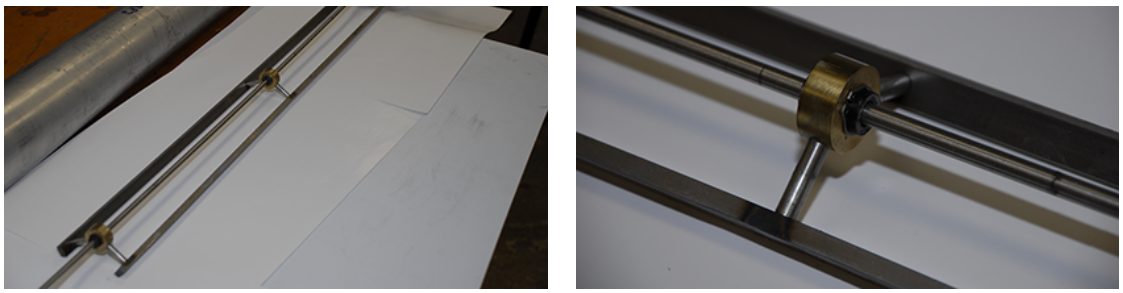

(a) Both bearings on rail (b) Linear bearing

Figure 4.4: Guide rails for linear bearings

The guide rail is a very simple design. A 24" long length of 1/8" x 1/4" steel stock was machined to place 1/8" diameter holes in the correct locations. The legs from the linear bearings was placed in the holes and welded in place once the bearing were properly aligned. A short tab was welded on at the back of each rail and a hole was positioned and drilled to allow a screw to attach the rail assembly to the driver flange with the proper threaded holes. This would prevent the rails from shifting forward over time and causing the misfire discussed above. However, the driver flange was

never drilled and tapped to allow this feature to be used, as the additional mass of the rail assembly along with the decreased drag on the linear bearings due to proper alignment of the bearing and the rod has proven to mostly stay in place for horizontal shots. Occasionally, it is still necessary to push the bearings back. But once a week is much better than once every hour or so with the original system!

### 4.1.2 Battery Backup For The Solenoid

Even with the guide rails, the cutter still occasionally failed to move forward when fired. Or, it would also occasionally move forward very sluggishly. Investigation showed we had some wiring issues to address.

The solenoid originally used was actually designed as an electric lock for a safe door. When activated, the steel output rod of the solenoid would go into holes in the door frame and secure it. Multiple solenoids were used on each door and the solenoid was ONLY moving it's own plunger and output rod.

We had added a heavy steel coupler, nearly 48" of 1/4" diameter steel rod and a heavy metal cutter head to the equation. The wiring coming out of the solenoid is 18awg wire. Additional 18awg wire was used to carry current from a 12V battery charger, over to the firing switch, back to the solenoid and then back to the ground on the battery charger. All in all, over 12 feet of 18awg wire was used to complete this little circuit.

The force of a solenoid is proportional to the current flowing through the windings and inversely proportional to the distance the armature is pulled out of the windings. Our attempts to maximize the throw of the solenoid has the added (and unwanted) effect of reducing the initial force the solenoid can generate. Given that it must overcome the friction of the bearings and the inertia of the cutter assembly, this initial force is critical to the cutter system operation.

The first approach used to improve the initial force (as well as the final velocity of the cutter head) was to simply rewire the cutter system with 14awg wire replacing everything right up to solenoid windings and to reroute the wiring to minimize the length of the wire used. 14awg wire has two and a half times less resistance for a given length than 18awg wire does. The solenoid pulls approximately 2 amps, which gives a voltage drop of just under 0.2V for the original cable. Given that our supply was only capable of putting out 14V (no load), this amounts to a 1% voltage drop. It isn't significant, the wiring upgrades pushed that down to less than 0.5% voltage drop. These measurements where taken with the battery attached, so the voltage drop listed here is much less than the actual voltage drop with just the charger attached.

This initial change did improve the cutter head's action slightly, but noticeably. It didn't, however, provide the force and velocity needed to ensure a clean, sharp rupture of the diaphragm in all conditions. The cleaned up wiring was, however, more aesthetically pleasing and more robust as well.

The next line of attack was the battery charger itself. The charger was not designed to be a power supply as it does not have any storage capacity, other than the magnetic field of the transformer. Because of this, when low resistance loads are attached to the charger, the output voltage collapses. Test shows that this charger will drop to a voltage of less than 10 volts when powering the solenoid. The charger by itself simply isn't designed to be a power supply and isn't a storage device.

A battery, on the other hand, IS a storage device.

A 12V motorcycle battery was sourced and connected into the circuit. The battery charger was simply set at the 2A charge rate and left attached to the battery to maintain it's charge. At the end of the day, the charger is disconnected to prevent overcharging of the battery and damaging it. The very first test with the battery

in place showed it was a winning upgrade. Estimates of the cutter head velocity improvements ranged from 50% to over 100%. These estimates were all based on individuals listening to the system firing with and without the battery connected and were not scientifically collected data. But there was no doubt that the battery gave the solenoid the extra jump it needed to cleanly rupture the diaphragm. For a before and after example, look at Figure 3.2 and compare it to Figure 4.5.

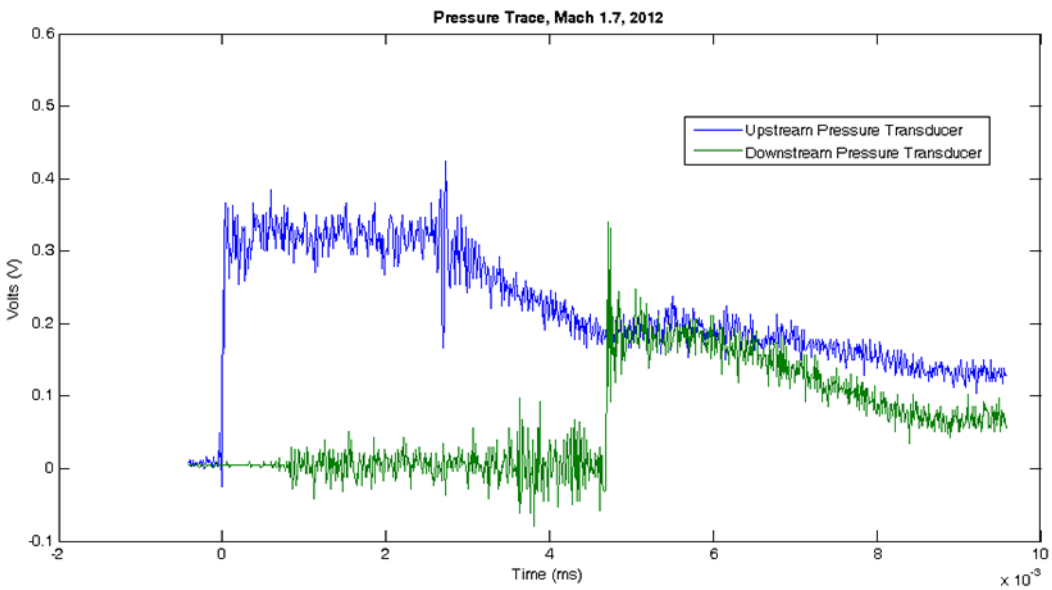


Figure 4.5: Pressure trace, 2012-06-01-shot-01, Pre Isolation

The first figure is an example of a poor rupture. Notice how the pressure trace from the upstream pressure sensor does not make a clean, vertical rise, but instead rises with a fairly pronounced slope. This is indicative of the normal shock wave not being fully developed when it passed the upstream pressure trace. Because we do not have a fully developed shock in the pressure trace, there is no real way to accurately measure the shock speed with this data, so the image captured is not useful, other than as a pretty picture.

On the other hand, the Figure 4.5 shows a nearly perfect vertical rise at the

upstream pressure transducer, clearly indicating that the shock was fully formed. This is data that can be used to accurately measure the shock wave velocity.

By increasing the velocity of the cutter head with the wiring and battery upgrades, the instances of a wasted shot due to poor pressure trace data was greatly reduced. Again, because failed shots are generally not recorded, there is only anecdotal evidence to support this claim. The general increase in the quality of the pressure traces that were saved is also supporting evidence for the usefulness of this upgrade.

### 4.1.3 Solenoid Coupler Optimization

Who would have thought that something as simple as a metal shaft coupler would actually be a source of issues with the shock tube? After all, it is nothing more than a 2" long piece of metal with a 1/4" hole in it and a couple of set screws. How could it cause misfires? Well, as was mentioned in section 1.3.2, this shock tube was originally fired dynamically. The driver is pressurized and it is fired the instant the pressure reaches the target pressure.

The reason for dynamic firing was fairly straightforward: very often, the shock tube would NOT fire if you brought the pressure up, let it sit for a few seconds and then tried to fire it. The cutter head would clank forward, but nothing would happen! The root cause of this behavior is yielding of the diaphragm. Under pressure, it starts to yield and bows out into the driven section, forming a hemispherical shape shown in Figure 4.6. The greater the driver pressure and the thinner the diaphragm material, the greater the bow. This diaphragm was deformed under 80 *psi* of helium which is normal for a Mach 1.7 shot. The Mach 2.0 shots are at 180 *psi* and even with two films as the diaphragm, they bow out nearly twice as much as the one in the image below.

Referring back to the cutter head Figure 4.3, you can see that the cutter head is

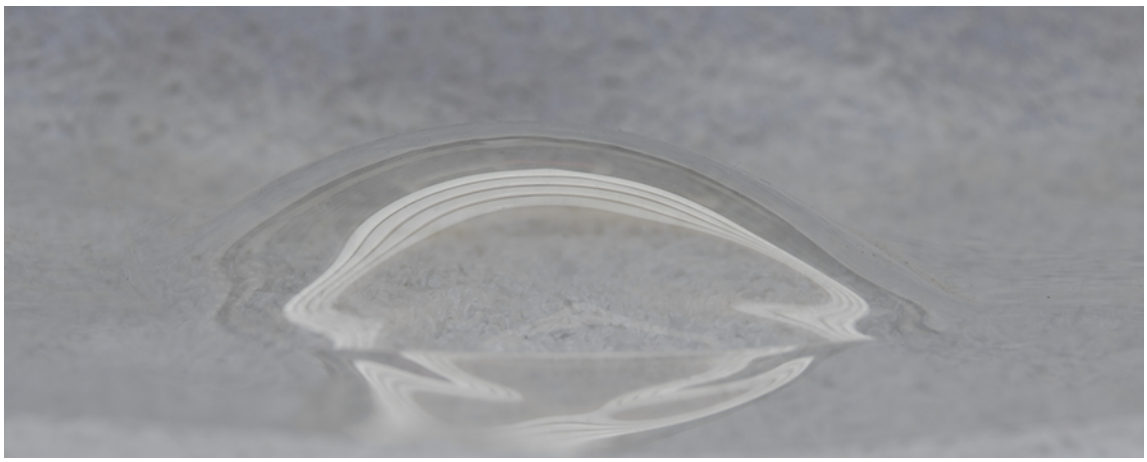

Figure 4.6: Diaphragm deformed under pressure

a very short and blunt cutter. It is NOT shaped like an arrowhead at all. Under low Mach number shots and especially with dynamic shooting, the point of the cutter head does puncture the diaphragm as you would expect. As the pressure rises for high Mach number shots, the diaphragm starts to yield more and more. Due to strain hardening, it does have limits on how far it will yield with a given pressure. As the bowing gets larger, a point is reached where the point of the cutter head is no longer puncturing the diaphragm, but instead the outside edge of one of the blades is puncturing the diaphragm off to one side. The bowing becomes more pronounced as the pressure rises, until eventually you hit a point were even the edge of the blade cannot reach the diaphragm due to limitations on the throw length of the solenoid.

Puncturing the diaphragm off to the side also impacts the quality of the Mach waves that are initially produced as the slower the diaphragm ruptures, the longer it takes for the Mach waves to coalesce into the normal shock wave. With a particularly slow shock formation, the normal shock may coalesce after it has passed the upstream pressure transducer, once again, leading to a lost shot.

This condition was made even worse as the helium bottle pressure fell below 1000 psi. The regulator used is not a constant flow rate regulator, so as the bottle pressure

decreases, the mass flow rate also decreases. Once the bottle dropped much below 1000 psi, the rise time of the pressure in the driver section increased dramatically, especially for the 180 psi Mach 2 shots. This slower fill rate gives more time for the diaphragm to yield into the driven section, moving it further from cutter and leading to more and more misfires as the bottle pressure drops. Quite often, a low bottle had to be set aside to be used on lower Mach number shots as the misfire rate was simply too high to be accepted at Mach 2. Unfortunately, this need to maintain a fast fill rate also made it more difficult for the operator to fire the shock tube at the desired pressure due to the limitations of human reflexes.

A partial solution was found in the solenoid coupler of all places! After all the low hanging fruit (such as adjusting the cutter head so it was less than 1mm from the back of the diaphragm to maximize the throw length) was consumed, additional investigations found that the original coupler sat over almost 3/4" of the output shaft on the solenoid! When the solenoid is fully retracted, the coupler is one of the limiting factors as the back of the coupler hits the front of the solenoid. Figure 4.7 shows the new coupler attached to the solenoid.

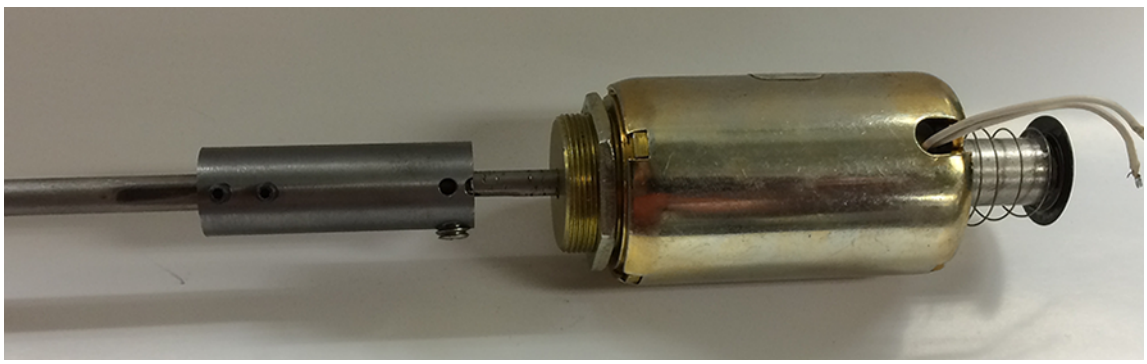

Figure 4.7: Close up of new coupler and solenoid, partially extended

The new coupler was made with as small a diameter as possible while maintaining full thread engagement on the set screw. In addition, the 3/4" coverage was reduced

to 3/8", providing 3/8" more throw with this one change! In addition, the shorter length of the coupler along with it's smaller diameter also produced a coupler that has significantly less mass than the original. Given that solenoids do not have a linear force curve, reducing the mass allows the solenoid to accelerate the cutter head to a higher speed before it impacts the diaphragm. The longer throw gives it a better chance of rupturing a severely yielded diaphragm as well. Figure 4.8 shows both the original and new coupler side by side.

Figure 4.8: Old and new couplers side by side

This new coupler significantly reduced the chances of a misfire occurring, especially for higher Mach number shots. Overall, it reduced sensitivity of the firing system to helium fill speed and diaphragm film thickness variations. The proof was on a single day in the summer of 2012 after these first changes were implemented. The previous record for the most good shots in a single full day (summer) was more

than doubled from thirty shots to sixty four shots!

The irritation and aggravation level was reduced as well...

### 4.1.4 Baffled Yet?

One very surprising result of the above modifications reared it's head when we went back to shooting Mach 2 shots after a very long time collecting Mach 1.7 data. From almost the very first attempt, we found that we had MORE misfires than before! This time, the tube would prematurely fire when the helium pressure reached around 50 to 60% of the target pressure.

A quick experiment showed why. All of the previous upgrades had greatly freed up the cutter head assembly so it moved much easier than before. Also, we now had the cutter head adjusted so it was very close to the diaphragm when it was initially closed up.

The test was simple: Insert a new diaphragm, flip the helium fill switch for a second or so, then vent the helium and take a close look at the diaphragm. Sure enough, on the very first test, we saw the root cause of the problem: The cutter head had slightly bumped the diaphragm and created a weak spot. On some shots, it was so bad that it was an actual leak you could hear.

Why was this happening at Mach 2, but the lower Mach numbers were unaffected? The answer is due to multiple issues. The first is simply the gas pressure. Mach 1.2 is shot around 8 to 9 psi. Very low. Moving to Mach 1.7 moves the pressure up to around 80 *psi*. And moving to Mach 2.0 has the pressure bumped up to 180 *psi*. It is a very nonlinear pressure curve.

This wouldn't be an issue except for a small design detail of the original driver flange. The helium gas port is in the exact center of the flange and blows straight

down the center of the driver. But the cutter solenoid is also mounted dead center in the driver. And, to keep it from blocking the helium gas when the diaphragm ruptures, it too is mounted up against the driver flange, just on the inside instead of the outside.

Now we combine this with the fact that all our work to maximize the cutter's throw ALSO moved the armature of the solenoid closer to the driver flange as well. And, as it turns out, the washer that the factory welded to the rear of the armature to contain the return spring just happens to be almost the exact same diameter as the 3/8 NPT hole used for the helium line...

Yup. When the switch was thrown, the puff of 180 *psi* gas would come rushing through the hose, into the driver flange and then right into the back of the solenoid armature who's washer was doing it's best to close off the helium from the driver section. The helium didn't like that, so it nudged the armature forward just a bit to make room to come roaring into the driver section. And that just a bit was just the right amount to create a weak spot in the diaphragm and cause a misfire!

If we hadn't increased the throw, this wouldn't have happened. If we hadn't freed up the cutter head assembly, this wouldn't have happened. If we didn't shoot at Mach 2, this wouldn't have happened...

Our original plan to address this was to simply make longer standoffs and move the whole solenoid further from the driver flange to give the helium plenty of room to enter the driver section without moving the armature.

But Dr. Vorobieff asked a simple question:

"Can't you just make a deflector or something?"

After the obligatory slapping of the foreheads, it was off to the machine shop. A small piece of thin gauge aluminum was found and with the help of a hammer and

dolly, tin snips and a few other small hand tools, the part shown in Figure 4.9 was created.

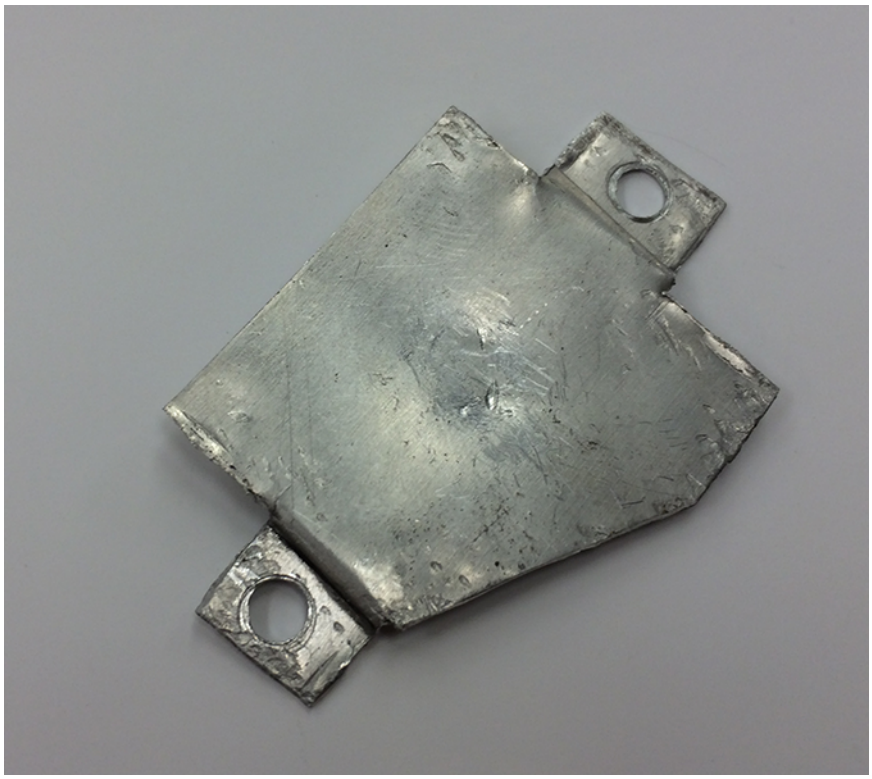

Figure 4.9: Top view of helium baffle

The view in Figure 4.10 shows the baffle being test fit on a blank flange and better demonstrates it's function.

This part was all made by hand shaping the metal. It's only job was to keep the helium from directly blowing on the armature while at the same time, allowing the armature to retract as far as it could (so it bottomed out on the coupler at the front). Using the two mounting tabs, it was attached between the driver flange and the solenoid's stand-offs.

And it worked perfectly on the very first try! There was also no noticeable increase in driver filling time either.

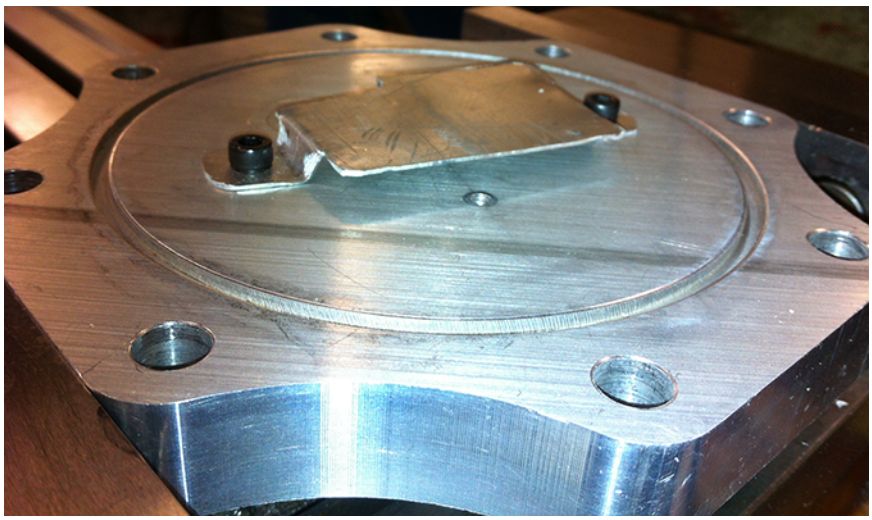

Figure 4.10: Baffle installed on flange

Scrap of aluminum. 10 minutes of work. Problem solved.

If only all problems could be addressed so easily!

### 4.1.5 Pneumatic Cutter System

While the solenoid based cutter head was much improved with the changes already discussed, firing of the shock tube was still based on the dynamic system. Some RAs had the touch and could get fairly consistent results, but other RAs had less luck with the process. And luck should never be counted on to collect good data!

This discussion began like many others (someone had a question) and ended like most (in an argument!) while trying to improve the Mach number variation one RA was getting while firing the shock tube. The question was simple:

"Can't we turn down the helium pressure a bit so it doesn't fill the driver section so quickly?"

The answer was equally as simple:

"Sure. But then you won't actually be able to fire it."

That launched into a discussion covering many of the issues with firing this shock tube that have already been discussed in this thesis. The short answer was simply that we had to replace the solenoid with a longer throw solenoid to do that. And getting one that was stronger would also help as well.

Researching possible solutions to this all showed a common theme: It is really hard to get long throw solenoids. The one currently used was very near the top of the commercially available list for throw. The problem is that the force of a solenoid is reduced by $\frac{1}{\sqrt{length}}$ that the armature is retracted from the windings. The result is the force falls off very fast and the solenoid becomes very complex and expensive to get the throw and power we needed. In addition, the solenoids get very large and use very high power levels which implies either high voltage or high current or even both to reach the performance that we needed to resolve these issues once and for all.

Eventually, the discussion swung around to pneumatic actuators instead of electrical actuators. On the face of it, pneumatics have many advantages over solenoids:

- Very compact for their force
- Long throws readily available
- No back EMF when you switch them off
- Easy to mount to the driver flange (a single threaded hole)
- Very strong for their size
- Cheap!

After digging through the McMaster-Carr catalog, we determined that we would be able implement a pneumatic system for less than $200. We already had a spare driver flange cut, it just needed the assorted threaded holes machined in it to support

the new system. We also already had a source of 125 psi compressed air in the lab as well. The cylinder selected used a very small threaded port (10-32 to be exact) for the supply and vent lines. The only concern we had was if this system would actually work inside the driver section after it had been pressurized with helium. Eventually, we decided to give it a try, so parts were ordered and the new driver flange was machined. Figure 4.11 shows the new cylinder mounted to the driver flange.

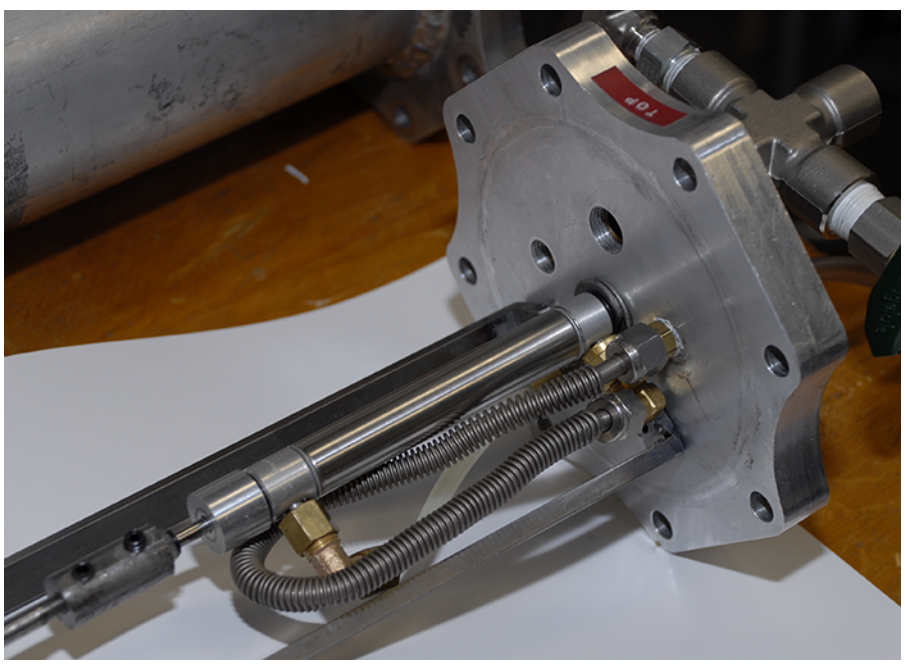

Figure 4.11: Pneumatic cylinder mounted to driver flange

The pneumatic system used a 2" throw, 5/8" diameter piston cylinder. It was significantly smaller than the solenoid it replaced. The firing system was through a double acting push button valve. When the button was up, air was directed to the retract port. When it was pressed, air was directed to the extend port and the retract port was vented back to the valve. The cylinder is made with a threaded stud on the back end to allow it to be simply threaded into the driver flange. There are no stand offs to get in the way and the cylinder is actually mounted closer to the flange (threaded into it!). That, along with it's very small size, presents even less of

an obstruction to the helium flow when the diaphragm is ruptured.

Instead of having a sealed electrical port into the driver section, we now had two 10-32 threaded holes for the hole nipples. Short lengths of the air hose connect the cylinder to the nipples and longer lengths connect the nipples on the outside of the flange to the firing valve. The hoses are secured with small zip ties, just to be safe. All in all, a very nice and tidy installation.

During the first test of the pneumatic system, one thing became very clear: The 22lb rating of the cylinder was not a marketing exaggeration! While it's velocity was only slightly faster than the improved solenoid system, the solenoid could easily be held stationary by hand (without the cutter head attached...) and that definitely was not the case for the pneumatic system.

With the bench test out of the way, it was time for in system testing. The driver was reassembled with a new cutter rod (it was longer than the solenoid's cutter rod as the cylinder is shorter than the solenoid plus it's stand offs) and everything was buttoned up for the first test at Mach 1.7.

And it worked almost perfectly. The reaction time of the system from pressing the button to the shock tube firing was definitely reduced even from the improved solenoid system. The rate of rise on the upstream pressure trace was improved, showing the diaphragm was bursting cleaner, allowing the shock wave to form faster. This was especially noticeable on low Mach number shots such as Mach 1.3 and lower.

A significant advantage to the pneumatic system over the solenoid system is that it retracts the cutter head automatically when you release the firing button. Plus, with 22 lbs of force on retraction, the cutter guide rails sliding forward was no longer a problem. The cutter would always pull it back and keep the cutter head point out of the next diaphragm.

Testing did show we had one issue that must be addressed: The o-rings on the cylinders shaft are very good and do their job well on the bench. But inside the driver section, when it is pressurized, the gas pressure from the outside of the cylinder could push the o-rings back, leading to a bad leak until the seals are repositioned. The manufacturer never envisioned their cylinder being used inside a pressure vessel, so they did not include any kind of retainer for the shaft o-ring. The air pressure would keep it pushed up were it needed to be.

A bit of time in the machine shop resolved this issue. A simple aluminum o-ring holder was constructed that allowed an external o-ring to be positioned on the shaft and sealed to the front of the cylinder. This o-ring was positively retained in all directions and prevent any helium from reaching the cylinder's internal o-ring. This stopped the leak!.

Like all things shock tube (one step forward, two or more steps back!), this also led to another issue with the pneumatic system: it took away 1/4" of our throw. While it was still 1/2" longer than the solenoid system, it wasn't quite long enough for Mach 2 shots with the new, non-dynamic firing we wanted to implement.

Before we addressed this issue, we also did additional testing and modifications to maximize the performance of the existing pneumatic system. The 1/8" ID air hose and the tiny 10-32 threaded fittings limited the mass flow rate of the air through the system. This had the effect of limiting the maximum velocity of the cutter head as well.

Testing was done by replacing the long runs of 1/8" hose with larger hose right up to the cylinder. A small reservoir was added right at the end of the driver section to minimize any pressure losses due to friction inside the airline. These tests showed the system could function much faster than the current system with these simple changes.

The Mach 2 testing once again hit a roadblock. It just wasn't reliable at that pressure. Occasionally, it worked perfectly. But usually, it would extend very slowly or not all. Often, when it wouldn't extend at all, continually pressing and releasing the firing button would "unstick" it. It continued to work perfectly at the lower Mach numbers, so we concluded it must be a pressure related issue. Given that the driver is pressurized to 180 psi and the supply pressure to the cylinder is only 125 psi, this was logical.

The first idea that everyone came to was it had to be the air lines being compressed shut by the helium. That is a 65 psi pressure differential on the retract line and a full 180 psi pressure differential on the extend line. The only problem was the airline was 1/8" ID with a 1/4" OD. That wall thickness was the same as the inner radius! Attempts to squeeze the line shut by hand pressure alone failed. On top of that, the helium would be applying hoop stress, which is the mode that the line would be strongest in.

After additional experiments failed to turn up any other possible root causes, the decision was made to simply test a stronger line inside the driver section. 1/4" semi-rigid plastic line was plumbed from the driver flange to the cylinder with custom adapters. The installation was definitely more error prone and the semi-rigid line was much less workable, but with a bit of work, it was successfully integrated into the firing system.

Once more, the driver was buttoned back up and test shots were conducted. The very first test proved we were right. The gas pressure was collapsing the original cylinder lines. But not the new lines. Not only did the system fire reliably, but it was faster than before, even at lower Mach numbers. The old line had been squeezed down enough to be a bit of a restriction for all the Mach numbers.

With the system reliably extending at every shot at every Mach number, a new

3" stroke cylinder was procured and installed. It was a drop-in replacement for the old cylinder with on a slight shortening of the cutter rod required. With a 2.75" effective stroke, there was no longer any doubt that the cutter head would rupture the diaphragm, which only bows a max of 1.5" away from the cutter head during Mach 2 shots. This led to the next change.

The old cutter head was not standing up to the abuse the new, faster and harder hitting pneumatic firing system was giving it. Looking back at the cutter head Figure 4.3, you can see it's construction.

The main item of interest is the method that is used to retain the cutter blades. As was discussed in the introduction, the blades are simply glued in place with JB-Weld epoxy. Usually, a couple times a year, we would lose a blade and need to rebuild the cutter. This was a messy process to remove the old blades and glue and then glue in fresh blades (after they had been modified in the machine shop). You always lost a full day of shooting when this did happen. Losing a day a couple of times a year was not significant. Often, you could find the blade loosening up, so you could plan on taking care of it at the end of a day to minimize the down time.

The pneumatic cutter was a different beast entirely. The forces on the blades were much greater due to both the acceleration of the cutter and the impact forces when the cutter hits the extend or retract limit. The blades started to loosen within a single day. Losing a day every other day due to damage to the cutter head didn't actually improve out shooting ratio.

The solution was actually already in the lab. The very first cutter head used with this shock tube proved to be unsuccessful. It was a common archery broad head arrow point. Unfortunately, with the original system, it could not reliably fire the tube at mid to higher Mach numbers. We know now that was due to limited cutter travel and the diaphragm bowing away under pressure. But we had taken the

cutter from less than 1.5" of travel to 2.75" of travel, almost doubling it. Figure 4.12 is a picture the current, and actually original arrowhead cutter.

Figure 4.12: Original and now current arrowhead cutter

The arrow point would also have several other benefits for us: they are easily sharpened by simply rubbing them on an oil stone. They came in a package of three, so replacing a damaged one can be done quickly and the damaged one can be reconditioned after the shooting is over. They are also always going to initiate the diaphragm rupture from the center of the diaphragm, where it can quickly "unzip" to allow the shock wave to form quickly and cleanly. The first shot, done at Mach 2, proved that the arrow points worked perfectly with the long throw pneumatic cutter system.

Of course, like most improvements to the shock tube, the pneumatic cutter also created a new issue. It was a mechanical firing system (the firing valve was a manual valve) and could not be used with the controller system. Also, because the firing valve had to be placed in the control station, this led to long tube lengths leading from the station, to the back of the driver section and then back down to the valve. With the small diameter of the tubing (1/8" ID), having 25 feet of tubing between the valve and the cylinder definitely slowed down the cutter.

The solution to both problems was fairly straightforward. A solenoid operated valve was purchased that used a pair of 120VAC coils to activate the valve. One pulled

it into "fire" mode and the other would pull it into "retract" mode. Figure 4.13 shows the solenoid valve mounted on the side of the shock tube right next to the driver flange and the pneumatic cylinder inside the driver.

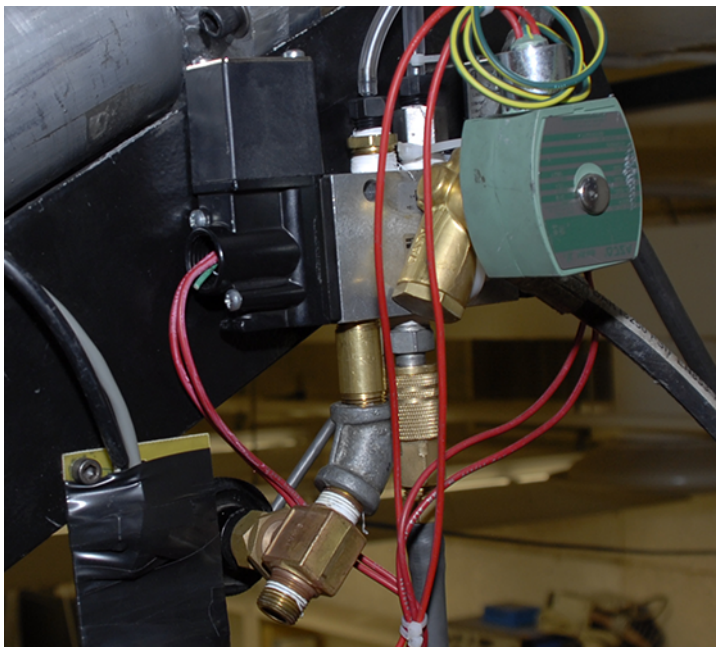

Figure 4.13: Solenoid operated pneumatic valve

The valve is in close proximity to the pneumatic cylinder allows for very short air lines between the valve and the cylinder. Where before we had over 25 feet of tubing (there and back) with the manual valve, we are now down to less than 3 feet. This significantly increases the flow rate of air through the tubing and improved the cutter velocity even more. In fact, it was retracting (and firing) so fast that the back of the cutter was hitting the front guide rod bearing when the guide rail moved forward.

It was hitting it hard enough that it eventually damaged the front linear bearing of the shaft support. Thankfully, the solution to this problem was also provided by solenoid valve itself. It had separate vent ports for the extend and retract sides, so it was possible to place a restricter on the vent line for the retract cycle that would

slow down the retract cycle from less than 1/4 second to right at 1.5 seconds. Now, when it retracts, if the guild rail has moved forward, the retract cycle will gently pull it back into position for the next shot.

With the solenoid valve mounted on the end of the shock tube, the 120VAC wiring to the solenoids ran down the length of the shock tube to the control station. A concern from the beginning was that we may pick up noise in the pressure transducers from the back EMF from the solenoids deenergizing. While things worked perfectly at higher Mach numbers (for a change!), when low Mach number shots at Mach 1.13 were attempted, the induced noise was greater than the signal (less than 200mV) from the pressure transducer.

To interface the controller to 120VAC solenoids was already going to require some new hardware as the PCB for the controller was only designed to switch DC current. The solution to both problems was to design a solenoid driver board that could be mounted next to the solenoid valve and keep all the high voltage AC power and noise safely at the far end of the shock tube.

The circuit designed had three snubberless triacs on board to drive each of three solenoids:

- Helium gas solenoid
- Extend solenoid
- Retract solenoid

The triacs chosen were vastly overkill for the job as they are rated at 600VAC and 30A. But they had two important features: They were on hand and they were snubberless triacs. Adding an external snubber circuit to absorb the back EMF produced by the solenoids to the driver board took up significant board space as

well as required high voltage AC rated capacitors that were not on hand. Using the snubberless triacs with these low current solenoids eliminated the need for the snubbers.

To trigger the triacs, each gate was connected to a MOC3022 random phase optoisolator with triac output. The optoisolator decoupled the 120VAC power and noise from the DC control wiring. This provides greater safety to the operator as there is no 120VAC in the control station and there is no high voltage noise being carried down the shock tube near the pressure transducers. They are also very easy to trigger from any microcontroller as all it is is turning on a small LED internal to the optoisolator.

While the helium solenoid's isolator is directly connected back to the controller, the solenoid valve was added on after the controller PCB was made and it only has an output for firing and not for retracting. To address this, a small, 8-pin Atmel ATtiny85 microcontroller was incorporated into the triac driver board. It is connected to the fire signal from the controller and executes a fairly simple program. When ever a valid (and valid means software debounced) fire signal is received, it activates the extend solenoid. It holds this for as long as the fire signal is received. Once the fire signal is no longer valid, it turns off the extend solenoid and activates the retract solenoid. An internal timer is then started and after two seconds, the retract solenoid is turned off. The friction in the system and the residual air pressure hold the cutter in the retract position after that without needlessly heating the retract solenoid.

This little firing controller has proven quite robust and reliable. Testing with the triac drive installed showed we can trigger the oscilloscope as low as 25mV without the firing system causing any false triggers. That is a 10 fold improvement over the direct 120VAC wiring system. The schematics for this firing controller are in the appendix.

## 4.2 Laser Trigger Errors

The laser has to be triggered at the correct time, as measured in microseconds. If it is triggered at the wrong time (or not triggered at all!), the shot is wasted. An accurate delay is a function of a good delay generator and a good trigger signal to the delay generator. The DG535 delay generator has proven itself quite accurate, but we did have some issues with the signal.

### 4.2.1 Pressure Transducers

The timing for the UNM shock tube is controlled by two pressure transducers. The up streams transducer triggers the oscilloscope that captures the pressure trace used in Mach number timing while the rear transducer triggers the delay generators that actually trigger the laser pulse at the correct time. These are high speed PX101 piezoelectric pressure transducers from Omega that have a rise time of $1\mu s$ and with a sensitivity of 0.002 psig. In the original system, these transducers were screwed directly into the driven section with the end of the transducer slightly protruding into the air stream. This direct mounting system worked reasonably well, but it did lead to an issue at low Mach numbers.

### 4.2.2 Signal to Noise Ratio

With the transducers directly threaded into the aluminum shock tube driven section, noise traveling through the walls of the aluminum tube is directly conducted to the pressure transducers, which shows on the pressure trace as a very noisy signal. For high Mach number shots, this is not an issue as the pressure spike when the shock wave passes the transducer is very high relative to the conducted noise.

The issues start at the low Mach number studies. The conducted noise does decrease, but not as fast as the shock wave's pressure spike. When attempting to shot much below 1.4, the signal to noise ratio collapses and it can become impossible to trigger the lasers as the conducted noise is now at the same magnitude as the shock wave pressure spike. One spike greater than the setpoint on the trigger to the delay generator and the lasers are fired prematurely. You increase the trigger level to prevent this spike from causing a false trigger and the signal from the shock wave is no longer strong enough to trigger the delay generator. The classic Catch 22.

Figure 4.14 shows a Mach 1.94 pressure trace. At approximately $400\mu s$, you can see how the noise on PT 2 (green) jumps several orders of magnitude. This jump is caused by the all the mechanical noise and the noise from the Mach waves upstream being conducted to the pressure transducers ahead of the shock wave in the aluminum driven section.

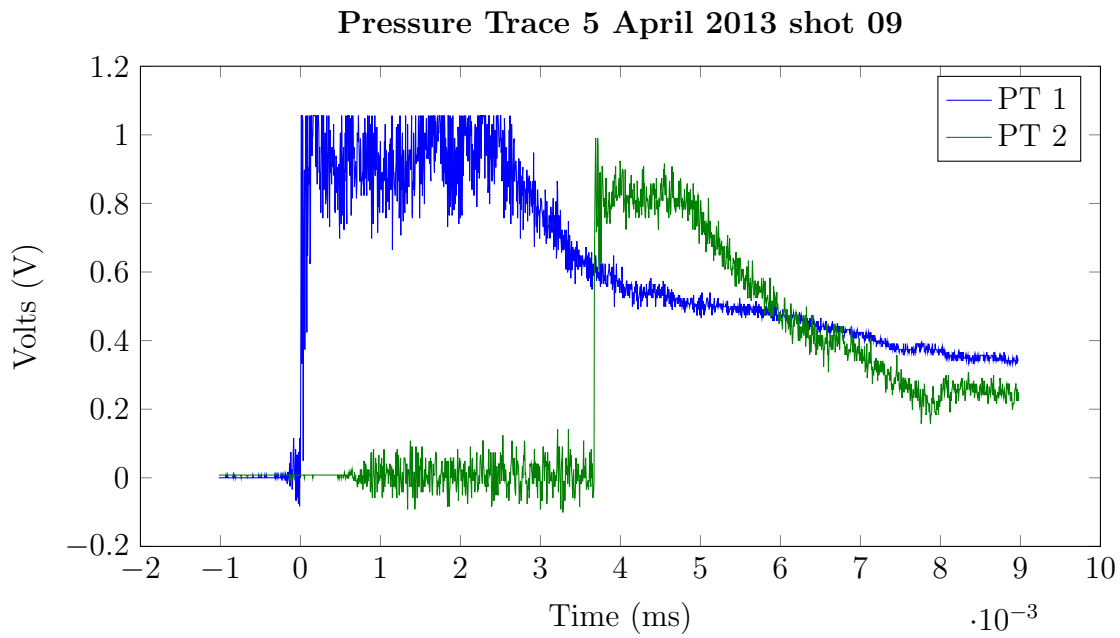


Figure 4.14: Mach 1.94 shot, pre isolation

At approximately $3.9ms$, the shock wave arrives and causes the signal from PT

2 to jump significantly. You can also see that the signal level on PT 2 when the shock arrives is right at 1 Volt where the noise is less than 200mV. For this shot, it was very easy to set the trigger level on the delay generator so that it could cleanly trigger on the shock without false triggering on the noise.

Pressure trace 4.15 shows a different case. The Mach number is lower so the signal level has decreased. The noise signal has also decreased, but not as much as the shock signal. In the worse case scenario, the signal disappears into the noise completely and it isn't possible to trigger the lasers on the shock. This is actually a very good preisolation pressure trace. The signal at PT 2 is peaking at 100mV, but the noise is only peaking at 50mV, giving a small 25mV window were the trigger level could be set to trigger on the signal but not the noise. Again, none of the "bad" shots pressure traces were kept as they are of no value to the experiment, but would have been great to have for this thesis.

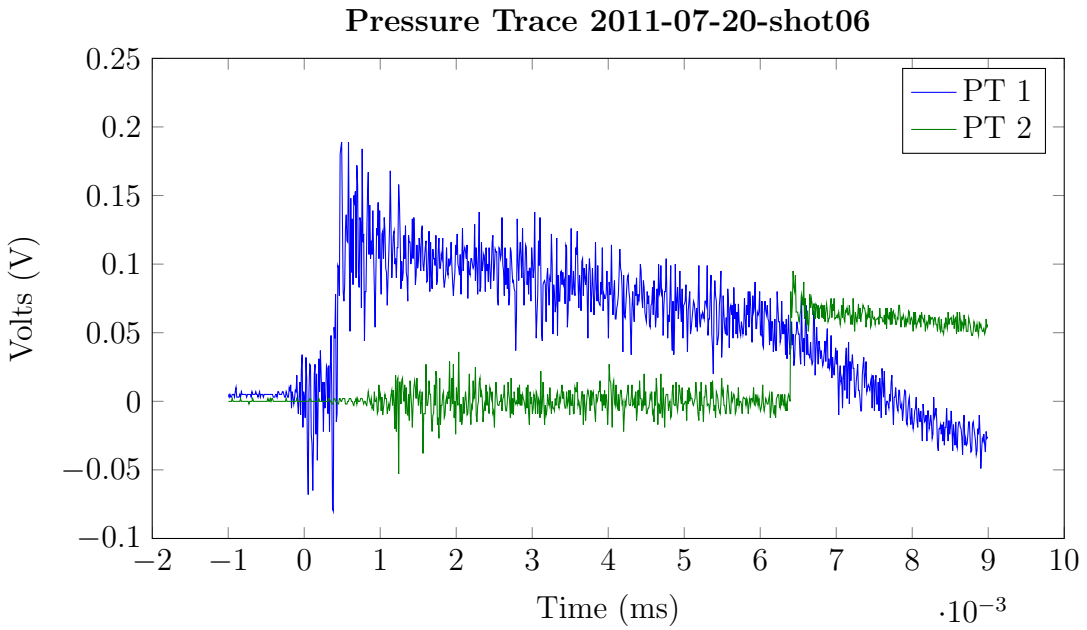


Figure 4.15: Mach 1.20 shot, pre isolation

### 4.2.3 Pressure Transducer Isolation

We can't increase the shock wave's pressure spike, so we decreased the noise by isolating the pressure transducers from the shock tube. Research showed that the pressure transducer did not need to be grounded to the driver section (it is connected to its power supply / signal conditioner via a SMA coaxial cable) to operate. A material, ultra soft polyurethane, or sorbathane, was found that would effectively absorb much of the conducted noise.

The trick was how to mount the sensors precisely in the driver section what attaching them through a very soft, very flexible material. This was made more difficult with the requirements to maintain accurate center-line mounting for the pressure transducers and keeping the face of the sensor flush to the inside of the driven section. In addition, there could only be minimal clearance around the tip of the pressure sensor to minimize disruptions to the normal shock. All of this was compounded by the normal shock itself and the significant pressure pulse it applied to the sensor every time the shock tube is fired.

Figure 4.16 shows the small aluminum adapter that was designed that had a large, 1" diameter flange around a central cylindrical mounting area. The mounting area was designed so that with the adapter epoxied to the driver section and the pressure sensor torqued down, it would hold the sensor at the correct height. The driver section was then machined to provide positive clearance around the body of the adapter while providing minimal clearance around the tip of the pressure transducer. Any contact between the tip and the driver section would mitigate the effects of the isolation adapter. Finally, a torus shaped piece of 1/8" thick sorbathane was cut and bonded to the adapter and the driver section with structural epoxy. Weights were used to keep the adapter firmly in contact with the drive section while the epoxy cured.

Figure 4.16: Pressure transducer mounted to driver section in isolation adapter

The centering issue was resolved by the simple trick of wrapping a single, thin layer of tape around the tip of the pressure transducer. It would just fill the clearance space between the transducer tip and the hole in the inside of the driven section, forcing the transducer to remain centered on the hole, preserving both the necessary isolation as well as maintaining the correct center line spacing of the transducers. Once the epoxy fully cured, the transducer was removed and then the tape was removed to restore the isolation.

The final task before testing was verify the face of the transducer did not protrude into the driven section nor sit too far back. The downstream transducer was perfect as installed. The upstream transducer sat a tiny bit proud, so a custom precision ground washer was made in the ME machine shop to space it back to being flush.

The final result yielding the pressure trace shown in Figure 4.17 demonstrates the dramatic improvement in signal to noise ratio.

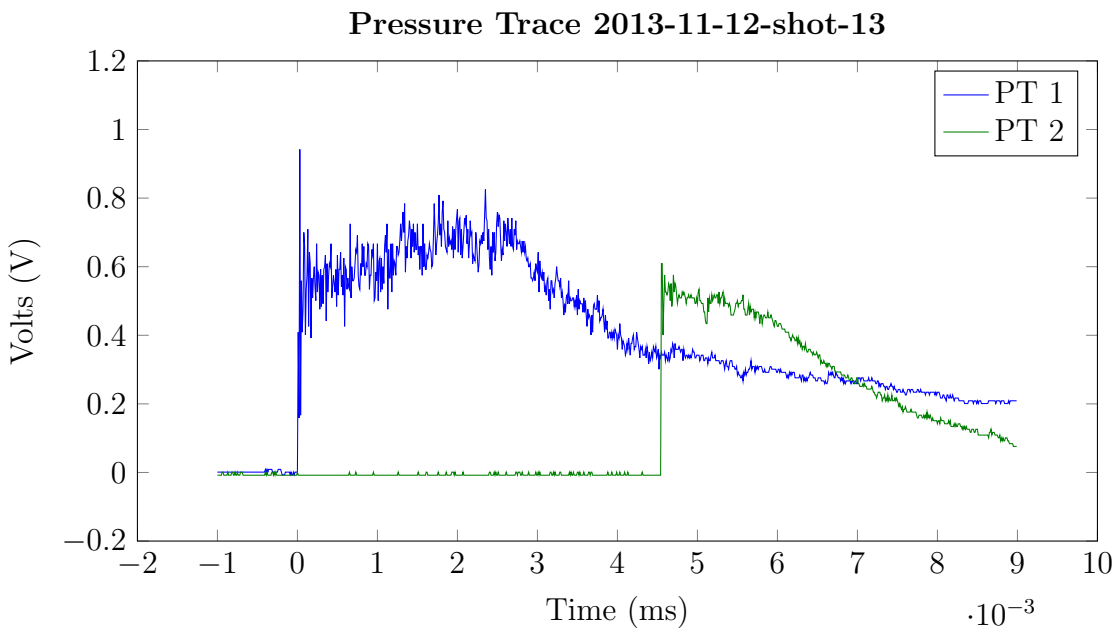


Figure 4.17: Mach 1.70 shot, post isolation

Notice the almost complete lack of any signal on the green PT 2 signal. There are tiny bits of noise that pops up along the trace, but the magnitude of this noise signal is orders of magnitude reduced from the the pre isolation pressure traces.

This change not only decreased the number of false (or no) trigger events with the wasted effort and materials that go with a bad shot, but also increased the effective low end of the shock tube. Prior to the isolation, it was very difficult to shoot below Mach 1.3. Mach 1.2 was almost impossible if everything didn't line up perfectly.

After this upgrade, shots have been reliably and repeatably taken at Mach 1.13. That uses only 7 psi of helium. Even with such a low pressure (and correspondingly low shock pressures), the signal to noise ratio was still more than good enough to enable reliable triggering at only 25mV as seen in Figure 4.18 below. The actual

noise floor for this shot is on the order of 10mV.

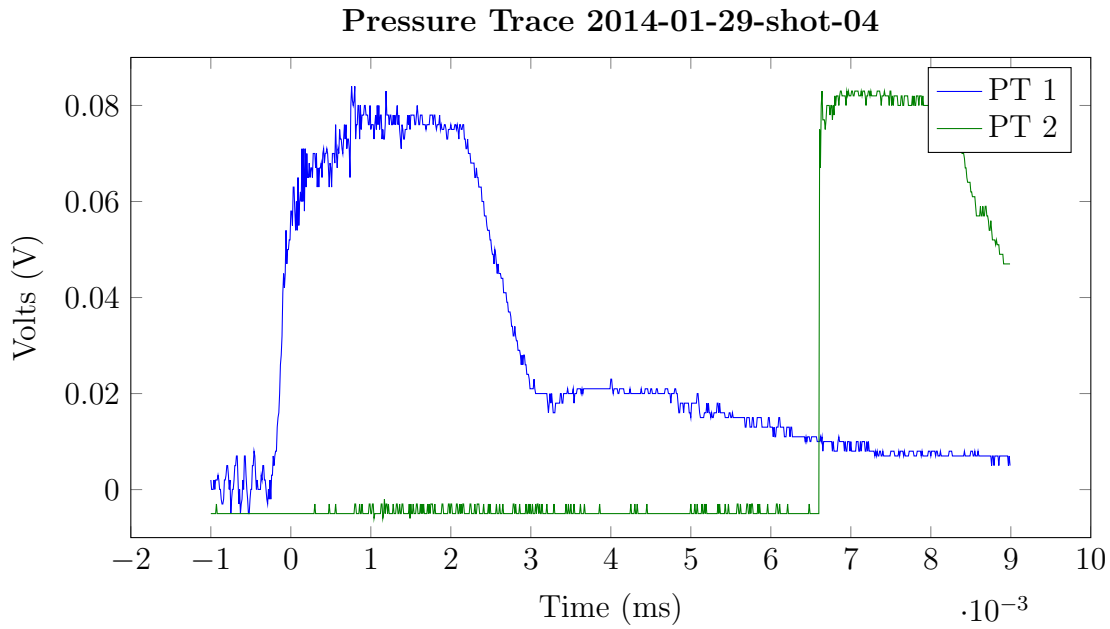


Figure 4.18: Mach 1.13 shot, post isolation

This change has taken the pressure traces and the related delay generator triggering from one that must be monitored closely and often causes loss of data and productivity to something that is nearly ignored. That is a win as it allows more time and energy to be expended upon items that truly impact the quality or even quantity of data collected.

## 4.3 Camera Trigger Errors

The camera iris has always been manually triggered by the operator. This is all driven by simple timing issues: the shock wave is taking less than $10ms$ to travel the length of the shock tube (not just between the pressure transducers) while the shutter on the camera takes $25ms$ to open. It simply is not possible to open the

shutter based on any shock generated signal.

The workaround for this has always been the same: use a long iris open time along with manually opening the iris just before triggering the experiment. The long open iris causes noise issues with the image, as was previously discussed while the manual trigger must occur during a time that almost complete attention must be given to the rapid pressure rise in the driver section while filling the driver section.

As it turns out, humans don't really multitask all that well! Anecdotally, approximately ten percent of all shots are lost because the camera iris was triggered either too soon (usually when the helium bottle pressure is low and the driver pressure is rising slower and slower) or too late (new helium bottle). Without the shutter open, all the work, supplies and time that went into that shot are completely wasted.

The ultimate solution to this issue is to bring the camera control under the control of a system that has better "reflexes" than a human. The next chapter discusses the microcontroller based system controller that does just that.

The work done to address the Mach number variations in the qualitative section led to the elimination of the dynamic firing system. Going to static firing also had a secondary effect: It is much easier for a person to press one button (camera iris control) then a second button (firing button) one after the other from a static situation than from a dynamic one.

Click. Click. Boom. That simple sequence is much easier to get correctly every single time (well, ALMOST ever single time!) when you are not completely focused on a rapidly changing pressure display waiting for the right moment to start every thing.

# Chapter 5

# System Automation

## 5.1 Microcontroller Based System Controller

There is one area where no amount of mechanical improvements can fully address: the timing of the triggering of the camera. Due to the human limitations with manually triggering the camera, the iris must be held open much longer than necessary for the experiment. For example, from the moment the shock arrives at the ICs to the ICs being blown out of the test section, that will take less than 2ms. Yet the iris is held open for the experiment for a whopping one thousand times longer! This is completely due to the lack of timing accuracy in the human camera controller.

By holding the camera open much longer than necessary, we are exposing the CCD to outside noise sources that it wouldn't otherwise be exposed to and increasing the noise level of our images. After all the work that has gone into reducing the noise and increasing the signal, leaving this low hanging fruit just didn't seem wise.

The controller was originally conceived early in the program while dynamic firing was still being conducted. The pressure sensor has a response time of 1ms, so it

was determined that an ADC oversampling this reading with a ratio better than 2000:1 and outputting the result to a microcontroller should be able to react much quicker and fire the shock tube much closer to the actual desired pressure than any human could. After much research, a final hardware specification for the controller was generated that included:

- Atmel ATmega328 microcontroller (the author was familiar with this MCU)
- 20x4 character display with $I^2C$ interface and 4x4 matrix keyboard controller
- Linear LTC2471 16-bit $I^2C$ analog to digital converter ($I^2C$ so low pin count interface)
- Maxim DS1307 $I^2C$ real time clock
- FTDI FT232RL USB virtual serial port
- LM1085 5.0V LDO voltage regulator
- Vishey SUM50N06-16L power MOSFET for IC solenoid an cutter solenoid
- Camera outputs direct through voltage divider (Camera is LVTTL 3.3V)
- Laser outputs direct through diode
- DS18B20 1-wire temperature sensors

From the beginning, it was understood that this controller would be based on an Atmel ATmega microcontroller as the author has completed several medium sized projects using this family and he has all of the development tools, programmers, debuggers, etc. to support them with only a minimal learning curve. As a bonus, much of the code for this controller could be based on existing code and libraries for this family. Figure 5.1 shows the populated PCB of the second revision of the controller.

Displaying what is going on is always important and often more than trivial to accomplish. For this project, a generic 20x4 LCD character display with an attached $I^2C$ controller was selected. It can display the required information in all modes without being TOO cramped. Because it uses the $I^2C$ interface, it is very low pin

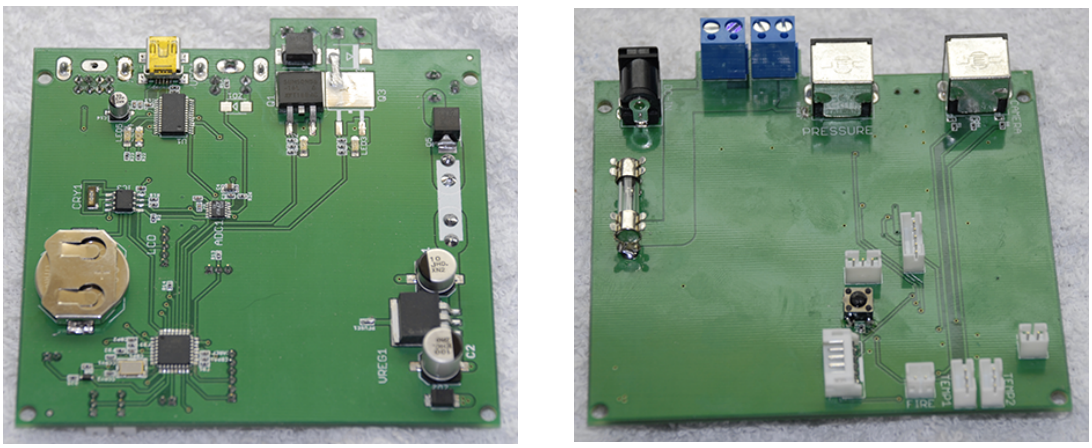


(a) Controller Front (b) Controller Back

Figure 5.1: Rev 2 shock tube controller PCB, front and back

count. In addition, it also has a built in 4x4 matrix keypad interface that can also be used as an input for up to 8 control switches. These switches are debounced internally to the controller and only require a single additional wire (key press interrupt) back to the controller to allow full function for the switches.

Plus, I had already used this display for another project, so I had a fully functional and debugged library ready to go...

The ADC was chosen for similar reasons. 16-bit resolution provided more than enough per bit resolution over the voltage range we would be using. It is also an $I^2C$ part, so a device driver library could easily be constructed using existing and understood base $I^2C$ libraries. The reduced pin count of $I^2C$ also simplified the board layout around the ADC, making it easier to produce a low noise layout. This ADC also could run in either single reading mode, 250 sample/s mode or 1000 sample/s mode. In the 250 sample mode, this device over-samples the input 8,192 times while in 1000 sample mode it can still over-sample at 2,048 times, which would help reduce spurious noise from the pressure transducer.

One limitation of this ADC is that VREF is fixed at 1.25V. The Omega PX303 pressure transducer outputs a 0.5 - 5.5V signal covering a 0 - 1000 psi pressure range. At Mach 2.0, we are shooting at approximately 280 psi, which corresponds to an output pressure of approximately 1.9V, which is well above the input range for the ADC. An optimal solution to this issue would be to scale and offset the input range to the ADC into 0 - 1.25V range using a pair of op-amps. Given the performance requirement of the controller, it was decided that this would be more work than necessary and instead, a pair of 10K resistors was used as a 2:1 voltage divider at the input. This reduces the input at Mach 2 from 1.9V to only 0.95V. The controller code was easily adapted to handle this scaling and simply shifts the incoming value from the ADC left by one place to restore the original value before calculating the pressure reading.

If high Mach number shots are needed in the future, either a revised controller with proper op amp based input conditioning to allow the full scale of the pressure sensor to be used will have to be designed, or the voltage scaling will have to be changed via a change to the voltage divider resistors and a change to the rescaling code in the firmware will have to be made. The first option is the optimal solution, but the second option is much easier to implement.

A Maxim DS1307 real time clock (RTC) was also added to the controller. It is a fairly low cost part and also uses the $I^2C$ interface. Perhaps the most significant reason to add this RTC is that it contains 56 bytes of battery backed up RAM. This RAM is where the program settings for the controller are stored. It would be possible to hold everything in RAM and then burn them to flash in the ATmega, but writing flash is a bit more convoluted than writing RAM (byte addressable versus page addressable, etc.) and flash must be wear leveled if many writes are going to be done. If we shoot 50 times per day (including tests, failures, etc), that would damage the flash in six years or so without wear leveling. Storing the default parameters in

flash and the adjustments in battery backed RAM is a more elegant solution that uses each type of memory to best effect.

In addition, I already had a fully debugged library for this device from previous projects, so adding it added very little to the programming time. Future uses of this part are mainly focused on data logging with date and time stamps.

This was also the reason the the FTDI FT232RL USB virtual serial port was added. It will allow an easy program interface as it acts like a serial port to the host, but because it uses the USB interface, it will work on modern computers which generally do not have a real RS232 serial port on them. If data logging is enabled, this will be used to export the data from the controller.

In the original specification, the controller was going to be directly controlling the high current cutter solenoid and it was also decided that it should be able to control an IC solenoid if it was ever decided to automate turning on and off the ICs. For these reasons, Vishey SUM50N06-16L N channel power MOSFET rated at 60 volts and 50 amps where chosen to provide significant headroom. Given the very low duty cycle, the FET would not have time to overheat, so it could be used with a small temperature derating if required. As it is, with no heatsink it should still be able to handle far more current than the board traces can handle on a continuous basis. With the change to a pneumatic firing system documented in chapter 4.1 above, there is no longer a need for a high current firing output, so the cutter output just acts like a VERY over sized input buffer to the micro controller.

Interfacing to the camera was much simpler, even if it was a bit more nerve racking. It was simpler because the ATmega could directly output to it through a current limiting resistor. It was nerve racking because the Apogee documentation ONLY lists the inputs as "LVTTL Compatible" without bothering to specify exactly which LVTTL specification they were talking about. Some of the specifications

are backwards compatible with old school TTL (5V) signals with no extra input conditioning required.

There were a few, however, that were not compatible with a 5V input and would in fact be damaged by it. The thought of damaging a $\$40,000$ camera did not appeal to me for some reason, so a simple voltage divider was created for each output that would reduce the 5V TTL output down to a 3.3V LVTTL compatible level. At the very least, it would prevent any damage to the camera even if it did cause issues that prevented the camera from being successfully triggered by the controller! Test day was a nervous day for some reason...

The laser outputs are very straight forward. We do not directly trigger the lasers. Instead, the trigger input to the delay generator is given a false trigger (versus a real trigger caused by the shock wave passing over the downstream pressure transducer PT 2) to its trigger input. It then counts down the programmed delays and fires which ever lasers we are using for that experiment. This signal is simply connected in parallel with the output from the PS 2 power supply. To isolate the signal from the controller, a diode is used on the output of the controller.

The controller also has inputs for two DS18B20 digital temperature sensors (and more can be daisy chained off of these if needed). These small, digital temperature sensors are not currently used by the controller. The interface and core software was added so that it would be trivial to add temperature sensors to assorted parts of the shock tube (such as the driver section which tends to warm up with long days of shooting) and monitor these temperatures if it became necessary to fine tune the control of the system even further.

The full schematics and board layout image of this controller is in the appendix with the first sheet of the schematic starting in appendix A.1. There are eight schematic sheets and one PCB layout sheet.

## 5.2 Controller Firmware

The largest task in building this controller was programming it. The core code started life as a copy of the code base for the SMD reflow oven controller I build a few years ago. This core code probably makes up 30% of the current code base. In addition, the LCD, RTC, USART and DS18B20 libraries were already written for other projects, so they were very easy to include as well.

The single biggest challenge in writing this controller was the state machine. In previous projects, I either did not need a state machine, or the states were so simple that the state machine was very easy to write and debug.

Not so for this application. The file that defines the state machine, menu.c, is 201 lines long and it defines 39 separate states for this controller. As I had never wrote a state machine anywhere near as complex as this, debugging this took longer than expected. This was compounded when I (eventually) found that avr-gcc (the open source compiler behind AVR Studio 5.1) had a bug in the pin configuration header file for the specific AVR part, the ATmega169P I was using for testing that caused the program to look at the wrong input pins even though they were correctly configured in my code. That was fun.

Due to reasons of pride, I won't say how long it took me to find the root cause of the problem! Let's just say it was WAY longer than it should have been and it wasn't found until I hard coded the pin definitions into my source that things started working...

With the switch to Rev 1 controller hardware from the testing hardware (an AVR Butterfly card), development accelerated. Once the state machine was roughly implemented, it was fairly straightforward to develop each function that implemented each of the many states.

## 5.3 The Rev 2 Controller

Like many electronics projects, the first revision of the hardware (and software) did not perform up to specifications. From a software point of view, the biggest problem was the firing function and its implementation. Basically, when you fired the shock tube, the controller would open the helium valve and monitor the pressure in the driver. In every 1 $ms$ loop, the controller would also calculate the rate of rise of the pressure from the current and previous pressure readings. It would then use this derivative to try and calculate the correct time to open the camera iris based on the iris preroll value (usually around 50ms) and then to calculate exactly when to trigger the cutter system taking into account the reaction time of the cutter system and the current rate of rise and pressure.

The problem was that like all derivatives, it was very easy for even slightly noisy pressure data to lead to the system shooting before it was actually at the correct pressure. In addition, it was possible for it to prematurely trigger the camera and then try to trigger it again when it actually was the correct time, but the camera can only be triggered once for each shot, so the shot would still be lost.

From a hardware point of view, the main issue was lack of sufficient protective elements in the power section to prevent damage under abnormal conditions. The need for these protective elements came to light during a debugging session in the lab. While probing voltages in the controller, a short occurred (root cause has not been identified) that overloaded the voltage regulator that regulates the 14VDC input power down to 5VDC for the controller's use. The LM1085 is a fairly standard linear regulator and it failed in the most common mode: it shorted.

This short had the effect of blowing through all of the output pins on the ATmega328 microcontroller. This raised every pin above VCC and enabled all the active

high outputs simultaneously and permanently. I was looking at the display at the time of the short and saw a glitch on the display. As fast as I was unplugging the controller (not the first time I've released the magic smoke...), I was still way, way to slow to save this controller.

The final tally of the damage was significant:

- ATmega328 IC
- 20x4 character LCD display
- I2C LCD display controller
- LTC2471 16-bit ADC IC
- DS1307 Real Time Clock IC
- FTDI FT232RL USB virtual serial port
- One 100 mils wide trace on the PCB

While the original controller was rebuilt and in fact functions to this day as a development board for software development, the fact that the high power outputs activated outside of software control spelled the end for this revision of the controller. Once the root cause of the event was understood (5V power shorted to ground causing the regulator to short), discussions began on how to prevent this and other types of failures from causing an out of control shock tube.

In the end, the changes made to produce the Rev 2 controller were fairly straightforward, but still significant:

- Additional power conditioning added to ATmega328
- High current self resettable fuse and high current zener diode added to 5V power supply
- Self resettable fuse added to excitation supply voltages on external sensors
- RS232 interface changed to USB interface
- Circuit added to trigger delay generator directly

The single biggest change was the self resettable fuse and the high current zener. Basically, the zener is a diode that starts to conduct at $5.1V$ in our case. It is placed just after the polyfuse that is placed directly on the output of the 5V regulator and connects directly to the ground plane. If the output of the regulator goes above 5.1V, the zener will conduct. It is rated for 10 times the current of the polyfuse which will open due to the power surge. This action protects all of the other devices on the PCB from an over volt condition like the one that destroyed the first revision of the controller. Polyfuses were also added to the power supply lines feeding external sensors to prevent external shorts from damaging the controller.

We had also devised a couple of changes that needed to be made to the controller before the melt down. Specifically, we needed a way to trigger the delay generator directly so the controller could generate background images without directly firing the lasers. a simple diode isolated circuit was tested and then added to the new boards design.

In addition, this refresh was also used to replace the functional but outdated RS232 serial port with a much more up to data FTDL USB interface. This circuit used had been previously tested out on my aquarium light controller project and worked perfectly. Eliminating the RS232 port removed the reliance on an interface that is fast fading from modern computers.

One additional upgrade was discovered just prior to frying the first controller. During testing for a Mach 2.0 shot (which fires around 180 $psi$), it was discovered that the display would stop climbing at 150 $psi$. A bit of math showed that aligned with an input voltage of $1.25V$. A bit of head scratching and referencing the ADC datasheet provided the answer to this strange behavior: the ADC uses an internal voltage reference which is $1.25V$ and not the $5.0V$ reference that I thought it did. It would never be able to fire Mach 2.0 shots with the current hardware configuration.

Two different hardware solutions were discussed:

- Implement a full op amp based input signal conditioning circuit
- Add a two resistor voltage divider before the ADC input

The op amp solution was the most elegant. It would allow the full scale output of the PX303 pressure transducer to be used which gives the controller the ability to control up to 1000 *psi*. The down side to the op amp solution was complexity. It would require a dual op amp along with several external components to both shift the transducers $0.5V$ to $5.5V$ output down to a $0V$ to $1.25V$ input for the ACD. Op amps are not expensive and either were the additional components, but the did add additional complexity that was not wanted.

In the end, the decision was made to go with a simple voltage divider circuit composed of a single 1K Ohm resistor and a single 2K Ohm resistor. This divider would drop the input voltage at the ADC from $1.30V$ down to $0.86V$ which is well within the input range for this ADC. It would also leave plenty of headroom for faster shots up to Mach 2.5 and slightly above.

These updates have been made to the design and Rev 2 PCBs have been fabricated. A Rev 2 controller has been fabricated and tested. The firmware updates to support static firing are being implemented at this time and will be completed prior to the end of the semester.

# Chapter 6

# Recent RMI Results

## 6.1 Post Upgrade RMI Studies

The modernization of the UNM shock tube has produced significant results. First, we are able to reliably fire the shock tube using the static firing method which greatly reduces the Mach number variation. The improvements to the camera and laser plane focusing methods an apparatus have allowed sharper, more detailed images to be captured than ever before.

### 6.1.1 Mach Number Variation Visualization

Figure 3.1 is perhaps the best proof of the improvements in the Mach number variation. Six images were captured in back to back experiments with a fixed timing of $570\mu s$ after delay generator trigger and five of the six images have the shock captured in the ICs which is only $8mm$ in diameter at this point. More impressively, the goal of that shot sequence was to move the shock back to the beginning of the IC (right side) by making small changes to the firing pressure. When you compare the shock

position with the firing pressure listed for each shot, you can see the level of control achieved.

### 6.1.2 Mach Number Variation Data Analysis

In the "Early RMI Results" section, I reviewed the Mach timing data from a sample of shots at Mach 1.2, 1.7 and 2.0. The data anlysis in the section will be very similar, but I will directly compare the early results to the current results. The standard warning remains, this is not a statistically random sample, but effort was made to ensure the data presented does represent the general case.

Table 6.1 below shows before and after data in a single table.

Table 6.1: Mach Number Data Analysis

| **Pre or Post Upgrade?** | **Target Mach Number** | **# Samples** | **Standard Deviation** | **Average** | **% Error** |
|---|---|---|---|---|---|
| Before: | M = 1.20 | 17 | 0.030339 | 1.227592 | 2.299 |
| After: | M = 1.13 | 20 | 0.004206 | 1.129932 | 0.006 |
| Before: | M = 1.70 | 17 | 0.037856 | 1.557438 | 5.587 |
| After: | M = 1.70 | 19 | 0.021063 | 1.693486 | 0.383 |
| Before: | M = 2.00 | 13 | 0.075581 | 1.960902 | 1.955 |
| After: | M = 2.00 | 20 | 0.024908 | 1.991622 | 0.419 |

Each of the sample sets was selected as a representative sample and every sample was taken as a block (no interior shots removed) with up to 20 shots per sample. Each block represents a single day of shooting to minimize any changes to the setup that would artificially inflate the average and standard deviation values.

Looking at the average Mach number values, the percent error for each group was calculated as

$$\frac{(average - target)}{target} \cdot 100\% \tag{6.1}$$

The average and standard deviation were calculated using Microsoft Excel 2010's built in AVERAGE and STDEV functions.

Looking at the result, we first notice that the before average error was running from 2 to nearly 6%. After the modernization, the % error has dropped from less than $\frac{1}{100} \cdot \%$ to less than $\frac{1}{2} \cdot \%$! In this sample, the worse case improvement is a 75% reduction in error for the Mach 2 shots. The best case sample for Mach 1.2 / Mach 2.0 is far, far better were the Mach 1.7 sample has a nearly 15 fold improvement in error. From just an error off target perspective, there is no doubt that the modernization has dramatically improved the performance of the UNM shock tube.

Perhaps more important, the standard deviations also improved, but not as dramatically. The best standard deviation before was 0.03 and after was 0.004. This is nearly a 10 fold improvement. The worse case is also better with the worse before being 0.076 and the worse after being 0.038, which is still a factor of 2 improvement.

We can also compare the 95% confidence window is also illustrative. Table 6.2 is a summary of the statistical confidence interval data calculated from our data sample.

Table 6.2: Mach Number Data Statistical Analysis

| **Pre or Post Upgrade?** | **Target Mach Number** | **95% Confidence Window** | **95% Window Size** |
|---|---|---|---|
| Before: | M = 1.20 | 1.2203 to 1.2350 | 0.014717 |
| After: | M = 1.13 | 1.1290 to 1.1309 | 0.004206 |
| Before: | M = 1.70 | 1.5959 to 1.6142 | 0.018363 |
| After: | M = 1.70 | 1.6887 to 1.6983 | 0.009664 |
| Before: | M = 2.00 | 1.9819 to 1.9400 | 0.041925 |
| After: | M = 2.00 | 1.9861 to 1.9972 | 0.011140 |

Once more, we can clearly see the trend where the 95% confidence window has been reduced by factors ranging from 2 to 4 for all after cases.

All of the data presented demonstrates that the modernization of the shock tube has resulted in improved capability and the ability to target and hit more specific Mach numbers (for example, Mach 2.1 instead of Mach 2.0). This capability can be used to further refine Mach number studies with a much greater degree of confidence in the precision of the results.

### 6.1.3 Image Resolution

This last section is just to demonstrate some of the very sharp, very clear images that have recently been captured by the UNM shock tube. The upgrades to the shock tube have paid dividends in its ability to capture high quality data and these images bare that out. The image in Figure 6.1 has been false colored by intensity level (the Apogee U42 is a monochrome camera) to high light the features. And the features are beautiful! Not only is the RMI instability very clear and very symmetrical, but you can see the beginning of secondary instabilities developing in the image as well. In addition to all that, it is also just a very beautiful image!

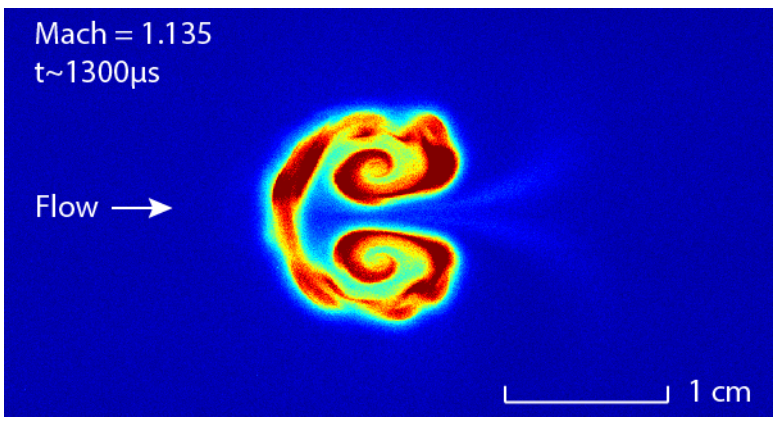


Figure 6.1: Secondary instabilities in RMI

The image above was captured in the horizontal plane. The image in Figure 6.2 was taken not only in the vertical plane were we are using the laser to "cut in half"

the IC column from top to bottom vertically, but it was also shot with the shock tube inclined at a 30° as well. The vertical striation pattern also appears to be indicative of secondary instabilities forming in the column and also demonstrates that turbulence is inherently a three dimensional phenomenon. This image is also false colored by intensity.

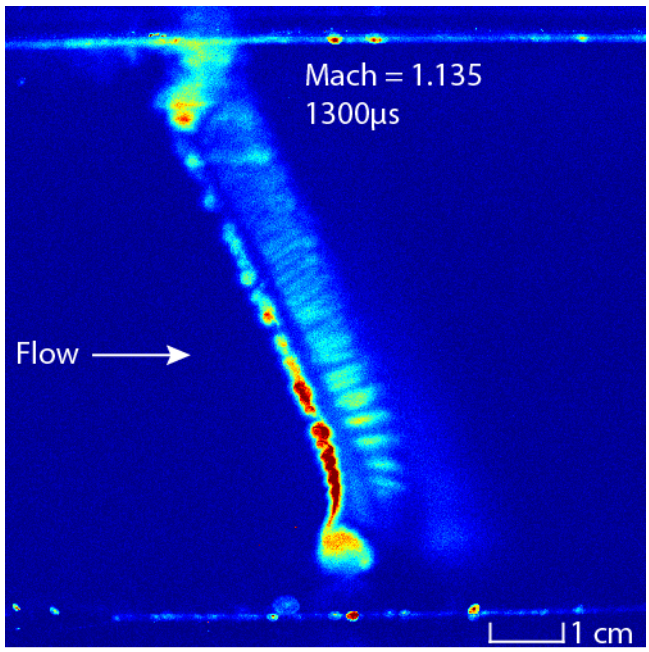


Figure 6.2: Vertical plane with secondary instabilities

Figure 6.3 is left monochrome. The sharpness of the features in this image was described in the shot log simply as "incredible!" I have to agree. This level of detail was not apparent before the improvements to the camera and laser focusing systems.

The final image in this section is Figure 6.4. This image is monochrome and is a vertical inclined shot. Notice at the base of the image, you can clearly see the outlet hole in the bottom of the test section were the IC gas column falls out of the test section. Also, you can clearly see that this opening DOES have an effect on the gas column as the shock wave passes through it.

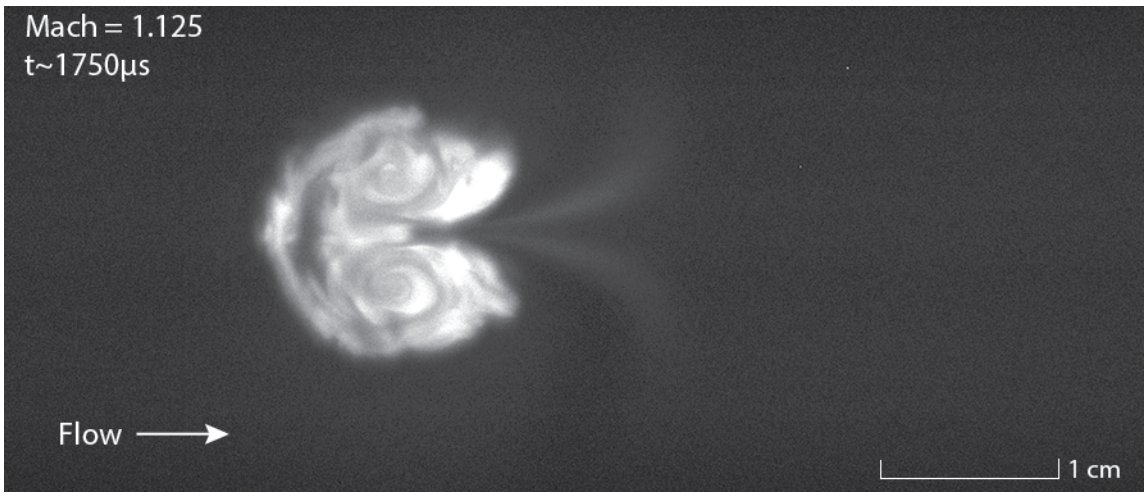


Figure 6.3: Very sharp horizontal plane image, 2014-01-29-shot-20

Taken together, these images demonstrate the quality of the images now being captured by the UNM shock tube.

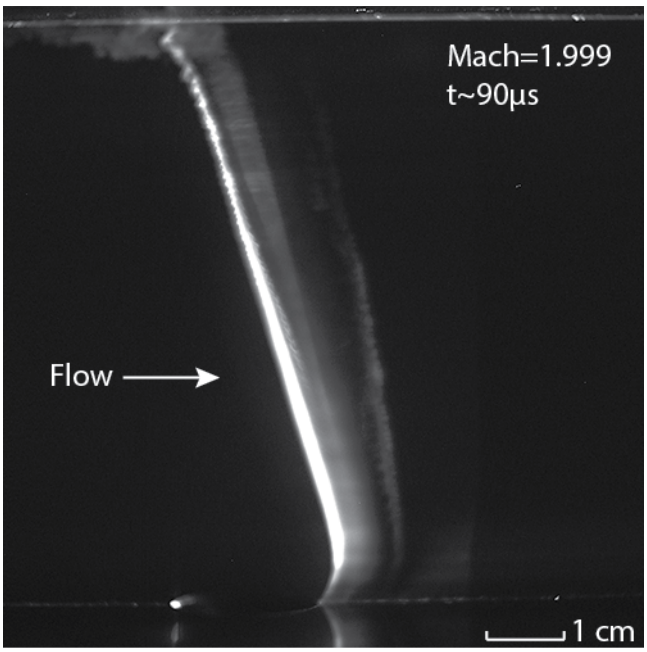


Figure 6.4: Very sharp inclined vertical plane image, 2014-02-21-shot-16

# Chapter 7

# Conclusions

What started out as simply a need to reduce the aggravation of trying to shoot the shock tube and collect good data grew into much more as small upgrades proved there worth and paved the road for more expansive upgrades. With the "changing of the guard" in early 2012 and the new PhD student coming on board, the pace of upgrades became faster and faster as the improvements demonstrably simplified the life of the RAs in the lab while increasing the quality and quantity of data collected. Often, the early upgrades enabled some of the later upgrades. At other times, the simple act of correcting one big issue brought to light another, slightly smaller issue that had been hiding in the shadows of it's big brother.

Many of the upgrades implemented actually allowed future upgrades to be likewise implemented. The cutter system upgrades are a perfect example. Originally, the custom made cutter head was used instead of an off the shelf arrowhead because the original cutter system simply couldn't always get the tip of the arrow through a bowed diaphragm. Correcting the length of throw and power limitations of this system allowed us to return to an arrowhead for a cutter which improved the pressure traces as well as simplifies maintenance on the cutting system.

Moreover, these upgrades also allowed us change not only the hardware on the shock tube, but the procedures used as well. Changing from dynamic shooting to static shooting demonstrably decreased the Mach number variation for the experiments. This improvement was dramatic and was an unexpected side effect of improving the cutter system.

Overall, the modernization of the UNM shock tube was a complete success. These improvements mentioned here, along with countless smaller ones, have significantly improved the performance of this shock tube and have positioned it perform new and unexpected experiments in the future.

# References


[1] Vorobieff, P., Anderson, M., Conroy, J., White, R., and Truman, C. R., "Vortex formation in a shock-accelerated gas induced by particle seeding," *Physical Review Letters*, Vol. 106:184503, 2011.

[2] Vorobieff, P., Wayne, P., Bernard, T., Corbin, C., Truman, C. R., and Kumar, S., "Experimental studies of shock interactions with a multiphase medium," *To be published in Proceedings of 29th ISSW*, 2014, University of New Mexico.

[3] Bernard, T., Truman, C. R., Vorobieff, P., Corbin, C., Wayne, P. J., Kuehner, G., Anderson, M., and Kumar, S., "Observation of the development of secondary features in a Richtmyer-Meshkov instability driven flow," *Submitted to Shock Waves*, 2014, Submitted to Experiments in Fluids.

[4] Brouillette, M., "The Richtmyer-Meshkov Instability," *Annual Review of Fluid Mechanics*, Vol. 34, 2002, pp. 445–468.

# Appendices

# Appendix A

# Rev 2 Controller Schematics

## A.1 Sheet 1 - Microcontroller

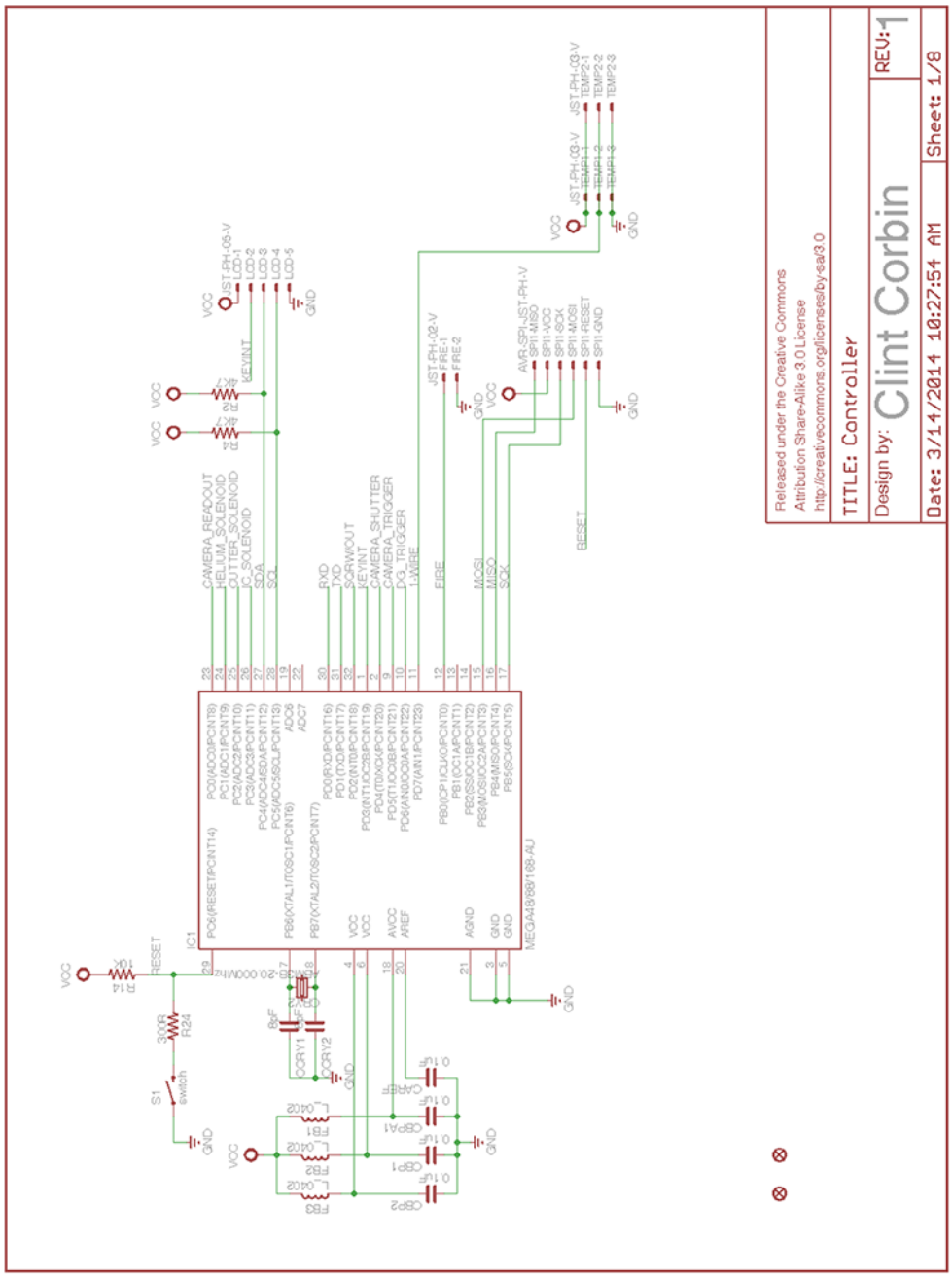


Figure A.1: Rev 2 Controller Schematics Sheet 1

## A.2 Sheet 2 - Power Regulation and Conditioning

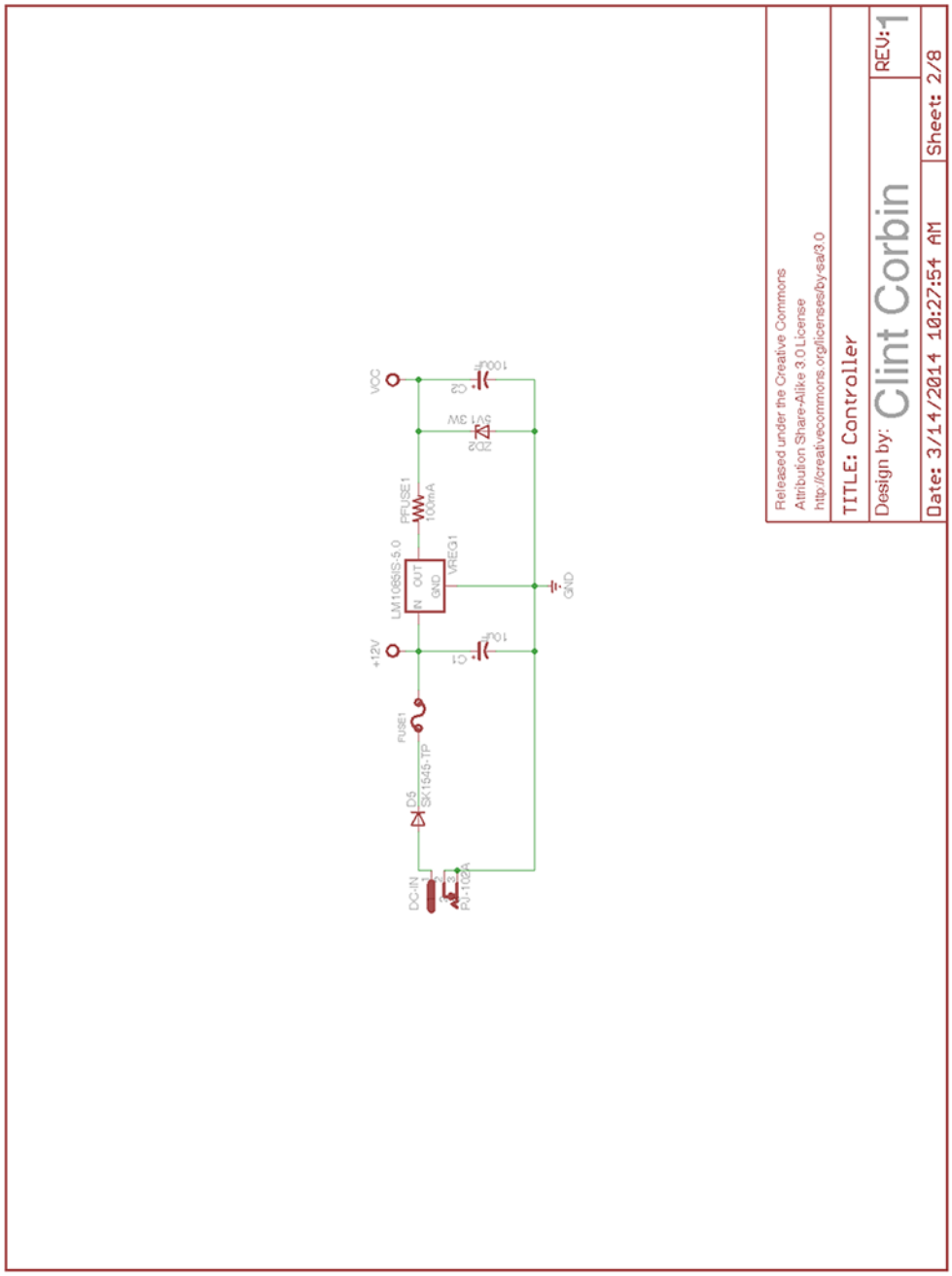


Figure A.2: Rev 2 Controller Schematics Sheet 2

## A.3 Sheet 3 - Solenoid Control Interface

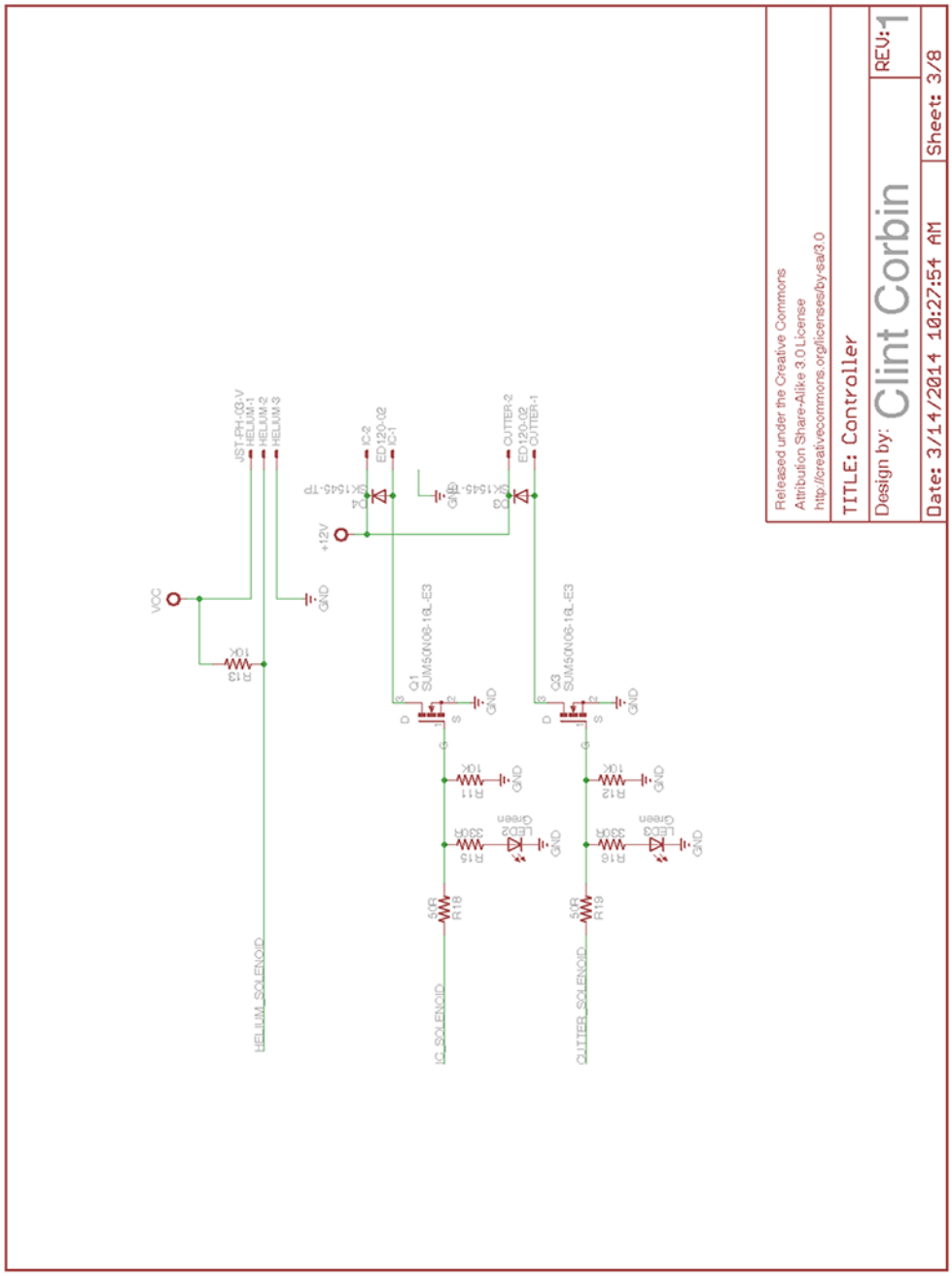


Figure A.3: Rev 2 Controller Schematics Sheet 3

## A.4 Sheet 4 - ADC Circuit

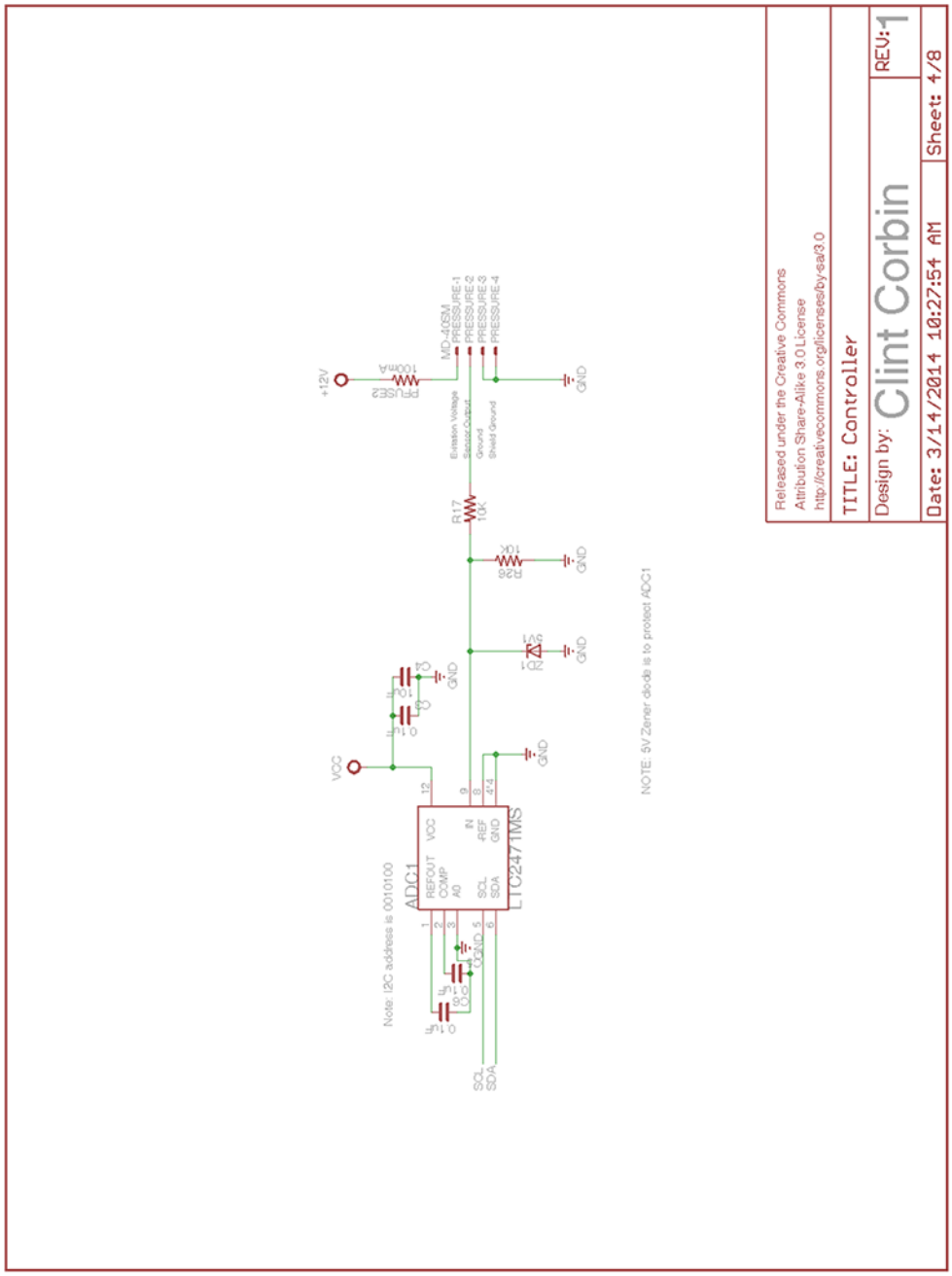


Figure A.4: Rev 2 Controller Schematics Sheet 4

## A.5 Sheet 5 - Camera Interface

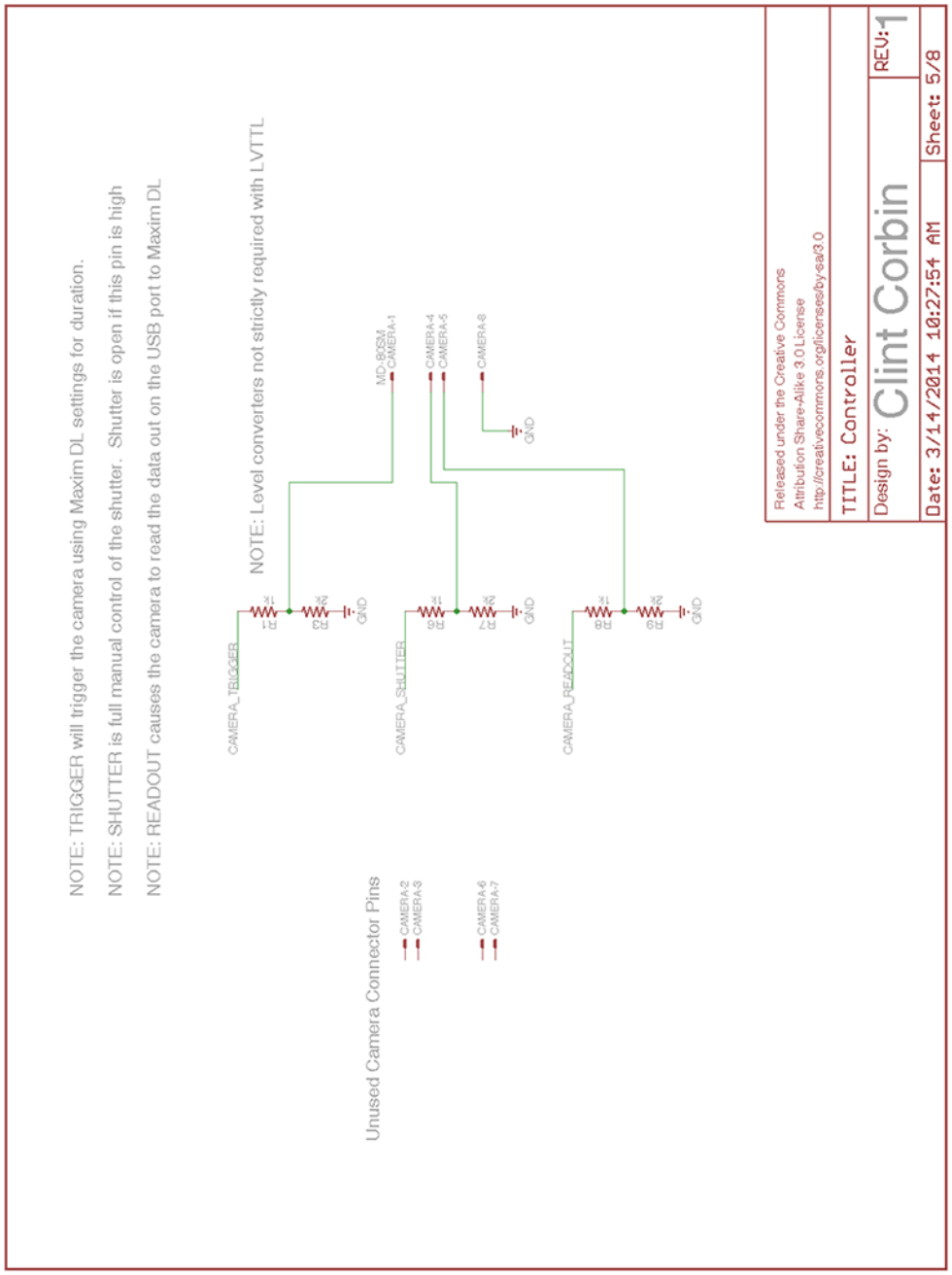


Figure A.5: Rev 2 Controller Schematics Sheet 5

## A.6 Sheet 6 - Delay Generator Trigger

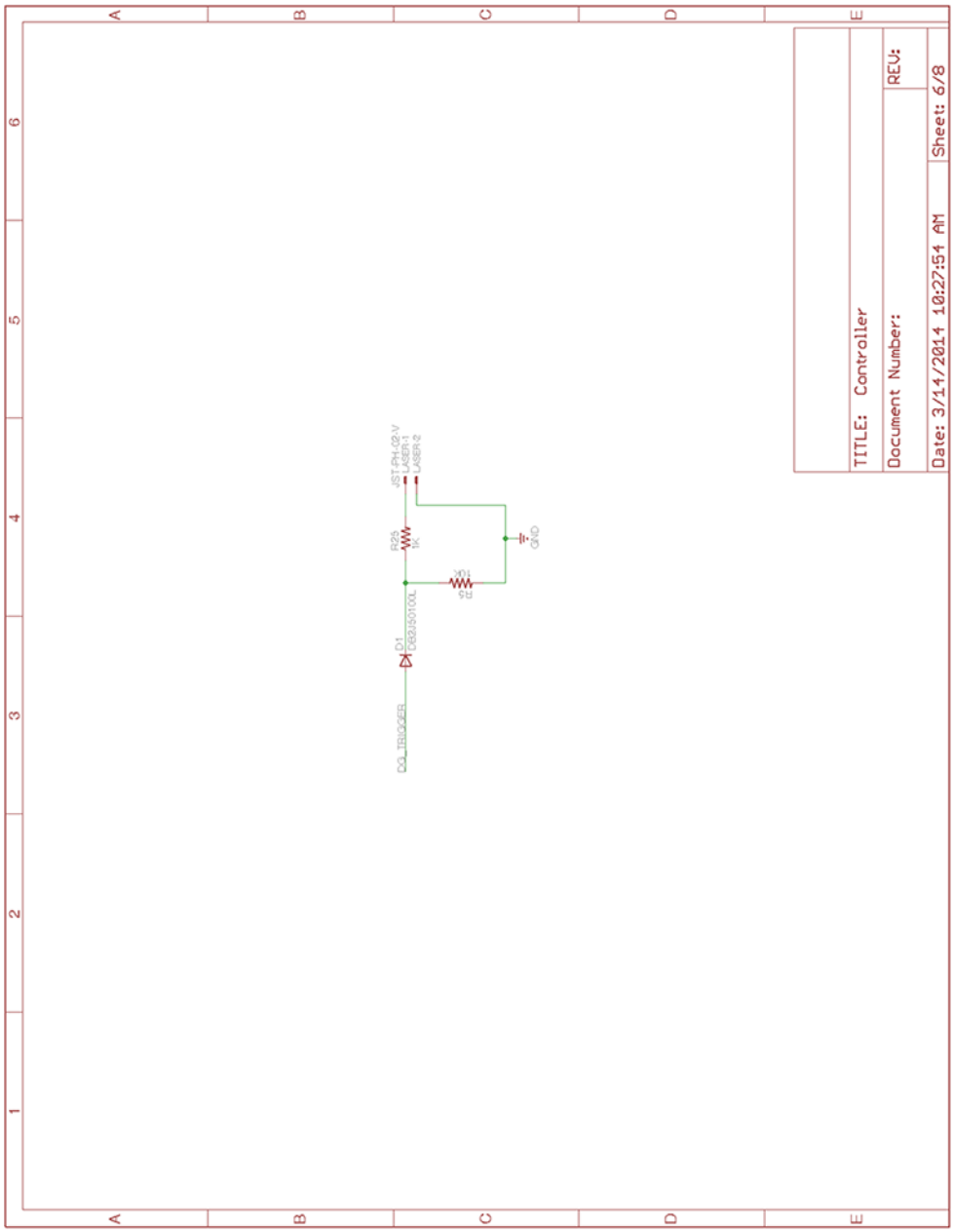


Figure A.6: Rev 2 Controller Schematics Sheet 6

## A.7 Sheet 7 - Real Time Clock

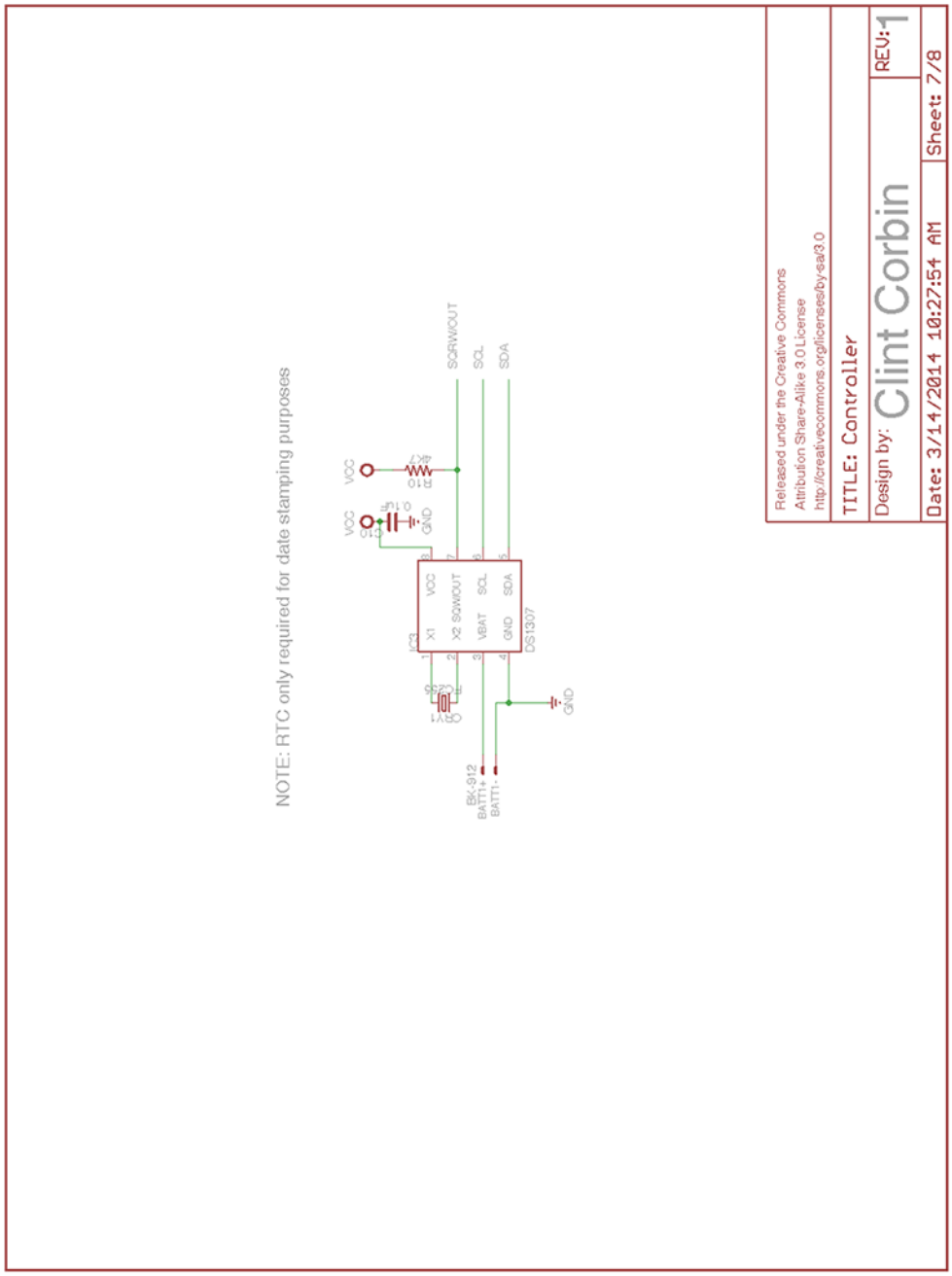


Figure A.7: Rev 2 Controller Schematics Sheet 7

## A.8 Sheet 8 - USB Interface

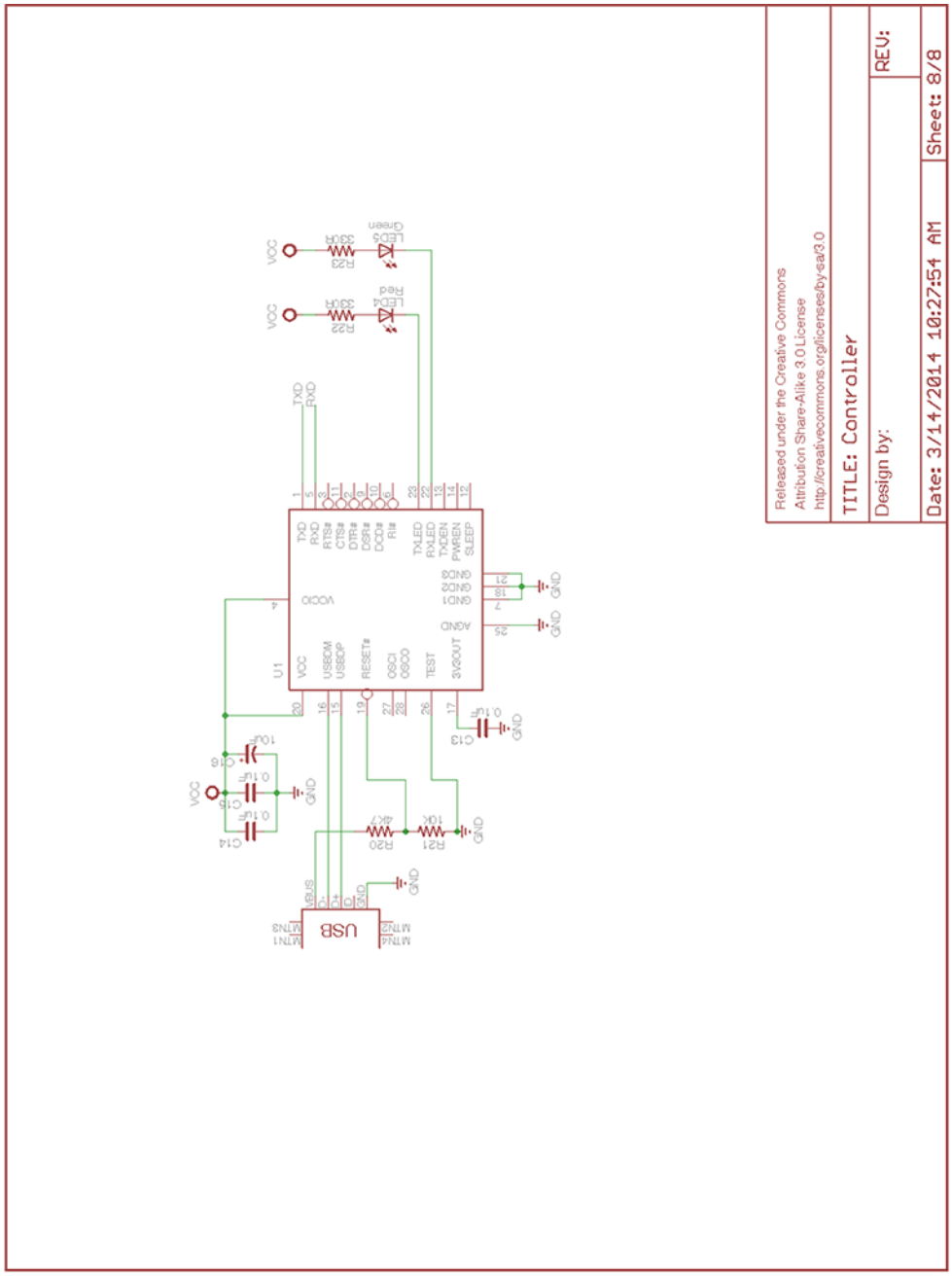


Figure A.8: Rev 2 Controller Schematics Sheet 8

# Appendix B

# Rev 2 Controller PCB Layout

## B.1 Sheet 1 - Controller PCB Layout

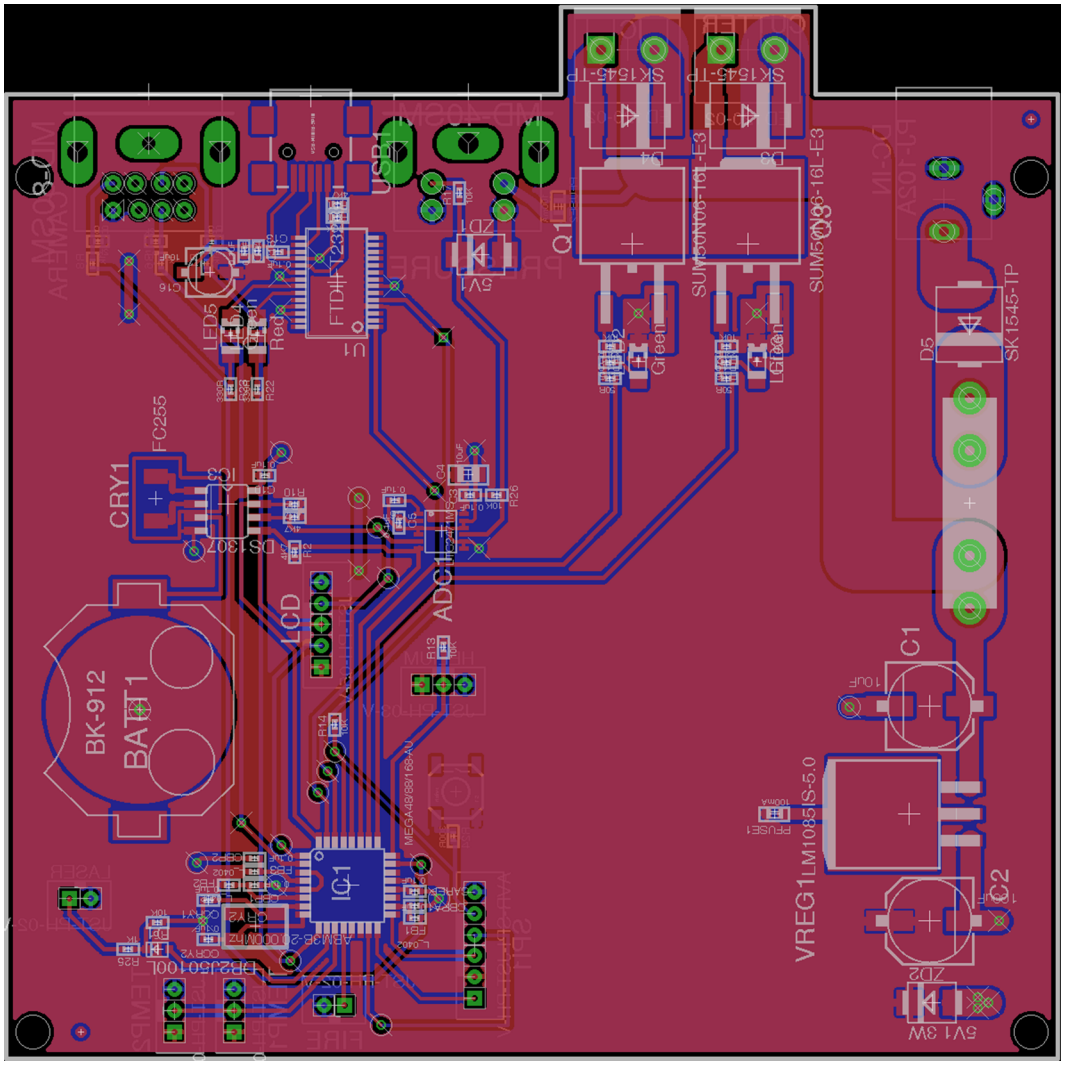


Figure B.1: Rev 2 Controller PCB Layout

# Appendix C

# Solenoid Driver Board Schematics

This board has three outputs. One output is used to turn on and off the helium fill solenoid and the other two outputs activate the extend and retract solenoids. There is an Atmel ATtiny85 8-pin microcontroller that controls the timing

## C.1 Sheet 1 - Solenoid Driver Board Schematics

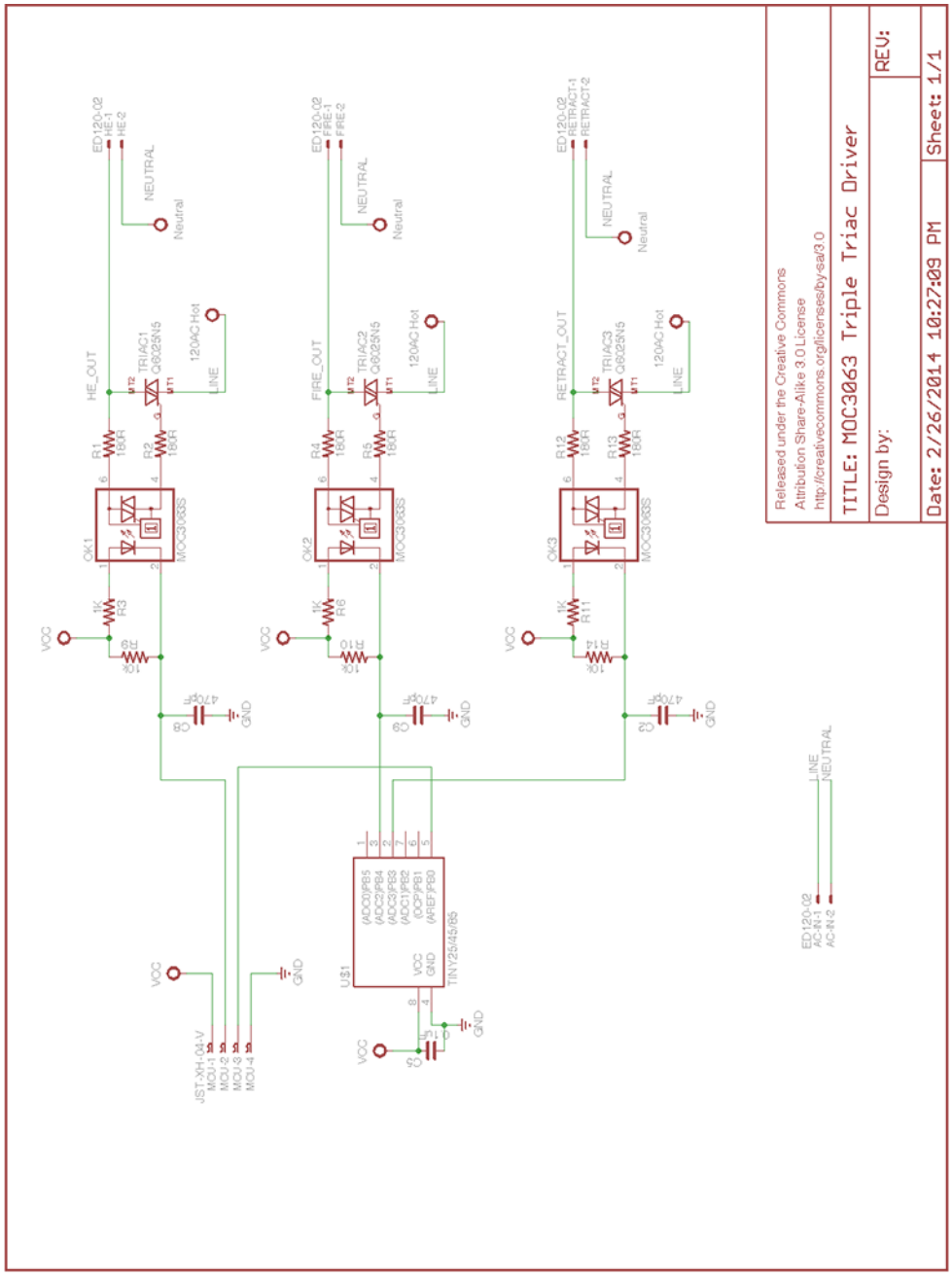


Figure C.1: Solenoid Driver Board Schematics

# Appendix D

# Solenoid Driver Board PCB Layout

PCB layout of the solenoid driver board. on the extend and retract solenoids.

## D.1 Sheet 1 - Solenoid Driver Board PCB Layout

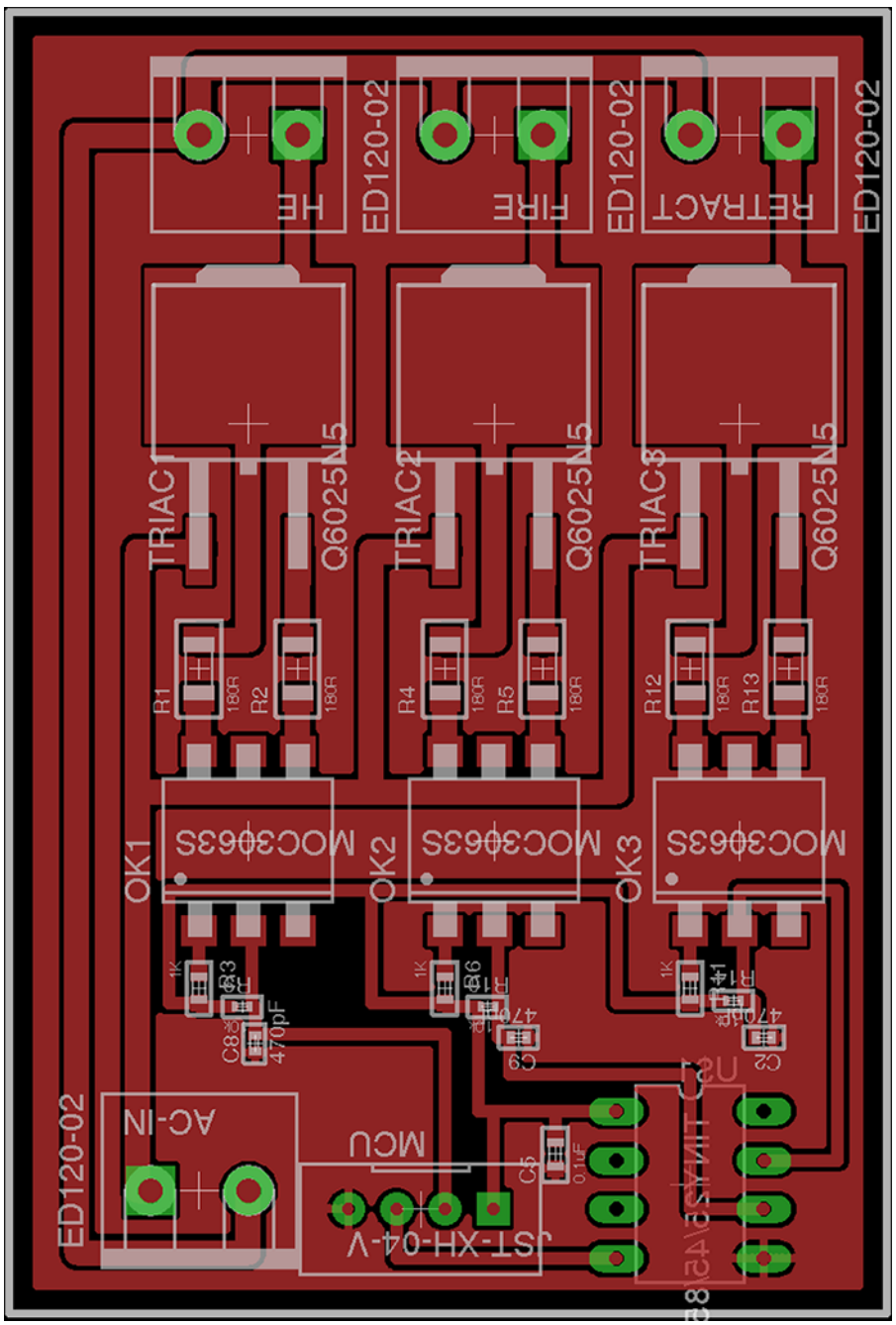


Figure D.1: Solenoid Driver Board PCB Layout